Microbiologically Influenced Corrosion (MIC) Mechanisms and Mitigation

A dissertation presented to

the faculty of

the Russ College of Engineering and Technology of Ohio University

In partial fulfillment

of the requirements for the degree

Doctor of Philosophy

Dake Xu

August 2013

This dissertation titled

Microbiologically Influenced Corrosion (MIC) Mechanisms and Mitigation

by

DAKE XU

has been approved for

the Department of Chemical and Biomolecular Engineering

and the Russ College of Engineering and Technology by

Tingyue Gu

Professor of Chemical and Biomolecular Engineering

Dennis Irwin

Dean, Russ College of Engineering and Technology

ABSTRACT

XU, DAKE, Ph.D., August 2013, Chemical Engineering

Microbiologically Influenced Corrosion (MIC) Mechanisms and Mitigation

Director of Dissertation: Tingyue Gu

Microbiologically influenced corrosion (MIC) has become a major problem in the oil and gas industry due to frequent use of water flooding in enhanced oil recovery that leads to water wetting of pipeline walls. MIC is also of concern in many other industries such as water utilities and nuclear power plants. As infrastructures are aging, MIC threat increases.

Sulfate reducing bacteria (SRB) are regarded as the primary culprit for pipeline failures caused by MIC. Due to a lack of understanding, MIC has even been considered to be a "myth" in corrosion research. Until recently, there has been no clear mechanism that clarifies why and how MIC happens in the field because of its complexity. Indeed, a mechanism that can cogently explain MIC phenomena is needed.

The new biocatalytic cathodic sulfate reduction (BCSR) theory proposed by Gu et al. (2009) is bioelectrochemistry based. In BCSR, the bioenergetics can explain why MIC occurs, while the extracellular electron transfer (EET) theory is able to explain how MIC happens. In this work, solid evidence was found to support BCSR. Additional experimental data suggested that MIC can also be caused by nitrate reducing bacteria (NRB), which led to an analogous biocatalytic cathodic nitrate reduction (BCNR) theory. Another experiment to support BCSR was an electron mediator test designed to verify the EET process proposed in BCSR. The experimental results indicated that common

electron mediators like riboflavin and FAD were capable of accelerating MIC by promoting electron transport between an iron surface and a biofilm. A starvation test demonstrated that when lacking organic carbon, elemental iron replaced organic carbons as an energy source/electron donor for SRB to obtain their maintenance energy. The output of the test showed that under severe starvation of organic carbon, the largest pit depth was achieved, which was consistent with the prediction of BCSR.

The emerging demand and urgent need in the oil and gas industry is to find an efficient method to prevent and mitigate MIC at a reasonable cost. A mixture of D-amino acids, signal molecules to disperse bacterial biofilm, was selected to act as biocide enhancers. The efficacy of the D-amino acid mixture containing D-tyrosine (D-tyr), D-methionine (D-met), D-tryptophan (D-trp), and D-leucine (D-leu) in equal moles was evaluated. The potential of D-tyr and D-met as individual biocide enhancers was also investigated. Considering the cost, toxicity and their biocide enhancement ability, D-amino acids appear to be very attractive.

DEDICATION

To all who encouraged and helped me during my PhD study

And my special gratitude to my wife, Miaomiao Wang.

ACKNOWLEDGMENTS

I would like to express my sincere gratitude to my academic advisor, Prof. Tingyue Gu, for his continuous support during my PhD study. His guidance, motivation, and enthusiasm encouraged me not only to grow as a researcher but also to be an independent thinker. His rigorous training improved my research ability, and helped me to explore more deeply into the academic field.

I would also like to thank Prof. Srdjan Nesic, director of The Institute for Corrosion and Multiphase Technology (ICMT), for providing a stimulating work environment for research.

My sincere appreciation also goes to my former senior labmate Jie Wen, who not only helped me in my research, but also taught me how to deal with the daily challenges of being a graduate student. My gratitude also goes to all the members in our MIC group, Yingchao Li, Wenjie Fu, Peiyu Zhang, and Amy Lindenberger. I would like to thank Mr. James Caesar for his help on repairing and maintaining of the instruments in the lab. My appreciation also goes to all members in the ICMT for their help with my experiments and professional corrosion training.

Grateful appreciation goes to my dissertation committee members, Professors Darin Ridgway, Peter W. Coschigano, Xiaozhuo Chen, and Monica M. Burdick for their valuable discussion, comments and suggestions to help me fulfill my program of study. I would also like to acknowledge the following sponsors who supported my research at Ohio University: M. D. Anderson Cancer Center, ExxonMobil, and US Department of

Transportation Pipeline and Hazardous Materials Safety Administration (PHMSA) via a subcontract through Gas Technology Institute and Southwest Research Institute.

Finally, and most importantly, my appreciation and gratitude go to my wife Miaomiao Wang. Her support, encouragement, patience and love were the bedrock of this academic venture. Her support and tolerance helped me overcome all the difficulties in both my personal life and my research. I am also grateful to my father Kuijun Xu, my mother Huimin Luan, and my parents-in-law Zhongjun Wang and Shulan Liu for their love and support.

TABLE OF CONTENTS

Page

LIST OF TABLES

Page

LIST OF FIGURES

Page

CHAPTER 1 INTRODUCTION

Microbiologically influenced corrosion (MIC) was first confirmed more than a hundred years ago according to Axelsen and Rogne (1998). MIC was defined by Videla (1996) as "an electrochemical process in which the microorganisms are present to initiate, facilitate, and accelerate the corrosion reactions." MIC has become a major problem in the oil and gas industry, as well as in numerous other industrial areas such as water utilities. MIC can cause corrosion and leakage in pipelines, as well as the plugging of injection wells – all of which, as Flemming (1996) and Videla (2002) reported, could decrease production and raise potential safety concerns. The serious crude oil pipeline leakage at Alaska Prudhoe Bay in 2006 triggered the turmoil in the global oil market. MIC was suspected to be the primary culprit for this failure which was caused by a 1/4 inch pinhole pit (Jacobson, 2007). Bhat et al. (2011) reported another serious MIC case where a new 8-inch ID pipe transporting oil and produced water failed due to MIC in only eight months.

Billions of dollars are lost annually due to MIC in the U.S. alone (Walsh et al., 1993). According to Flemming (1996), nearly 20% of all corrosion of metals and building materials is caused by MIC. Koch et al. (2001) reported that the estimated annual cost of all forms of corrosion to the gas and oil industry is around $13.4 billion, and MIC alone is responsible for $2 billion annually.

Due to the skyrocketing price of oil and gas in recent years, previously unproductive wells are being brought back into production by injecting water or CO_2 into

the wells to enhance the oil recovery pressure. In this water injection procedure, called flooding, the injected seawater and produced water contain readily available nutrients for microbial growth. This seawater and produced water may also contain bacteria such as sulfate reducing bacteria (SRB) and perhaps even nitrate reducing bacteria (NRB). It was also reported by Rosnes et al. (1991) that SRB may have existed in the reservoirs since geological time. Another reason that attracts the attention of engineers and researchers is that microorganisms, such as SRB, in the oil reservoir can cause serious souring due to sulfate reduction, allowing for the formation of H_2S gas, which is not only highly toxic, but also can be a very corrosive agent to carbon steel, and can even cause cracking corrosion of stainless steel (Bagarinao and Vetter, 1989; Kane, 1985).

Given both the latent and active corrosion potentials of MIC, much more attention is currently being placed on the conditions of new pipelines and storage tanks before they are commissioned (Xu et al., 2013a). Hydrotesting to determine the mechanical strength of the pipeline and to check for possible leaks is becoming a routine practice to ensure system integrity. Water (seawater, produced water, or brackish water) is the test fluid of choice due to its low cost and availability. Microorganisms are always naturally present in these fluids, and given the presence of microbes, MIC can occur during or after the hydrotesting. Once a hydrotest is completed, the test fluids often remain in the pipelines for an extended period–lasting for months, until they are commissioned for service. During this period, if the local environmental conditions such as nutrients, pH, and temperatures are favorable, MIC will occur.

To better understand this multidisciplinary research area, various fields of knowledge such as microbiology, bioelectrochemistry, electrochemistry, and corrosion are needed. Due to the complexity of MIC, much confusion still remains in MIC literature. The new biocatalytic cathodic sulfate reduction (BCSR) theory based on bioelectrochemistry and bioenergetics, proposed by Gu et al. (2009), is a new milestone in MIC study and can explain why and how microbes cause corrosion. Much evidence and supporting data can be found in non-corrosion literature such as those in microbial bioenergetics and microbial fuel cell (MFC) research. In this work, lab experiments were designed to verify and support BCSR from the aspect of bioelectrochemistry as well as to investigate the extension from BCSR to biocatalytic cathodic nitrate reduction (BCNR).

Hall-Stoodley et al. (2004) defined biofilm as a community of microorganisms that can attach itself onto either living or non-living surfaces. It is believed that the sessile bacteria within the biofilms are directly responsible for MIC–rather than the planktonic bacteria in the bulk fluid. Biofilm is able to protect the sessile cells against such changes in external environmental conditions as pH, fluid shear stress, and anti-microbial agents (Hall-Stoodley et al., 2004; Zuo, 2007). When biofilm mitigation is needed, physical scrubbing methods such as pigging, or chemical biocide treatment are often used (Videla, 2002) separately or together. The pigging treatment is used for cleaning the interior surfaces of the pipelines. However, pigging has limitations given its cost and production down time. Some pipelines are not designed for pigging.

Biocide is the most common and effective method for treating biofilms. It is reported that sessile cells in a biofilm are much more tenacious than planktonic cells in

the bulk fluid. Thus, in order to effectively treat a biofilm, a 10 times higher biocide dosage is often required compared with the dosage needed to mitigate planktonic cells (Videla, 1996). Extreme concentrations as high as 1000 times have also been reported (Mah and O'Toole, 2001). Repeated biocide treatment to control biofilm film is normally required (Vance and Thrasher, 2005) because a pipeline system cannot be kept sterile. Tetrakis (hydroxymethyl) phosphonium sulfate (THPS) and glutaraldehyde, which are both biodegradable, are presently the most widely used biocides in the oil and gas industry. However due to increasingly stricter environmental regulations, high dosages of biocide are not desirable, and large-scale biocide applications in oil and gas pipelines are becoming more costly. More effective biocide dosing is needed. In this work, green biocide enhancers that can improve the performance of current biocide, THPS, were investigated.

CHAPTER 2 LITERATURE REVIEW

Oxygen is very corrosive and thus is usually removed from oil and pipelines by using oxygen scavengers. However, anaerobic corrosion still occurs. For example, abiotic corrosion by CO_2 and H_2S causes major problems. Apart from abiotic corrosion, anaerobic MIC is also a problem. Because of its complexity, there has been a lack of a clear mechanism to clarify why and how MIC happens. Due to its incomplete understanding, MIC has been called a "myth" in the field of corrosion research (Little and Wagner, 1997). Indeed, there is a need for a mechanism that can cogently explain MIC phenomena. The emerging reasons for MIC attack on pipelines are closely related to frequent operations like hydrotesting, water flooding and water wetting of internal pipeline walls. Based on the urgent needs and demands of the oil and gas industry, better understanding of MIC mechanisms and efficient methods to prevent and mitigate MIC at a lower cost are highly desired.

2.1 Sulfate reducing bacteria

Microbes relevant to MIC are pervasive. Various bacteria are able to cause MIC attack such as sulfate reducing bacteria (SRB), acid producing bacteria (APB), iron oxidizing bacteria (IOB), metal reducing bacteria (MRB), metal depositing bacteria (MDB), and slime producing bacteria (Beech and Gaylarde, 1999). Archaea and fungi have been shown to cause MIC attack in oil pipelines (Larsen et al., 2010). Methanogens reported by Uchiyama et al. (Uchiyama et al., 2010) were found to be corrosive to carbon steel. SRB are considered the primary culprit for MIC in localized pitting corrosion, causing pipeline failures (Abedi et al., 2007; Bhat et al., 2011). SRB are also capable of

attacking various materials such as stainless steel, mild steel, and even concrete (Abedi et al., 2007; Xu and Gu, 2011; Monteny et al., 2000). In non-corrosion situations, SRB can be beneficial. In 2008, Muyzer and Stams (2008) reported the benefits of SRB found in bioremediation applications by removing sulfate and heavy metals in wastewater systems. In addition, radionuclides like chromium and uranium can also be alleviated by SRB (Muyzer and Stams, 2008).

SRB are omnipresent because sulfate is widely available in aqueous systems. SRB can be found in places such as oil fields, waste water, marine sediments, hydrothermal vents, and even mud volcanoes (Jeanthon et al., 2002; Ravenschlag et al., 2000; Stadnitskaia et al., 2005). SRB are able to utilize the energy from dissimilatory sulfate reduction of different sulfur compounds–such as sulfate, thiosulfate, sulfite, and even sulfur reduced to sulfide (Lovley and Phillips, 1994). Hydrogen sulfide is highly toxic to almost all life forms including human beings.

SRB have previously been considered to be strictly anaerobic microbes. It has been demonstrated that SRB can survive when exposed to oxygen, but they don't grow. Some SRB can even be detected at saturating oxygen concentrations in hypersaline microbial mats (Minz et al., 1999; Risatti et al., 1994). Bade et al. (2000) showed that some extremely oxygen tolerant biofilms are able to stay alive up to 72 days. The pH for SRB growth ranges from 4 to 9.5. Reported extreme examples include that the habitat pH of SRB in acid-mine drainages sites can be as low as two, while the pH can reach 10 in soda lakes (Geets et al., 2006; Sen, 2001). The highest temperature at which special thermophilic species of SRB can grow is approximately 90°C (Stahl et al., 2007; Fukui

and Takii, 1990). The highest pressure that SRB can tolerate is 500 atm (Stott et al., 1988). Little et al. (2000) divided SRB into two groups: heterotrophic bacteria and mixotrophic bacteria.

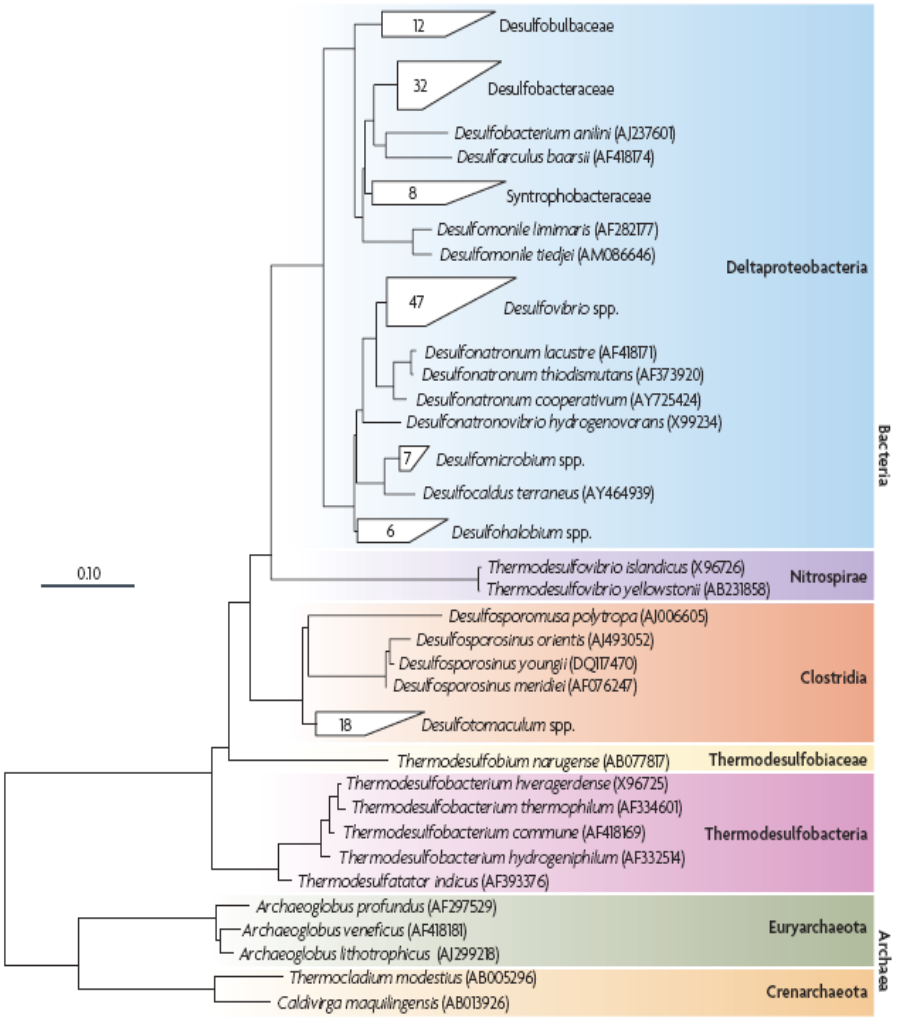

Figure 2-1. Phylogenetic tree describing sulfate reducing bacterial species based on the 16S rRNA identification technology. The scale bar represents 10% sequence difference. (Muyzer and Stams, 2008).

Based on 16S rRNA molecular identification technology, the currently known SRB can be divided into seven groups phylogenetically. Muyzer and Stams (2008) reported, as shown in Figure 2-1, five groups belonged to the bacteria, while the other two groups were archaea.

It is known that various organic carbons such as ethanol, formate, lactate, pyruvate, malate and succinate can be digested for SRB growth. Some SRB incompletely oxidize these organic compounds to acetate, while others completely degrade the organic substrate to CO_2. Various substrates can also serve SRB as electron donors including sugars, amino acids, and one carbon compounds like methanol and CO (Baena et al., 1998; Henstra et al., 2007; Nanninga and Gottschal, 1987; Sass et al., 2002). Several novel SRB strains isolated from marine sediment are capable of oxidizing long-chain fatty acids and aromatic compounds like benzoate and phenol (Muyzer and Stams, 2008).

2.2 Mechanistic study of MIC caused by SRB

Numerous mechanisms have been proposed to explain MIC since the 1900s (Videla and Herrera, 2005). The first pioneering work, is the classical cathodic depolarization theory (CDT), that was proposed by von Wolzogen Kuhr and van der Vlugt (1934). Since then, many other MIC mechanisms have been proposed. However, there is still confusion and limitations that remain unaddressed in published literature due to the complexity of MIC. To investigate MIC, a clear understanding of its mechanisms is needed to guide field operators on how to mitigate and inhibit MIC.

2.2.1 Cathodic depolarization theory

CDT, which is still a prevailing MIC theory due to SRB, was also considered to be the first theory to explain MIC from the aspect of electrochemistry (Videla, 1996; von Wolzogen Kuehr and van der Vlugt, 1934). The following reactions were used to explain SRB corrosion:

Anodic reaction (iron dissolution)	$4Fe \rightarrow 4Fe^{2+} + 8e^-$	2-(1)
Dissociation of water	$8H_2O \rightarrow 8H^+ + 8OH^-$	2-(2)
Cathodic reaction	$8H^+ + 8e^- \rightarrow 8H_{ads}$	2-(3)
Cathodic depolarization by hydrogenase	$8H_{ads} (\rightarrow 4H_2) \rightarrow 8H^+ + 8e^-$	2-(4)
Sulfate reduction by SRB	$SO_4^{2-} + 8H^+ + 8e^- \rightarrow S^{2-} + 4H_2O$	2-(5)
Corrosion product formation	$Fe^{2+} + S^{2-} \rightarrow FeS$	2-(6)
Corrosion product formation	$3Fe^{2+} + 6OH^- \rightarrow 3Fe(OH)_2$	2-(7)
Overall reaction	$4Fe + SO_4^{2-} + 4H_2O \rightarrow 3Fe(OH)_2 + FeS + 2OH^-$	2-(8)

It is necessary to state that HS^- is the dominant species compared with S^{2-} in the bulk solution. Only under the condition of very high pH (e.g., pH=10), $[S^{2-}]$ will become significant.

$$HS^- \leftrightarrows S^{2-} + H^+ \qquad 2\text{-}(9)$$

Under acidic condition, H_2S will be formed through the pathway of reaction 2-(10), which may consume H^+ and then increase the pH in the culture medium (Gu and Xu, 2013).

$$HS^- + H^+ \leftrightarrows H_2S \qquad 2\text{-}(10)$$

"Cathodic polarization" is the process where H atoms adsorb onto the cathode, which can stop the corrosion reaction unless H_{ads} is removed by either of the following reactions:

Chemical desorption $\qquad 2H_{ads} \rightarrow H_2 \qquad 2\text{-}(11)$

Electrochemical desorption $\qquad H_{ads} + H^+ + e^- \rightarrow H_2 \qquad 2\text{-}(12)$

Due to the high activation energies required for the desorption process, these two reactions are regarded as rate-limiting steps. SRB cells secrete hydrogenase, a group of enzymes that catalyze the conversion of H_{ads} by lowering the activation energy, which can convert H_{ads} to H_2 and then to H^+. This process is called cathodic depolarization.

There are several major flaws in the CDT theory. First of all, it neglects the significance of biofilm, which may be the most important surface active catalyst. Secondly, the CDT theory fails to explain the corrosion caused by hydrogenase-negative strains of SRB (Little et al., 2000). Moreover, Thierry and Sand (2002) reported that the H_2S effect to the cathode is not addressed in CDT and the corrosive metabolites produced

by the microbes are also ignored. The “depolarization” term in CDT is not an electrochemical reaction, which only indicates the reactions that happened at the cathode. Gu and Xu (2013) argued that a physical cathode is not a valid concept in this kind MIC. The reduction reactions (often called cathodic reactions in corrosion) actually happen inside SRB cytoplasm rather than on the surface of a physical cathode.

2.2.2 Other MIC mechanisms due to SRB

Since the publication of the CDT theory, as shown in Table 2-1, many mechanisms have been proposed to explain MIC due to SRB. Similar results obtained from different research groups confirm that SRB biofilm is involved in the corrosion process, and abiotic H_2S cannot reach the same aggressivity as the biotic H_2S produced by SRB (McNeil et al., 1991; Thomas et al., 1988). Many review papers published in the past 20 years clearly agree that there may be more than one dominant mechanism to explain MIC due to SRB. A combination of several mechanisms or various factors depending on environmental conditions might also be considered (Beech and Gaylarde, 1999; Hamilton, 1998a; Lee et al., 1995; Kakooei et al., 2012).

Table 2-1. Published mechanisms of MIC due to SRB (Beech and Gaylarde, 1999; Kakooei et al., 2012).

Corrosive process/substance	Reference(s)
Cathodic depolarization by hydrogenase	von Wolzogen Kuhr and van der Vlugt, 1934; Bryant *et al*., 1991.
Anodic depolarization	Salvarezza and Videla, 1986; Daumas *et a*l., 1988; Crolet, 1992.
Sulfide	Little *et al*., 1998.
Iron sulfides	King and Wakerley, 1973.
A volatile phosphorus compound	Iverson and Ohlson, 1983.
Fe-binding exopolymers	Beech and Cheung, 1995.
Sulfide-induced stress Corrosion cracking	Edyvean *et al*., 1998.
Hydrogen-induced cracking or blistering	Edyvean *et al*., 1998.
Three-stage mechanism	Romero, 2005

2.3 The new biocatalytic cathodic sulfate reduction (BCSR) theory

The new BCSR theory proposed by Gu et al. (2009) assumes that MIC due to SRB biofilm takes place in two overall steps: first, the dissolution of anodic iron releases electrons, and then, the electrons are transported to the SRB cells and utilized by sulfate reduction within the cytoplasm of the cells. This is a biocatalytic process. The theory requires a corrosive SRB biofilm on an iron surface which is directly responsible for MIC and causes the BCSR reaction to move forward due to biofilm biocatalysis. All the potential values ($E^{o\prime}$) in this work are under standard conditions of biological systems. $E^{o\prime}$ requires the same conditions as standard conditions that are 25^{o}C, 1 M concentration for solutes and 1 bar partial pressure for gases, the exception is that pH 7 instead of pH 0 is used for H^{+} concentration. More precisely concentrations should be activities. The apostrophe in $E^{o\prime}$ denotes pH 7 and all the potential values in this work use the standard

hydrogen electrode (SHE) as reference. $E^{o\prime}$ is commonly used in bioenergetics research (Thauer et al., 2007). The overall reactions for BCSR are listed as follows:

Anodic reaction: $4Fe \rightarrow 4Fe^{2+} + 8e^-$ $-E^{o\prime} = +447$ mV 2-(13)

Cathodic reaction: $SO_4^{2-} + 9H^+ + 8e^- \rightarrow HS^- + 4H_2O$ $E^{o\prime} = -217$ mV 2-(14)

In the BCSR theory, unlike in conventional corrosion thinking, there is no physical cathode. The cathode itself is the SRB biofilm working as a biocathode (Rosenbaum et al., 2011). The biocathode has already become a widely accepted concept in the MFC field and has been used in some MFC devices (Chen et al., 2008). The real sulfate reduction process in the SRB cytoplasm would be far more complicated than reaction 2-(14), where only the overall effect is considered in the BCSR. Normally, reaction 2-(14) reacts only at a negligible rate and can happen only with biofilm biocatalysis. Sulfate reduction is catalyzed by a complicated biological enzyme system. Reaction 2-(14) can move via the catalysis of the hydrogenase enzyme system in hydrogenase-positive SRB cells by using molecular hydrogen as an electron carrier (Gu and Xu, 2013). The hydrogenase can lower the activation energy and accelerate the reaction rate of the sulfate reduction. In hydrogen-negative SRB systems, other electron transfer methods are used to transport extracellular electrons for sulfate reduction.

2.3.1 Bioenergetics to explain why MIC happens

The BCSR theory provides a better understanding of MIC from a bioenergetics aspect. First, it can clearly explain why microorganisms attack iron. It is well known that SRB utilize sulfate as the terminal electron acceptor in their anaerobic respiration.

Lactate is a favored organic nutrient. The following oxidation reaction presented by Thauer et al. (2007) shows how SRB utilizes lactate:

$$CH_3CHOHCOO^- + H_2O \rightarrow CH_3COO^- + CO_2 + 4H^+ + 4e^- \qquad -E^{o\prime} = +430\ mV \qquad 2\text{-}(15)$$

When reactions 2-(14) and 2-(15) are coupled together with biocatalysis by SRB, this reaction takes place as follows:

$$SO_4^{2-} + 2CH_3CHOHCOO^- \rightarrow 2CH_3COO^- + 2CO_2 + HS^- + OH^- + H_2O \qquad 2\text{-}(16)$$

This redox reaction has a cell potential $\Delta E^{o\prime}$=+213 mV, which leads to $\Delta G^{o\prime}$=−164.4 kJ/mol <0 based on the formula,

$$\Delta G^{o\prime} = -nF\Delta E^{o\prime} \qquad 2\text{-}(17)$$

Reaction 2-(16) describes the anaerobic respiration of SRB, and its Gibbs free energy change of reaction is negative, and the energy is released by the redox reaction. The reaction can move forward spontaneously because it is thermodynamically favorable. In Equation 2-(17), $\Delta G^{o\prime}$ represents the Gibbs free energy change under the conditions defined for $E^{o\prime}$ (Hamilton, 1998b), n the number of electrons, F the Faraday constant, and $\Delta E^{o\prime}$ the cell potential of the redox reaction. A positive $\Delta E^{o\prime}$ value results in a negative $\Delta G^{o\prime}$, indicating an exergonic reaction. A negative $\Delta G^{o\prime}$ also means that the reaction is thermodynamically favorable and can occur spontaneously. However, thermodynamically favorable reactions do not guarantee that the reactions will happen at a significant rate. When lactate and sulfate are mixed together without the addition of

SRB, no noticeable reaction occurs without biocatalysis. Enzymes are required for lactate oxidation and sulfate reduction reactions.

Bioenergetically speaking, the oxidation of 2 mol lactate in Reaction 2-(16) can release 164.4 kJ of energy when 1 mol sulfate is reduced. It has been reported that a $\Delta E^{o'}$ value of +25 mV, equivalent to a Gibbs free energy change of reaction of $\Delta G^{o'}$=20 kJ/mol sulfate is sufficient to support SRB growth (Thauer et al., 2007). Energy is needed for such SRB metabolic activities as material transport, signal amplification and organic synthesis. Even when cells are not growing in the stationary phase, maintenance energy is still needed (Chen and Johns, 1996).

SRB cells do not really "eat" iron. Like most microbes, SRB utilize oxidation of organic carbon to obtain electrons, and carbon building blocks for organic synthesis. From a nutritional point of view, it is not necessary for SRB cells to obtain iron directly from steel because ferrous ions are readily available in the environment either as a nutrient supplied in lab tests or as a corrosion product in pipeline fluids. However, further explanation is necessary to understand why SRB corrode iron.

The most important contribution of BCSR is that, based on bioenergetics, the BCSR can explain why MIC occurs on iron. It is well known that MIC pitting corrosion due to SRB is caused by SRB biofilm. The planktonic SRB perform the so-called anaerobic respiration which utilizes organic carbons such as lactate as the electron donor and sulfate as the electron acceptor. This redox reaction is described as Reaction 2-(16) and takes place in the cytoplasm of SRB cells (Thauer et al., 2007). Planktonic SRB are not directly involved in corrosion, because electrons released by iron cannot "swim" in

water from iron surface to planktonic cells. Normally, organic carbons diffuse into SRB cytoplasm as electron donors. No external electrons are involved. Thus, there is no need for the microbes to attack iron to obtain electrons, and no direct electrochemical MIC will occur.

The morphology of the SRB biofilm on an iron surface is known to be very dense. This may result in a significant mass transfer barrier for the diffusion of organic carbon from the bulk to the iron surface (Gu and Xu, 2010). Typically, the driving force for the diffusion is the concentration gradient. The small driving force may cause insufficient organic carbon transport to the sessile SRB cells deep in the biofilm–especially the layer of SRB cells direct on the iron surface. Another factor that should be considered is that, due to their own metabolic need, the top layer of biofilm may consume the majority of the organic carbon diffused into the biofilm. Even though the concentration difference can offer a driving force large enough to make the organic carbon diffusion occur, after the consumption of the top layer of biofilm, it is still difficult to supply sufficient organic carbon to the sessile cells deep in the biofilm.

Maintenance energy is needed for the survival of the starved sessile SRB cells. In this situation, the starving sessile cells tended to switch from organic carbon oxidation to iron oxidation to supply electrons for sulfate reduction for energy production. This also means that the electron donor changes from organic carbon to iron (Figure 2-2). From the biological standard potential table (Table 2-2), it appears that the reduction potential for Fe^{2+}/Fe (−447 mV) is actually slightly more negative (more energetic) than CO_2+acetate/lactate (−430 mV). This suggests that when iron oxidation is coupled with

sulfate reduction, it can provide slightly more energy than lactate oxidation. Under this condition, the electron offered by iron oxidation is directly utilized by sulfate reduction with the help of biocatalysis. Compared with lactate, iron is insoluble, and cannot directly enter the cytoplasm to donate electrons for the sulfate reduction. This means an electron transport chain must be employed by the SRB to transport the extracellular electrons. Only a fraction of microbes have the ability to perform this kind of electron transport.

2.3.2 Extracellular electron transfer to explain how MIC happens

In BCSR theory, the electron transport chain from iron surface to the cytoplasm is the most important pathway to elucidate how SRB drive the corrosion process. Strong evidence from MFC research suggests that the electron transfer process described in Figure 2-2 does happen. According to Hernandez and Newman (2001), this transport phenomenon is the so-called extracellular electron transfer (EET), which is one of the most fundamental methods for some microbes to generate energy for survival.

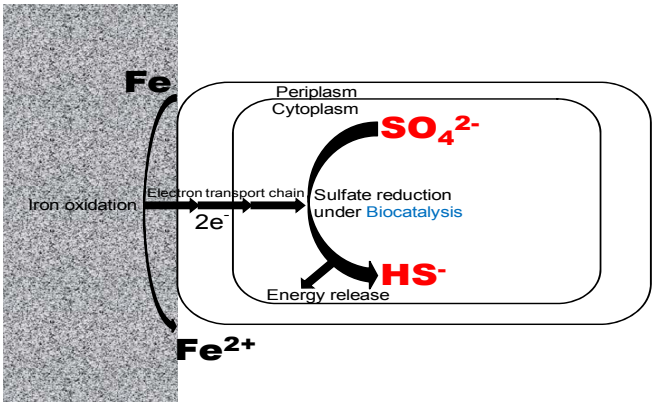

Figure 2-2. Mechanism for MIC by SRB utilization of electrons from iron oxidation for sulfate reduction.

Table 2-2. Standard reduction potentials of redox couples of biological systems at pH=7 (Thauer et al., 2007).

Redox couple	n	$E^{o'}$ (mV)
Fe^{2+}/Fe	2	−447
CO_2+acetate/lactate	4	−430
CO_2/formate	2	−432
$2H^+/H_2$	2	−414
$2CO_2$/acetate	8	−290
$4CO_2$/butyrate	20	−280
CO_2/CH_4	8	−244
SO_4^{2-}/HS^-	8	−217
NO_3^-/NH_3	8	+360
$2NO_3^-/N_2$	10	+760

Based on the MFC work by Du et al. (2007), electrons can be transferred into the cytoplasm through two primary methods: (a) direct electron transfer (DET), and (b) mediated electron transfer (MET). DET relies on special proteins such as c-type cytochrome or pili (also known as nanowires) to transfer electrons. Sessile cells can obtain electrons from direct contact via c-type cytochrome on their cell walls from an electrode surface, and they can also form pili to extract electrons from an electrode surface or iron. Sherar et al. (2011) found direct evidence that starving SRB produced nanowires to capture electron from iron when exposed to modified Postgate medium that

lacked organic carbon. When the culture medium had organic carbon, pili were not observed by them. The utilization of pili to transport electrons from steel to SRB cells as shown in Figure 2-3 is direct evidence to support the BCSR theory and to demonstrate that the SRB cells need electrons in order for sulfate reduction to take place in their cytoplasm.

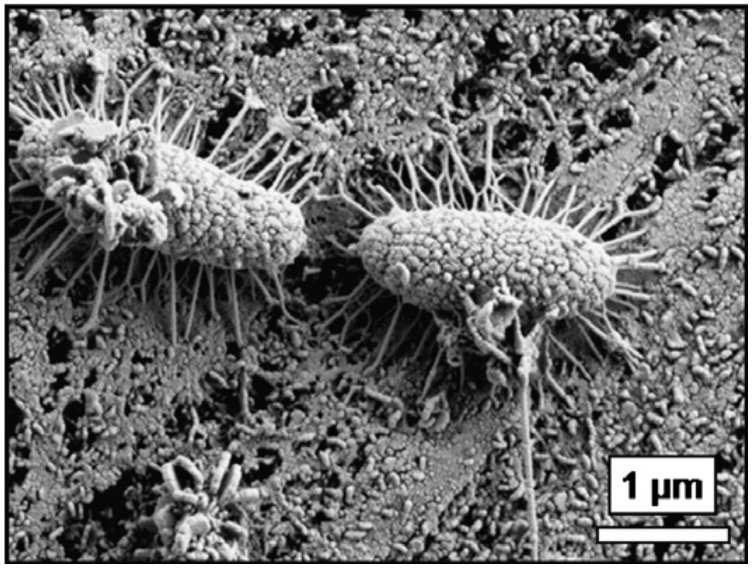

Figure 2-3. Nanowires produced by SRB to capture electrons from iron surface (Sherar et al., 2011).

MET, another pathway of EET, mainly relies on electron mediators to shuttle the electrons between the cells and the iron surface. Electron mediators, also called electron shuttles, are soluble chemicals that can transport the electrons through the cell membrane. FAD and riboflavin are the most common electron shuttles secreted by bacteria in the biological systems. *Shewanella putrefaciens* is a commonly found bacterium in oil and gas fields, and always co-exists with SRB in the same biofilm (Martín-Gil et al., 2004). It

is also reported that electron mediators such as FAD and riboflavin can be secreted by *S. putrefaciens*. These electron shuttles may help SRB to obtain more efficient electron transport resulting in faster corrosion. It is a fact that corrosion is an energy releasing process. In return *S. putrefaciens* can share the energy released by corrosion caused by the SRB. This may help to explain the co-existence of SRB and *S. putrefaciens*, and the so-called synergistic effect of a mixed bacteria biofilm. Normally, fast pitting corrosion does not occur automatically for a biofilm consisting of one strain of bacterium. The schematic illustration as shown in Figure 2-4 clarifies the detail of how DET and MET transfer electrons between electrodes and bacterial cells.

Venzlaff et al. (2013) found electrochemical evidence for direct uptake of electrons from carbon steel by SRB. Figure 2-5 is consistent with Figure 2-4 that explains the role of electron transfer in MIC. Figure 2-5 deliberately skipped detailed electron transfer mechanisms in order to accommodate various mechanisms including the one described in Figure 2-5.

As aforementioned, DET is one of the two main pathways of electron transfer between the cytoplasm of the cells and the external electron donors, which relies on nanowires or membrane bound protein like c-type cytochrome. The c-type cytochrome was confirmed to be an important membrane protein related to electron transfer, which is commonly distributed in the SRB cell membrane (Heidelberg et al., 2004; Semkiw, 2010). Based on the BCSR theory, DET can reasonably be considered to be the major player in the process of direct uptake electron by SRB from iron oxidation. The electrons captured

by cytochrome c are finally transferred into the cytoplasm and taken by the terminal electron acceptor SO_4^{2-} for its reduction.

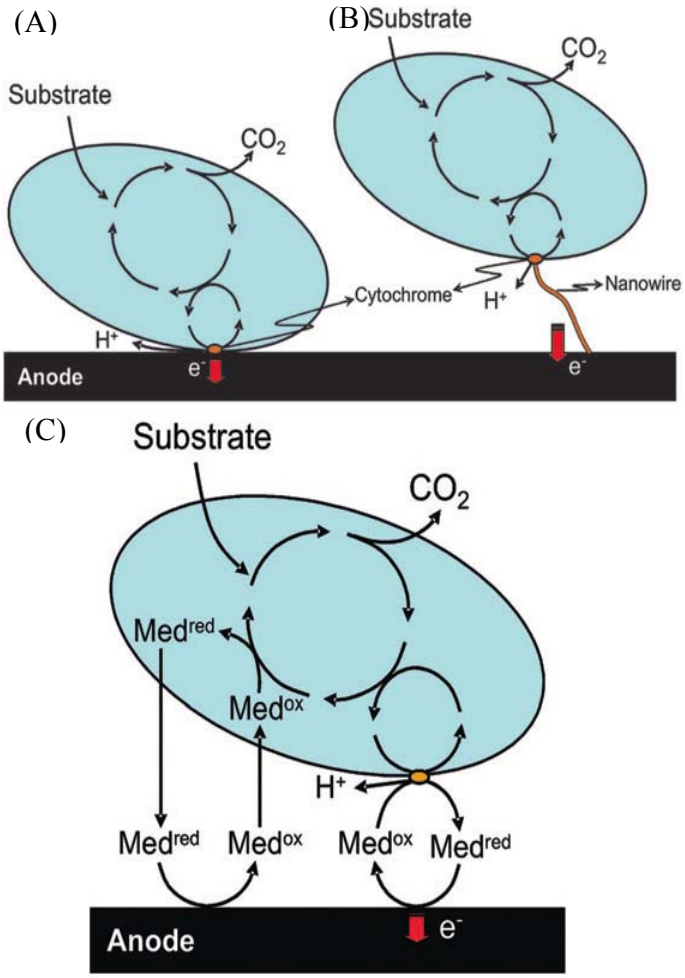

Figure 2-4. Schematic illustration of both DET and MET: (A) direct contact of cytochrome, (B) pili (nanowires), and (C) mediators (Du et al., 2007; Schröder, 2007).

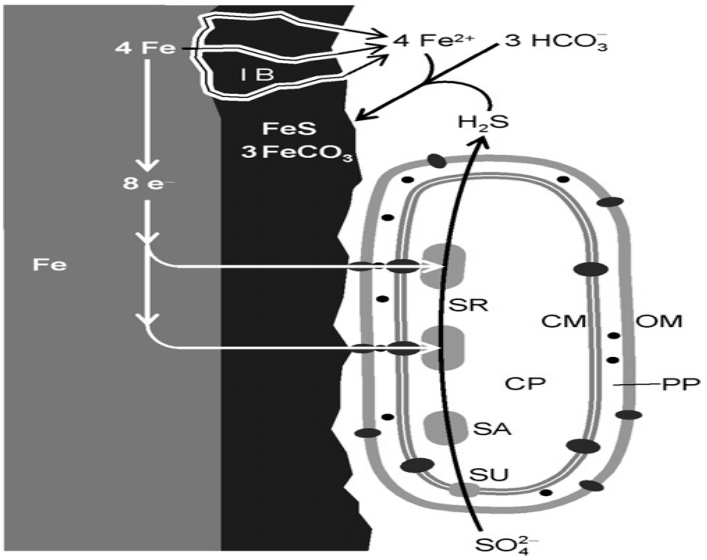

Figure 2-5. MIC due to direct electron uptake by SRB from iron corrosion (Venzlaff et al., 2013).

2.3.3 The thermodynamic verification of BCSR

$E^{o\prime}$ used in BCSR is defined under the conditions of 25°C, pH 7 and 1 M solutes (1 bar gasses). Real conditions may differ; thus, a calculation of ΔG values is necessary to confirm whether the thermodynamics is still favorable. The Nernst equation is used to calculate the equilibrium potential at given conditions. For Fe^{2+}/Fe^{0} and SO_4^{2-}/HS^{-}, Nernst equations lead to the following (Thauer et al., 2007; Pourbaix, 1966):

$$E_e = -0.447\,V + \frac{RT}{2F}\cdot \ln[Fe^{2+}] \qquad 2\text{-}(17)$$

$$E_e = 0.252\,V - \frac{2.591RT}{F}pH + \frac{RT}{8F}\cdot \ln\frac{[SO_4^{2-}]}{[HS^{-}]} \qquad 2\text{-}(18)$$

For instance, SRB are often cultured at 37°C in lab tests rather than the standard condition of 25°C. The actual concentration of ferrous iron may be far smaller than 1 M

underneath the biofilm. When [Fe^{2+}] is equal to 1, 10, 100, and 500 ppm, E_e values are −593, −562, −531, −510 mV at 37°C for Fe^{2+}/Fe^0 from Equation 2-(17), respectively. For SO_4^{2-}/HS^-, the E_e values calculated from Equation 2-(18) are −217 mV and −248 mV, corresponding to $[HS^-]/[SO_4^{2-}]$ values of 0.01 and 100, respectively at 37°C and pH 7. The cell potentials for iron oxidation coupled with sulfate reduction calculated from these E_e values are all positive, leading to negative Gibbs free energy change of reaction (ΔG) values. Thus, the thermodynamic driving force is still there despite the temperature and concentration variations.

Another factor that should be considered is that the pH always shifts toward an acidic direction of SRB medium. Equation 2-(18) indicates that a lower pH value may lead to a higher E_e value. This deviation results in a change of E_e value, but the cell potential difference remains positive; thus, a negative ΔG remains. Stripping of H_2S from SRB culture medium using nitrogen gas in the process of keeping the medium oxygen free as practiced by some researchers may result in a slight pH increase, but this increase is insufficient to change the sign of ΔG.

To summarize, changing conditions are unlikely sufficient to alter the sign of ΔG, except in borderline cases, and the ΔG value is far smaller than zero for iron oxidation coupled with sulfate reduction. This proves that the attack of SRB on iron is almost always thermodynamically favorable.

2.4 Prevention and mitigation of MIC

Due to frequent operations such as hydrotesting, water flooding and wetting, the microbes like SRB, NRB and APB are introduced into the reservoirs resulting in serious

souring and MIC problems. The H_2S produced by microbial sulfate reduction of SRB is often the main source of the H_2S reservoir souring (Korenblum et al., 2010). This condition often occurs during secondary oil recovery and is a serious problem, given that it decreases the quality of the oil and increases the cost of production (Vance and Thrasher, 2005). In addition to souring, SRB biofilms can cause serious MIC in the form of pitting corrosion. This has been considered to be the primary culprit in several pipeline failures (Abedi et al., 2007; Jacobson, 2007). Figure 2-6 depicts the process of water flooding. Another reason dramatically increasing the susceptibility of MIC is the aging infrastructures including many U.S. pipelines. Thus, research of how to prevent and mitigate biofilms in order to alleviate MIC and souring problems is becoming more important for the oil and gas industry.

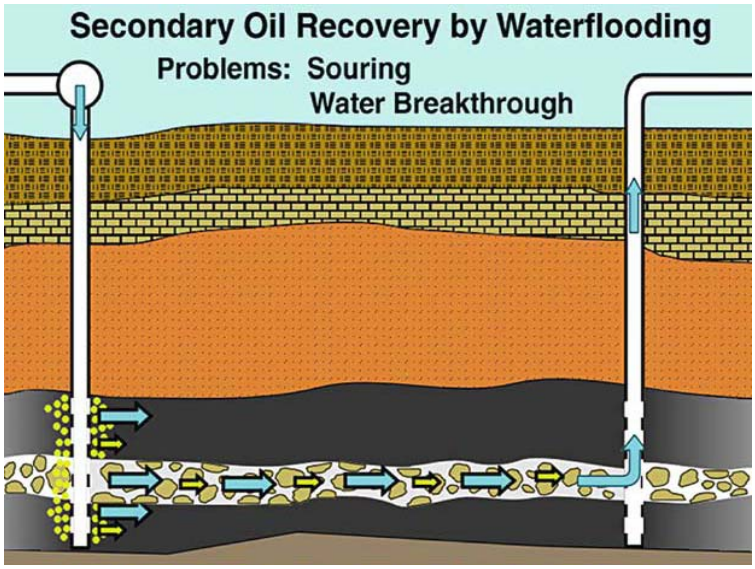

Figure 2-6. Water flooding process that introduces microbes and sulfate into the reservoirs resulting in reservoir souring and MIC downhole in pipelines. Yellow dot stands for sulfate (Costerton, 2007).

2.4.1 Biofilm and its development

A community of microorganisms that can attach itself onto either biotic or abiotic surfaces is a biofilm (Hall-Stoodley et al., 2004). A biofilm can be composed of a single microbial strain, but most biofilms are comprised of multiple synergistic microbial species (O'Toole et al., 2000). The immobilized microbes living in the biofilm matrix are called sessile cells while those living in the bulk solution are called planktonic cells. Sessile and planktonic cells have the same genotypes, but in their phenotypes may differ (Donlan, 2002).

Microbes embed themselves in the extracellular polymeric substances (EPS), a sticky secretion which provides protection against such changing external environmental conditions as pH, fluid shear stress, and antimicrobial agents (Hall-Stoodley et al., 2004; Zuo, 2007). The major components of EPS consist of polysaccharides, proteins, nucleic acids, phospholipids, and humic substances (Jahn and Nielsen, 1998). Based on its adhesive nature and matrix structure, EPS allows the biofilm to thrive in an anaerobic environment. The co-existence of aerobic and anaerobic biofilm is commonly found in nature because both types of biofilm actually benefit from biofilm colonization. Aerobic biofilm can consume all oxygen in the surrounding environment, which provides anaerobic biofilm with a suitable growing condition underneath it.

Biofilms develop in a dynamic 5-stage procedure as described in Figure 2-7. Stage 1 is when the cells initially attached to the surface. Stage 2 indicates that the production of EPS makes cells firmly adhere, which is an irreversible process. Stage 3 describes the early architecture of the biofilm. Stage 4 shows a mature biofilm and Stage

5 is the dispersion of the cells after the biofilm matures, which means that the cells will cycle back to Stage 1 to colonize other places.

2.4.2 Current biofilm mitigation methods

To mitigate biofilms and MIC, pigging (or scrubbing) is one of the effective methods and is commonly used in pipelines to reduce corrosion activity (Carew et al., 2009). It can go through the pipelines and physically scrub off the biofilm and other corrosion deposits (Gieg et al., 2011). More advanced smart pigs equipped with high resolution sensors to detect pitting corrosion are also used to clean pipeline interiors. However, in some complicated designed pipelines, pigs cannot be used. The cost of the pigging and biocide dosing is expensive on top of costly downtime.

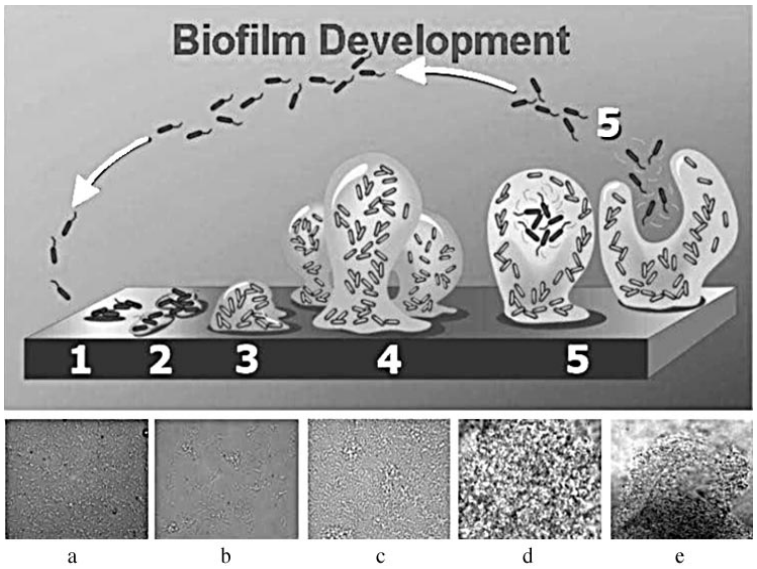

Figure 2-7. Illustration describing the five stages of biofilm development (Stoodley et al. 2002).

Chemical treatments with non-oxidizing biocides are routinely used in oil and gas industry (Videla, 2002). Among them are broad-spectrum biocides like glutaraldehyde, tetrakis (hydroxymethyl) phosphoniumsulfate (THPS), benzalkonium chloride, formaldehyde, and sodium hypochlorite. THPS and glutaraldehyde, which are both biodegradable and have low environmental toxicity, are the most widely used (Gieg et al., 2011; Videla and Herrera, 2005). With increasingly stricter environmental regulations, a high dosage of biocide is undesirable, and large-scale biocide applications in oil and gas pipelines are becoming more costly. Because field systems cannot be kept sterile, repeated or continuous treatments of biocide are necessary in practice to effectively control microbes. This promotes a microbial biocidal resistance problem (Vance and Thrasher, 2005). In some cases, even the combination of two biocides can only temporarily control the microbes. It is reported that sessile cells in a biofilm are much more tenacious than planktonic cells in the bulk fluid (Gardner and Stewart, 2002). To effectively treat a biofilm, a 10 times higher biocide dosage is usually required compared with the dosage needed for treating planktonic cells (Videla, 1996). An extreme case was reported by (Mah and O'Toole, 2001) where 1000 times was required. Based on the instruction of Dow Chemical for its AQUCAR THPS 75 formulation containing 76.5% (w/w) THPS, the recommended dosage for use in the oil and gas industry ranges from 93 to 350 ppm (active) THPS for two to six hours for shock treatment, or 14 to 100 ppm THPS for a continuous treatment (The Dow Chemical Company, 2009). Reduction of cell numbers in log scale is often used to measure the efficacy of the biocide treatment (Keasler et al., 2010; The Dow Chemical Company, 2009).

Biocide enhancers are designed to reduce the biocide dosages while improving their efficacies. Raad et al. (2003) demonstrated that ethylenediaminetetraacetic acid (EDTA), a commonly used chelator, can function as a co-inhibitor to improve the eradication efficacy of antibiotics against biofilms on catheters. Wen et al. (2009 and 2010) confirmed that chelators such as EDTA enhanced the biocide efficacy against planktonic SRB cells, SRB biofilms in lab investigations. The synergetic effect between biocide and biodegraded chelator ethylene diamine disuccinate (EDDS) reduced the planktonic SRB cells and also controlled the biofilm sessile cells. The drawback of this double combination is that a high dosage (often 1000 ppm) of chelators is required.

Ethanol at a concentration of 25% (v/v) significantly improved biofilm removal when it was combined with minocycline and EDTA (Raad et al., 2007). Thus alcohol is a potential candidate for lowering the chelator dosage and increasing the biocide cocktail efficacy against SRB biofilm. Xu et al. (2012) demonstrated that methanol can replace ethanol by using a triple combination of biocide, chelator, and methanol that achieved planktonic SRB cell control, prevention of biofilm establishment, and removal of established biofilm. Methanol is more practical for use in oil field applications because it is a hydrate inhibitor and winterizing agent, which is widely and commonly used in significant quantities in pipelines and oil wells. The shortcomings of this triple combination are that the high concentration of methanol is costly and there is a possibility of a reaction between biocide such as glutaraldehyde and methanol during long term storage and shipping, which is a concern.

2.4.3 D-amino acids as novel biocide enhancers

Amino acids exist normally in nature in the L-form, which is dominant in biological systems. The enantiomeric type of L-amino acids, D-amino acids, were once considered rare and were found only formerly in prokaryotes. Based on novel analytical tools and methods, D-amino acids were found not only in much larger quantities but also in more organisms such as plants and even mammals and humans (Konno et al., 2009). Recently, the existence and secretion of D-amino acids in various organisms has been reported (Cava et al., 2011; Friedman, 2010). D-amino acids such as D-aspartate and D-serine were even found in the central nervous system (CNS) of mammals. In fact, D-serine has been confirmed to be an indicator for some mental disorders (Oliet and Mothet, 2006; Pollegioni and Sacchi, 2010). D-amino acids were also found in some antibiotic peptides (Wade et al., 1990).

Several decades ago, researchers found that high concentrations of D-amino acids were capable of inhibiting bacterial growth. There was no mechanistic explanation for this phenomena until Cava et al. (2011) proposed that the possible mechanism was that D-amino acids may alter peptidoglycan synthesis in the cell wall. Peptidoglycan, a polymer consisting of β(1-4)-linked N-acetylglucosamine(GlcNAc) and N-acetylmuramic acid (MurNAc), is a very vital membrane component in the bacterial cell wall, which plays the key role of maintaining the shape of the cells and resistance to high osmotic pressure and osmotic lysis (Royet and Dziarski, 2007). There are two main types of peptidoglycan shown in Figure 2-8, for Gram-positive and negative bacteria. When meso-diaminopimelic acid (DAP) exists as the third amino acid, it is called DAP-type.

Whereas for some Gram-positive bacteria, L-lysine appears as the third amino acid, it is called Lys-type.

Lam et al. (2009) demonstrated that various bacteria can produce different D-amino acids, which were believed to be key signal molecules in regulating and modifying the cell wall. Kolodkin-Gal et al. (2010) reported that an equimolar mixture of D-tyrosine (D-tyr), D-methionine (D-met), D-tryptophan (D-trp), and D-leucine (D-leu) at a total concentration as low as 10 nM effectively dissembled the biofilm in aerobic cultures of *Bacillus subtilis* in both liquid and solid media. The same D-amino acid mixture also significantly reduced the sessile biofilm cells and biomass of *Pseudomonas aeruginosa* PAO1 biofilm grown in a flow chamber (Sanchez et al., 2012). Xu and Liu (2011) found that D-tyr could inhibit the secretion of EPS, while achieving the mitigation of membrane fouling and dispersal of the attached biofilm. A concentration of 3 mM of D-tyr was capable of effectively preventing the attachment of *Pseudomonas aeruginosa* to the nanofiltration membrane surface, while continuous additions of D-tyr into the membrane feed water successfully controlled the biofouling by dispersing the *P. aeruginosa* biofilm (Yu et al., 2012) .

Researchers have concurred that D-amino acids dissembled the biofilms without inhibiting bacterial growth (Kolodkin-Gal et al., 2010; Yu et al., 2012). The mechanism to explain this discovery was that D-amino acids can work as signal molecules to make the biofilms disperse. These D-amino acids can replace D-alanine (D-ala) terminus (Figure 2-8) in the cell wall resulting in the biofilm disassembling. This process naturally occurs in the peptide side chains of peptidoglycan of bacterial cell walls. D-amino acids

are supposed to make the bacteria adapt to the changing external environment by controlling the cell wall creation, modifying the cell wall assembly and biofilm attachment. The D-amino acids are considered to be potential candidates as biocide enhancers.

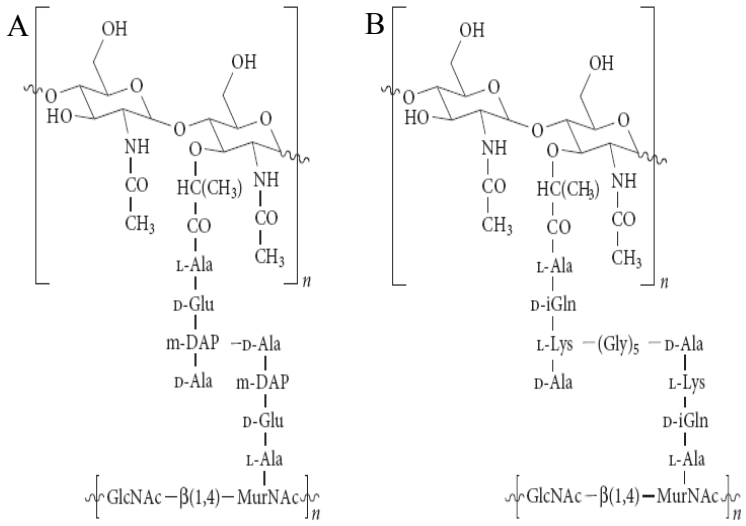

Figure 2-8. Two types of peptidoglycan: (A) DAP type and (B) Lys-type (Royet and Dziarski, 2007).

Researchers have concurred that D-amino acids dissembled the biofilms without inhibiting bacterial growth (Kolodkin-Gal et al., 2010; Yu et al., 2012). The mechanism to explain this discovery was that D-amino acids can work as signal molecules to make the biofilms disperse. These D-amino acids can replace the D-alanine (D-ala) terminus (Figure 2-8) in the cell wall resulting in the biofilm disassembling. This process naturally occurs in the peptide side chains of peptidoglycan of bacterial cell walls. D-amino acids are supposed to make the bacteria adapt to the changing external environment by

controlling the cell wall creation, modifying the cell wall assembly and biofilm attachment. The D-amino acids are considered to be potential candidates as biocide enhancers.

CHAPTER 3 MIC CAUSED BY NITRATE REDUCING BACTERIA

3.1 Introduction

In Chapter 2, the BCSR theory was introduced as the first bioelectrochemical theory to explain why and how MIC occurs. This theory is a foundation that helps researchers better understand MIC.

Anaerobic MIC of elemental iron is the process of iron oxidation coupled with such non-oxygen oxidants as sulfate, nitrate, proton or even CO_2. When the oxidant is sulfate, the electrons released from iron oxidation are captured by SRB. This can be explained by BCSR. The BCSR theory based on bioenergetics also extends to explain other MIC phenomena. If the oxidant is CO_2, based on the reduction potential Table 2-2 shown in Chapter 2, the $E^{o\prime}$ value of CO_2/CH_4 is −244 mV, which yields a positive cell potential (+203 mV) when coupled iron oxidation with Fe^{2+}/Fe (−447 mV). This means the redox reaction is thermodynamically favorable because of its negative $\Delta G^{o\prime}$ value as a result of a positive cell potential. If biocatalysis makes the reaction kinetically fast, the microbe reducing CO_2 to CH_4 may cause MIC. The microbes that are able to reduce CO_2 to CH_4 are methanogens. Solid evidence reported by Uchiyama et al. (2010) showed that a strain of methanogen isolated from an oil tank caused MIC. Gu (2012) lumped this type of MIC into Type I MIC, which is a result of anaerobic respiration utilizing extracellular electrons released by iron oxidation. Externally supplied electron acceptors such as sulfate and CO_2 are involved. Type II MIC is mainly based on anaerobic fermentation in which corrosive metabolites cause MIC. These metabolites do not require biocatalysis to

oxidize iron. For example, abiotic acetic acid corrosion is a well-known problem in the oil and gas industry.

Reservoir souring and MIC caused by SRB have been a serious concern in the oil and gas industry. Biogenic H_2S is not only a highly corrosive agent but is also extremely toxic (Gieg et al., 2011). Nitrate injection has been used routinely in oil and gas fields as a method to mitigate souring caused by SRB. Nitrate injection can effectively promote the growth of NRB to suppress SRB growth. This results in inhibition of biogenic H_2S production by SRB and successful mitigation of souring. Nitrate is also widely used as corrosion inhibitor in oil and gas fields because it can produce a ferric oxide barrier on the steel surface (Karim et al., 2010; Sakashita and Sato, 1977).

Only a few researchers are aware of the fact that NRB could be corrosive due to a lack of understanding of bioenergetics. If the injected nitrate is not fully consumed in the reservoir, NRB and nitrate could end up in the pipelines. It is very likely that NRB may corrode the iron in order to obtain maintenance energy when there is a lack of organic carbon under an NRB biofilm. Nitrate is an electron acceptor that is utilized in anaerobic respiration of NRB. In non-corrosion literature, Ghafari et al. (2008) claimed that iron oxidation coupled with nitrate reduction provides energy for NRB respiration in bioenergetics. Based on the understanding of MIC by SRB, we can reasonably speculate that, like SRB, NRB can cause Type I MIC as well.

Some special SRB strains are capable of utilizing nitrate instead of sulfate when sulfate is not available (Dunsmore et al., 2004; Feio et al., 2000). Unlike MIC caused by SRB, there are only a few published papers related to NRB corrosion (Dunsmore et al.,

2004; Halim et al., 2011). However, these investigators did not study detailed NRB corrosion mechanisms.

3.2 Bioelectrochemical mechanism of MIC caused by NRB

For NRB corrosion, the final electron acceptor is nitrate. In this work, the BCSR theory is extended to BCNR because of the analogy between sulfate reduction and nitrate reduction in which they both happen in the cytoplasm within the cells utilizing extracellular electrons released by iron oxidation. Through the process called biological denitrification, nitrate (or nitrite) can be reduced to N_2 gas (Ghafari et al., 2008). Biological denitrification is a common process that happens in the natural world. Most of the denitrifiers are heterotrophic bacteria, autotrophic denitrifiers have also been reported (Carlson and Ingraham, 1983; Lee et al., 2013). The genes of *nir* (nitrite reductase) and *nos* (nitrous oxide reductase) are required for microbes to perform denitrification (Zumft, 1997). Su et al. (2012) reported another process called Dissimilatory Nitrate Reduction to Ammonium (DNRA) in which it is able to reduce nitrate (or nitrite) to NH_4^+ directly. The DNRA, a less common denitrification pathway, is governed by nrf-genes in the microbes (Mishra et al., 2013). Thus, it is reasonable to speculate that N_2 and NH_4^+ may both be the products of nitrate reduction in an NRB culture as shown in the reactions below (Bard et al., 1985),

$$2NO_3^- + 10e^- + 12H^+ \rightarrow N_2 + 6H_2O \qquad 3\text{-}(1)$$

$$E_e = 1.246\ \text{V} - \frac{2.764RT}{F}\text{pH} + \frac{RT}{10F}\cdot\ln\frac{[NO_3^-]^2}{p_{N_2}} \qquad 3\text{-}(2)$$

$$NO_3^- + 8e^- + 10H^+ \rightarrow NH_4^+ + 3H_2O \qquad 3\text{-}(3)$$

$$E_e = 0.875\,V - \frac{2.879RT}{F}pH + \frac{RT}{8F}\cdot \ln\frac{[NO_3^-]}{[NH_4^+]} \qquad 3\text{-}(4)$$

In Equation 3-(2), p_{N_2} stands for the partial pressure of N_2 gas (in bar). At 25°C, pH 7 and 1 M solutes (1 bar gasses), the $E^{o\prime}$ values of $2NO_3^-/N_2$ and NO_3^-/NH_4^+ are equal to +749 mV and +358 mV, respectively. As introduced in Section 2.3.3, $E^{o\prime}$=−447 mV for Fe^{2+}/Fe^0, which means that when iron oxidation is coupled with either of the nitrate reduction reactions, it will yield a positive $\Delta E^{o\prime}$ value of +1196 mV for biological denitrification or +805 mV for DNRA. The cell potential difference of +1196 mV corresponds to $\Delta G^{o\prime}$=−577 kJ/mol nitrate, while +805 mV yields $\Delta G^{o\prime}$=−621 kJ/mol nitrate. Both of these reactions are highly favorable thermodynamically. With the help NRB biofilm catalysis, either of these two reactions, coupled with iron oxidation, can react at a considerable rate; thus, it is not surprising that NRB can attack carbon steel and cause MIC.

Figure 3-1 describes the MIC process wherein extracellular electrons released from iron oxidation are transferred into the NRB cytoplasm for nitrate reduction under biocatalysis. In non-corrosion literature, it is well known that Fe^0 can serve as the sole energy source for NRB (Biswas and Bose, 2005; Ghafari et al., 2008; Ginner et al., 2004).

Bacillus licheniformis is an anaerobe capable of respiring nitrate (Nijburg et al., 1998). It is also a facultative bacterium when no external electron acceptor is present. It is a common microbe that is omnipresent in the oil field biofilm consortia (López et al.,

2006). There has been no report of *B. licheniformis* as a corrosive microbe. Certain *B. licheniformis* strains have been investigated for corrosion inhibition due to the protective biopolymers they secrete (Örnek et al., 2002). In this study, we will investigate the MIC caused by *B. licheniformis* as an NRB.

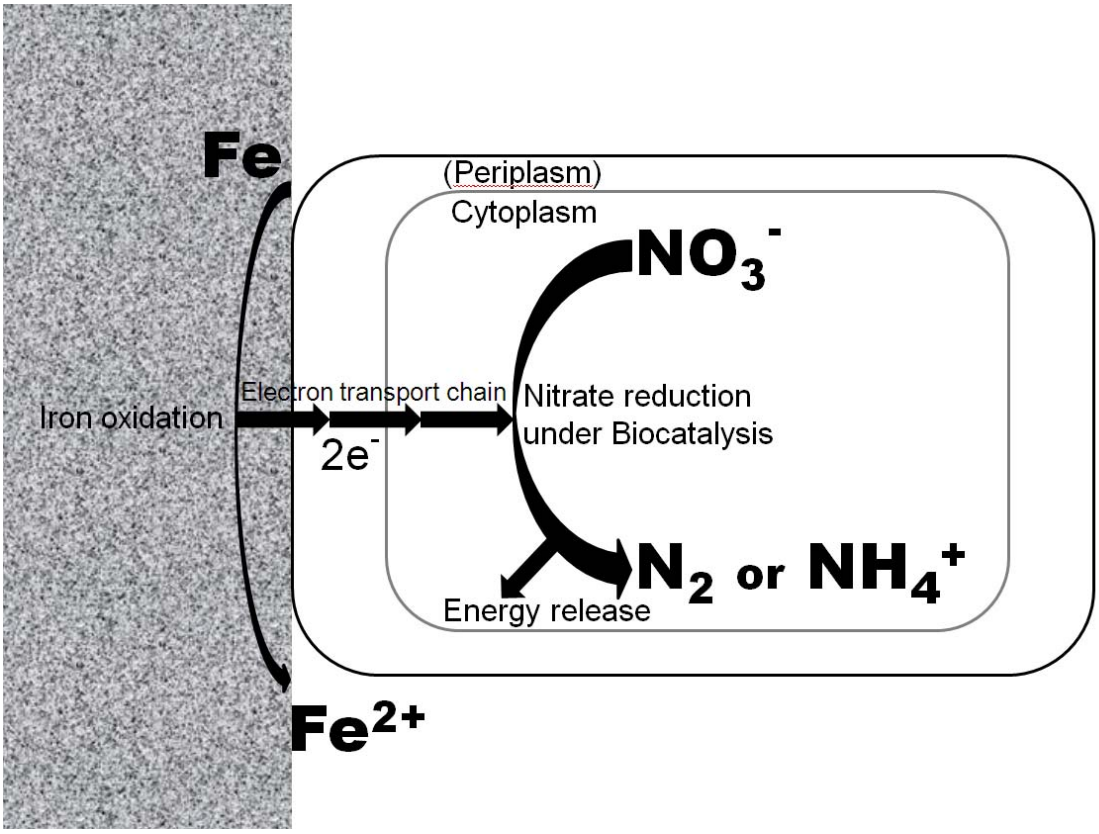

Figure 3-1. Schematic illustration of MIC mechanism due to NRB utilization of extracellular electrons for nitrate reduction.

3.3 Material and methods

3.3.1 Bacterium, culture medium and chemicals

In this work, a pure *B. licheniformis* strain (ATCC 14580, American Type Culture Collection, Manassas, Virginia) was used. The NRB culture medium contained the following components (concentration in g/L): sucrose (10), dibasic potassium phosphate (13.9), monobasic potassium phosphate (2.7), sodium chloride (1), yeast extract (1), sodium nitrate (1), and magnesium sulfate (0.25). Ten milliliters of a trace element stock solution was added to each liter of the culture medium. The stock solution contained (concentrations in mg/L): $MnCl_2 \cdot 4H_2O$ (18), $CoCl_2 \cdot 6H_2O$ (27), H_3BO_3 (5), $CuCl_2 \cdot 2H_2O$ (2.4), $NaMoO_4 \cdot 2H_2O$ (2.3), $ZnCl_2$ (1.9). The medium was modified based on Folmsbee et al. (2006) and sodium nitrate was the sole electron acceptor in the culture medium. The culture medium was autoclaved and then deoxygenated for more than 45 minutes using filter-sterilized N_2 sparging before inoculation.

3.3.2 Substratum for biofilm growth

Coin-shaped C1018 (UNS G10180) carbon steel coupons were used in this test. The composition of C1018 carbon steel was (wt%): C 0.14-0.20, Mn 0.60-0.90, P 0.04, S 0.05, Si 0.15-0.30, and Fe 98.81-99.26. The coupons were abraded with 200, 400 and 600 grit abrasive papers sequentially. Only the top surface of the coupon with a surface area of approximately 1.12 cm^2 was exposed to the culture medium while the other surfaces were coated with an inert Teflon paint. Isopropanol was used to dry and sterilize the coupon surface, which were then air dried under UV light for 15 min before use.

3.3.3 Biofilm culture and corrosion testing

Corrosion coupons were inserted into 125 ml anaerobic vials, in which there were three duplicate coupons with the top surfaces facing upside. Cysteine at a concentration of 100 ppm (w/w) was used as an oxygen scavenger to avoid accidental oxygen leaks. All the manipulations were operated in an anaerobic chamber filled with N_2. A 3-day old *B. licheniformis* was used as seed, and 1 ml of the inoculum was transferred to each vial. After the vials were sealed, they were incubated at 37^{o}C for either 3 or 7 days before the coupons were removed for analysis. The initial cell concentration in each vial immediately after inoculation was approximately 2×10^6 cells/ml, measured using a hemocytometer under a light microscope at 400X magnification.

3.3.4 Coupon surface analysis

A SEM (Scanning Electron Microscope, Model JSM-6390, JEOL, Japan) was used to observe the *B. licheniformis* biofilm on the coupon surfaces. The preparation procedure for biofilm observation by Wen et al. (2009) was followed. In order to study the pitting corrosion morphology underneath biofilms, the coupons were cleaned using Clark's solution (ASTM G1-90 solution for corrosion specimen preparation) to remove the corrosion products on the coupon surface. IFM (Infinite Focus Microscopy, Model ALC13, ALICONA, Austria) was used to measure the pit depth. An X-Ray Diffraction (XRD) analysis was then performed on a X-ray diffractometer (Rigaku Ultimia IV, Rigaku, Japan) with monochromatic Cu Kα radiation (λ=0.15405 nm) at a scanning rate of 2^{o}/min. The coupons for XRD analysis were rinsed with a graded series (25%, 50%, 75%, 100% v/v) of ethanol to dehydrate them before air-drying.

3.4 Results

Figure 3-2 shows that only mineral deposits appeared on the abotic control taken from the culture medium after 7 days. No sessile cells were detected, indicating that there was no microbial contamination. Figure 3-3 describes the morphology of the *B. licheniformis* biofilm grown on the carbon steel coupon surface. The rod-shaped sessile cells can be clearly seen after the 7-day incubation in the inoculated culture medium. The corrosion products and biofilm on the coupon surface were removed using the Clark's solution. Figure 3-4A demonstrates the pitting corrosion caused by *B. licheniformis* biofilm after 7-day incubation. The largest pit reached 15 μm in surface diameter. Figure 3-4B shows that the abiotic control sample in the identical culture medium was not visibly corroded indicating that the culture medium itself was not corrosive under anaerobic conditions.

The normalized weight losses caused by *B. licheniformis* at 37^{o}C after 3 and 7 days are shown in Figure 3-5A. The average normalized weight losses were 0.24±0.1 mg/cm^2 for 3-day samples and 0.89±0.25 mg/cm^2 for 7-day samples. In comparison, the weight loss of the abiotic control coupon after 7 days in the culture medium was only 0.05 mg/cm^2. This was consistent with Figure 3-4B where the polishing line is clearly visible. As shown in Figure 3-5B, the general corrosion rate of *B. licheniformis* biofilm after 3 days was 0.037 mm/year, while it increased to 0.059 mm/year after 7 days.

Figures 3-6A and 3-6B show the profiles for the deepest pits obtained by IFM after 3 days and 7 days, which were 13.5 μm and 14.5 μm, respectively. The largest pit depth obtained in this work was significantly larger than the pit depths caused by SRB

biofilm produced in our lab, which was usually approximately 10 μm for a 7-day test with the same carbon steel coupon. The largest pit depth of carbon steel caused by SRB reported in the literature was usually not greater than 10 μm (Chan et al., 2002; Xu and Gu, 2011; Xu et al., 1999). Thus, *B. licheniformis* in the laboratory MIC pitting corrosion test was more corrosive than typical SRB under strict anaerobic condition against carbon steel. Assuming that the pitting corrosion rate remained unchanged in the vertical direction, pitting corrosion rates of a worst-case scenario were 1.64 mm/year and 0.76 mm/year based on the largest pit depth caused by the *B. licheniformis* biofilm after 3 days and 7 days, respectively. These values were considerably larger than the general corrosion rate calculated from weight loss. It is well known MIC causes pitting corrosion rather than uniform corrosion. Pitting corrosion rate over 1 mm/year will definitely attract attentions from researchers and engineers in the oil and gas industry, serving as a warning that neglect of MIC caused by NRB could cause serious pipeline integrity problems.

The corrosion products on the coupon surface caused by the *B. licheniformis* biofilm after 7 days were examined and analyzed under XRD. As shown in Figure 3-7, the major corrosion products were ammonium iron sulfate and iron nitride. Iron nitride may consist of FeN, Fe_3N, and Fe_4N based on the XRD analysis. When K^+ cation as catalyst is available in the culture medium, it can catalyze the reduction of N_2 to nitride, which can react with iron, forming iron nitride (Rodriguez et al., 2011). Based on the presence of the iron nitride complex, it can be confirmed that Reaction 3-(1) is at least one of the possible pathways by which nitrate is reduced.

The bulk pH of the culture medium and the surface pH on the coupon surface were measured with a flat-tip pH meter. The electrode of the pH meter was firmly attached onto the coupon surface until a stable reading was obtained when measuring the surface pH of the coupon. As shown in Figure 3-8, after 3-day and 7-day incubation, both the bulk pH in the culture medium and the surface pH on the coupon surface had decreased slightly–0.5 unit, from initial neutral pH to approximately 6.5. *B. licheniformis* is known as a strain of APB that is capable of producing lactic acid under fermentation conditions (Sakai and Yamanami, 2006; Wang et al., 2011), but the existence of the nitride complex indicates that the acidity produced by *B. licheniformis* was not aggressive because the nitride complex could be dissolved at a more acidic pH (Rodriguez et al., 2011). This is consistent with pH values shown in Figure 3-8, which are only slightly lower neutral pH. It should be noted that the pH meter can only estimate the surface pH because the true pH underneath a biofilm may differ. Micro-electrode or color-changing nanoparticles may be deployed to sense pH more accurately.

The presence of nitride complexes also confirmed that the corrosion caused by *B. licheniformis* was mainly Type I MIC due to iron oxidation coupled with nitrate reduction, because the metabolites of *B. licheniformis* were not aggressive enough to cause Type II MIC corrosion under the experimental condition. The DNRA process was also adopted by *B. licheniformis* in the culture medium because of the presence of ammonium iron sulfate, which indicated that at least part of the reduced nitrate went through the DNRA process and, when reduced, formed ammonium by *B. licheniformis*.

This finding was consistent with López et al. (2006) who found that *B. licheniformis* was able to directly reduce nitrate to ammonium.

3.5 Discussion

The biocatalysis of *B. licheniformis* plays a key role in the whole corrosion process; the c-type cytochrome cell membrane protein may be the major player in extracellular electron transfer. Membrane bound c-type cytochrome exists in the *B. licheniformis* cell wall (Woolley, 1987). In recent MFC research, c-type cytochrome has been proven to be the vital protein in the extracellular electron transfer. It was also found that c-type cytochrome can help the biofilm uptake electrons from the cathode through direct contact with the electrode surface (Inoue et al., 2010; Nevin et al., 2009). In this study, it is reasonable to speculate that c-type cytochrome in the *B. licheniformis* cell wall helped the transport of electrons from iron dissolution to the cytoplasm inside the cell wall.

As in the aforementioned discussion of BCSR, the parameters such as temperature, chemical concentration or pressures can change significantly from standard conditions; thus, making the actual ΔG value differ from $\Delta G^{o\prime}$. But the sign of ΔG remains the same. A similar scenario occurred in this study when *B. licheniformis* attacked iron. The test temperature and pH were set at 37^{o}C and 7, respectively. For iron oxidation coupled with nitrate reduction to N_2 gas, if it was assumed that the actual $[Fe^{2+}]$ under the *B. licheniformis* biofilm was 100 ppm (1.8×10^{-3} M), the $[NO_3^-]$ was 0.01 M and the partial pressure for N_2 was 1 bar. The cell potential difference ΔE shifted from +1196 mV (under the conditions defined for $E^{o\prime}$) to +717 mV, indicating that the ΔG was very

negative and could still provide a sufficiently large thermodynamic driving force to make the reaction spontaneously move forward. The same trend could also be argued when iron oxidation coupled with nitrate reduction to NH_4^+.

Abiotic nitrate reduction was able to occur spontaneously when coupled with iron. However, the reaction was extremely slow even when iron powders were used to increase the surface area and improve the kinetics of the reaction (Ghafari et al., 2008). Without the help of biocatalysis, nitrate reduction reaction rate was negligible. In this study, the coupon surface area was approximately 0.6 cm^2/g, which was several orders of magnitude smaller than the surface area of iron powders which went up to 2 m^2/g (Till et al., 1998). The weight loss of the abiotic control coupon in both the 3 day and 7 day test in this work were negligibly small, which means that it was a kinetically slow reaction. This is consistent with the literature. All of the above helps to confirm that biocatalysis by the *B. licheniformis* biofilm was needed for aggressive MIC pitting corrosion.

3.6 Summary

(1) *B. licheniformis* was able to cause severe anaerobic MIC pitting against C1018 carbon steel as a nitrate reducer.

(2) The proposed thermodynamics of MIC by NRB was verified and supported by analysis of the corrosion products.

(3) The BCNR mechanism was able to fully explain the MIC caused by *B. licheniformis* from the aspect of bioenergetics.

(4) The pitting corrosion caused by *B. licheniformis* was more aggressive than typical SRB reported in MIC lab investigations under strict anaerobic conditions.

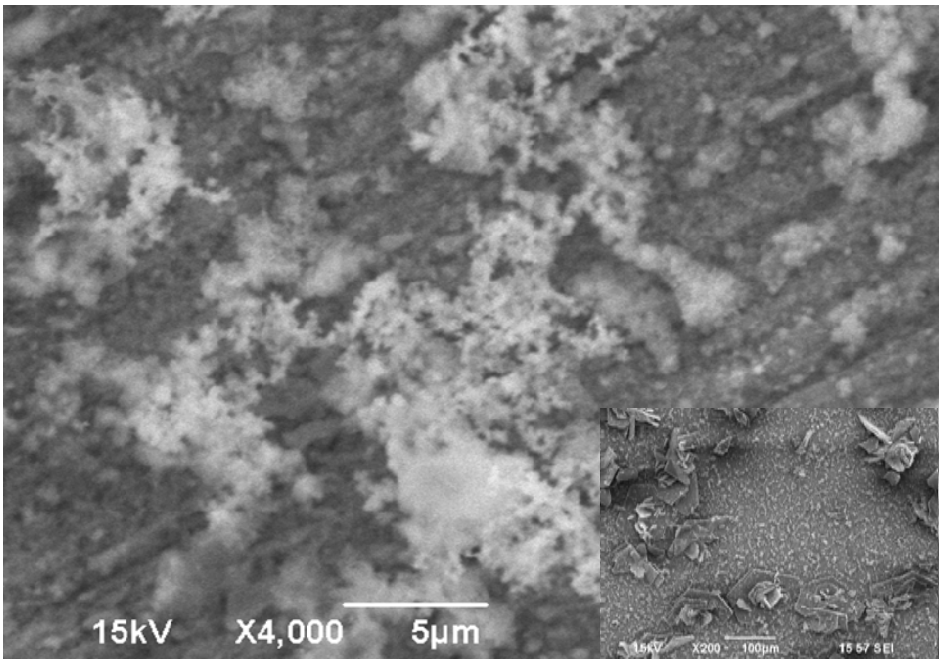

Figure 3-2. SEM image for a control coupon taken from culture medium after 7 days.

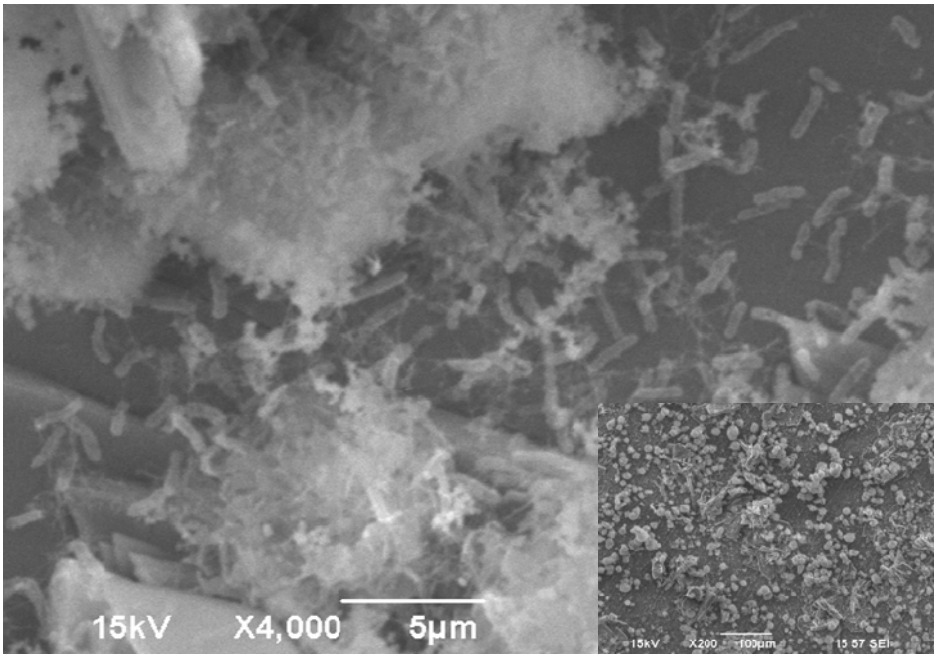

Figure 3-3. SEM image for a *B. licheniformis* biofilm on a coupon taken from a 37^{o}C *B. licheniformis* culture after 7 days.

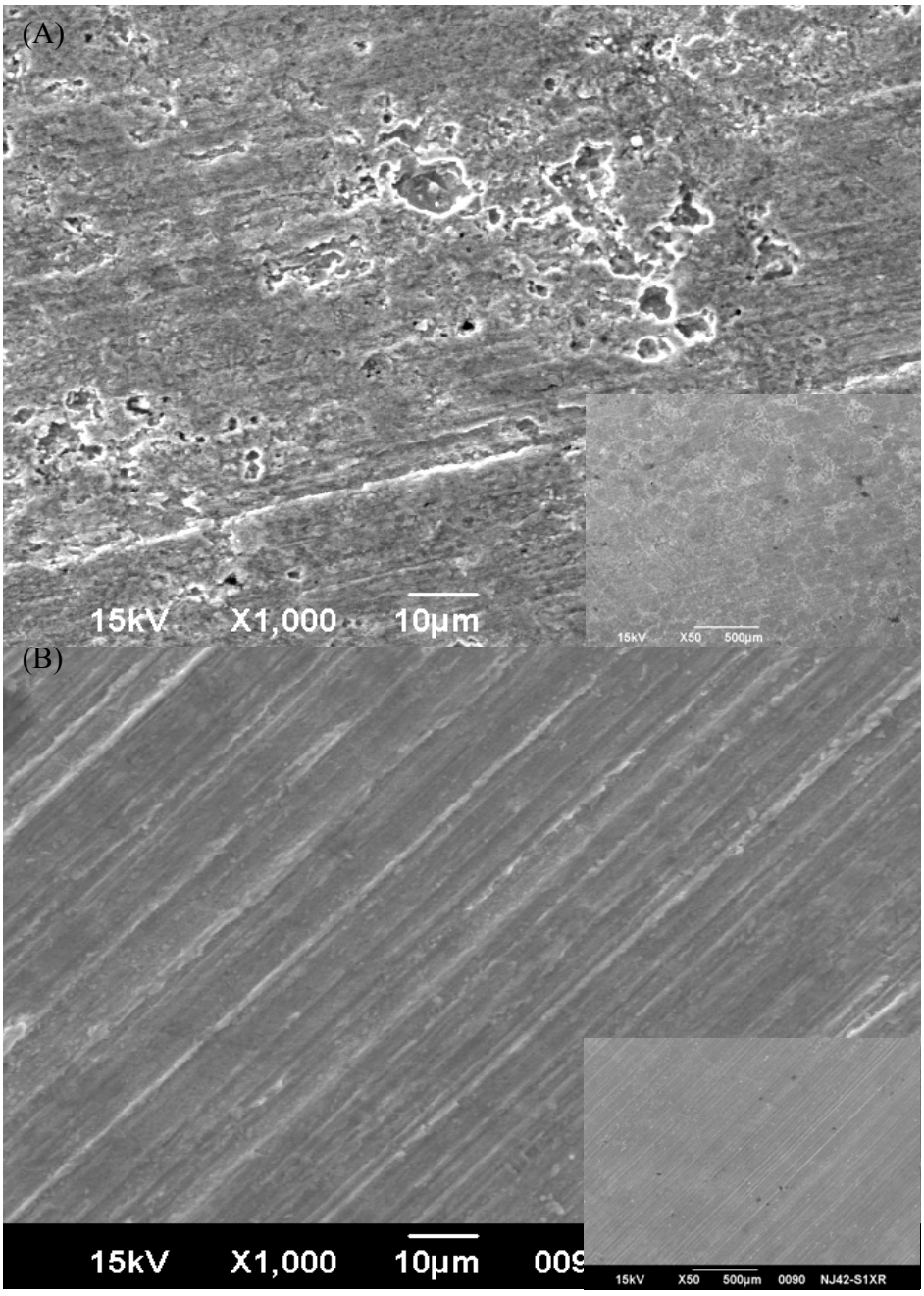

Figure 3-4. (A) SEM image of pitting corrosion on a C1018 coupon taken from a *B. licheniformis* culture at 37 ^{o}C after 7 days. (B) Control coupon without bacterium at 37^{o}C after 7 days. (The scale bars in the inserted images are 500 µm.)

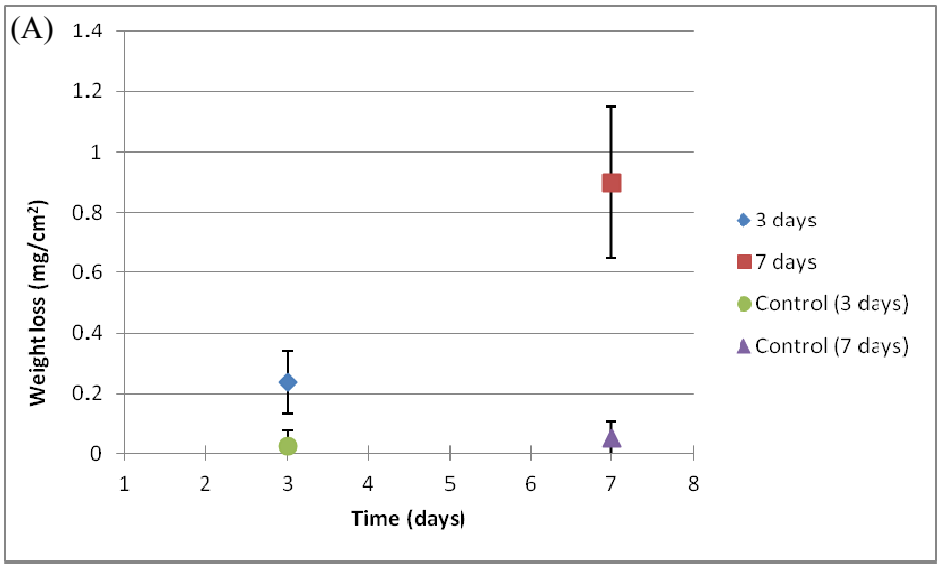

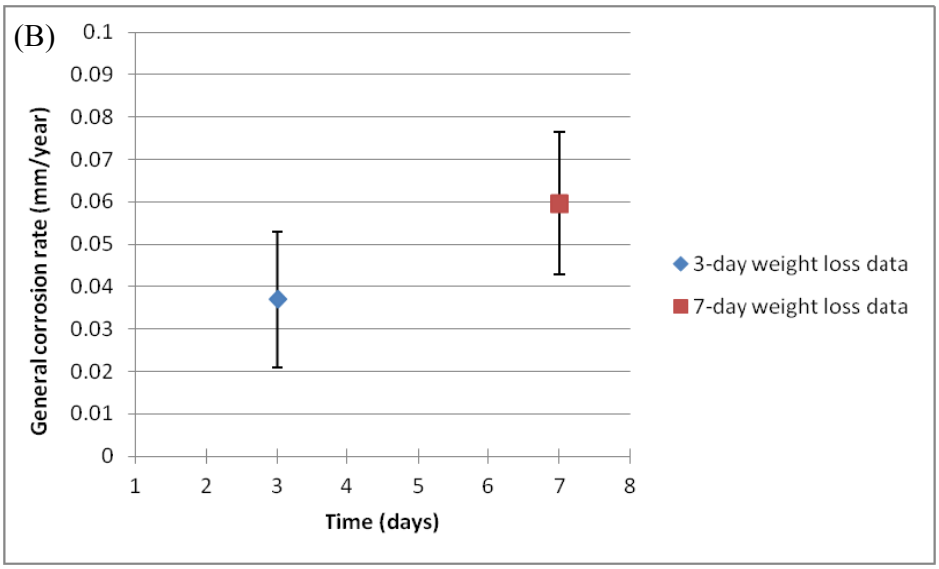

Figure 3-5. (A) Normalized weight loss data for coupons taken from 37°C *B. licheniformis* cultures after 3 and 7 days. Each data point was the average from 10 coupons (5 coupons for each abiotic control data point), and error bars represent standard deviations. (B) General corrosion rate data are converted from the weight loss.

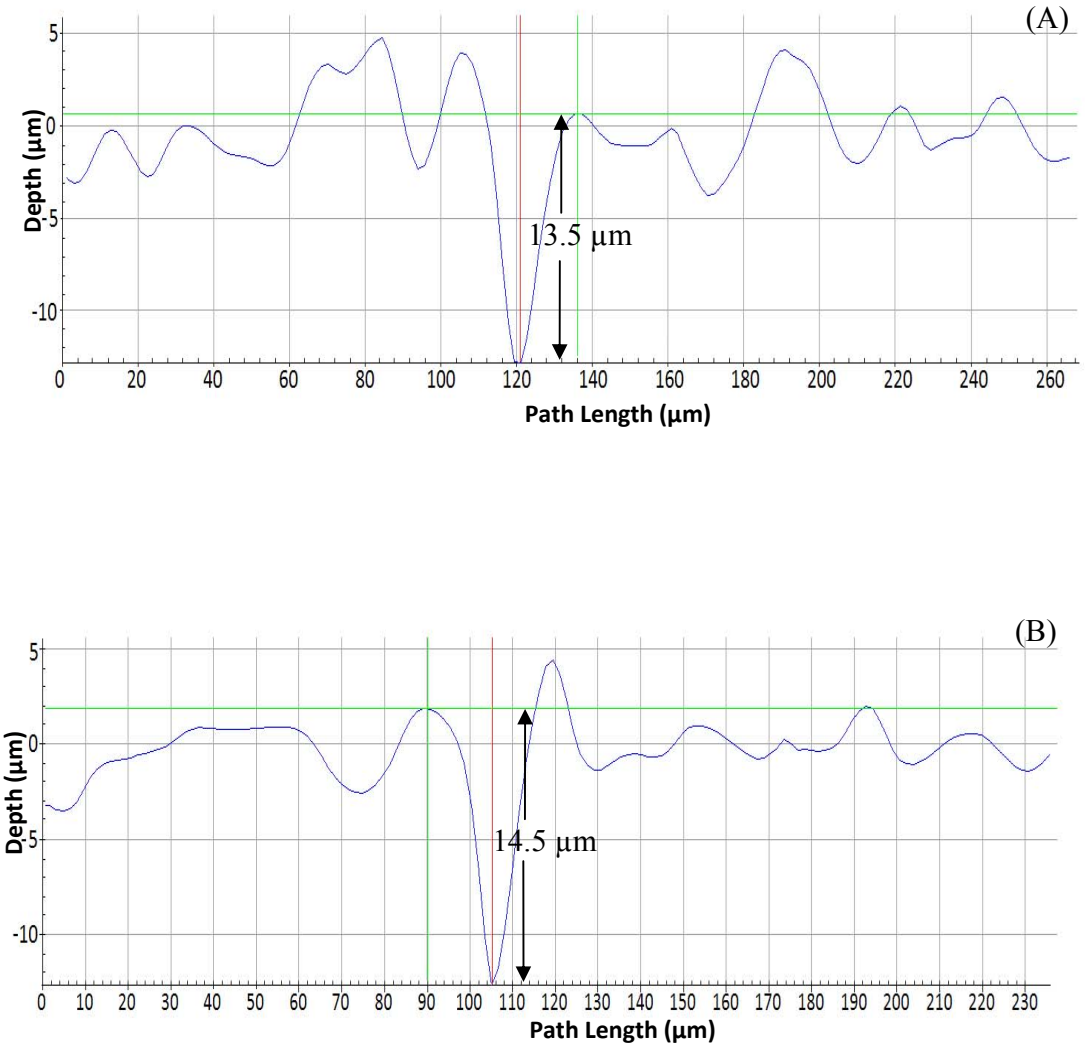

Figure 3-6. (A) Largest pit depth found in the 37°C culture medium after 3 days was 13.5 µm. (B) Largest pit depth found in the 37°C culture medium after 7 days was 14.5 µm.

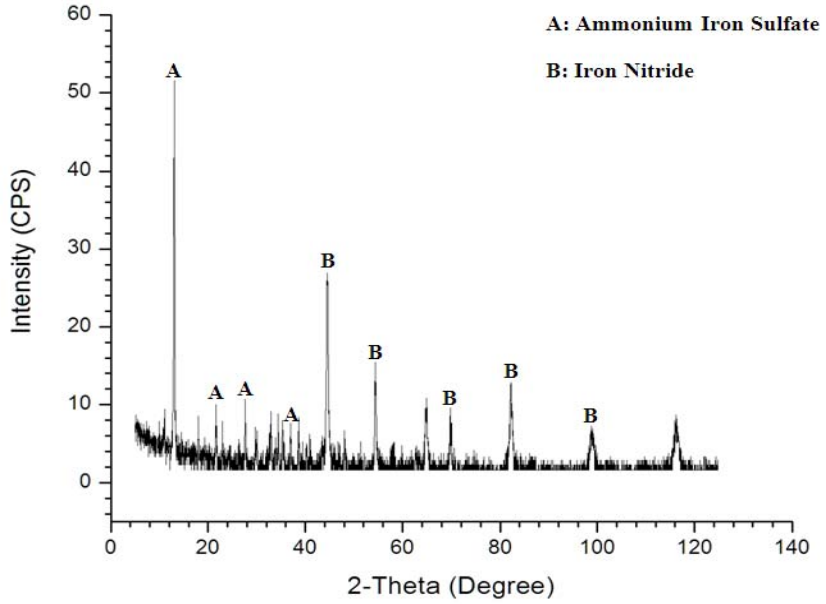

Figure 3-7. X-ray diffraction patterns of the corrosion products on the C1018 coupon surface in the 37°C culture medium after 7 days.

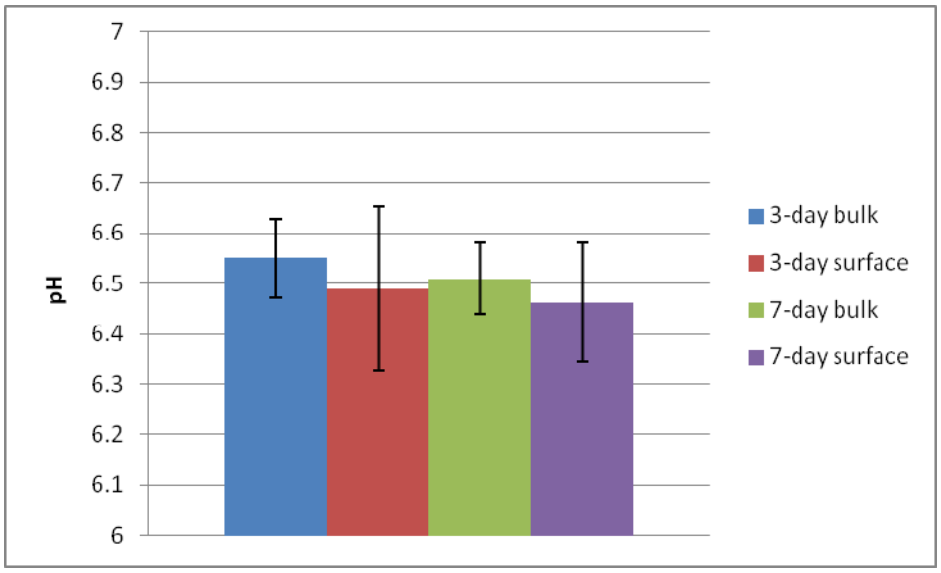

Figure 3-8. Bulk pH in the culture medium and the surface pH on the coupon surface after 3-day and 7 day incubation. (Error bars represent standard deviations.)

CHAPTER 4 ELECTRON MEDIATOR STUDY TO SUPPORT BCSR

As discussed in Chapter 2, the extracellular electron transfer (EET) is an essential concept in MFC research. EET has been further developed in recent years. Based on the BCSR mechanism, it can be argued that EET was a critical concept in Type I MIC research because it can be used to explain electron transfer between the cells and the iron, which is a key step for clarifying how MIC happens. It could also be the most important connection among corrosion, microbiology, and bioelectrochemistry.

4.1 Connections between MFCs and MIC

Since the 1970s, an energy crisis has been triggered by overuse and rapidly escalating demand for oil and gas. The skyrocketing rate of usage of fossil fuels including oil has resulted in a serious global warming problem. The development of the global economy has also been greatly hampered by a serious global energy shortage. Many researchers are seeking a source of electricity produced by renewable resources that do not emit greenhouse gas such as CO_2.

To supplement the conventional energy sources and alleviate global warming, renewable energy such as bioenergy is considered to be one of the alternative methods (Davis and Higson, 2007; Lovley, 2006). The utilization of MFCs is an emerging technology which can convert chemical energy stored in organic/inorganic matters to electrical energy through the catalysis of microbial biofilm (Du et al., 2007; Zhou et al., 2013). The most attractive and valuable merit of MFC technology is that it can digest low-grade organic matters and even wastewater while generating electricity, during which the organic pollutants are treated; thus, producing the green bioelectricity.

Figure 4-1 shows a classical two-chamber MFC design. The electrons released through the oxidation of organic carbon (glucose) by bacteria under anaerobic conditions were transferred to the anode through direct contact with proteins like c-type cytochromes, pili (nanowires) or electron mediators. The protons produced in this process move through the membrane (usually a proton exchange membrane) to the cathode. The electrons pass through the external resistor and used for the reaction of protons with oxygen (air cathode). Carbon materials like graphite, graphite granules, graphite felt, carbon cloth, and carbon paper are often the materials of choice for anodes/cathodes. Pt or Pt black is also used, but are limited to lab tests due to their high costs. With a better understanding of the mechanism of extracellular electron transfer, a biocathode was used in recent MFC research to replace the conventional air cathode (Cournet et al., 2010; Rosenbaum et al., 2011).

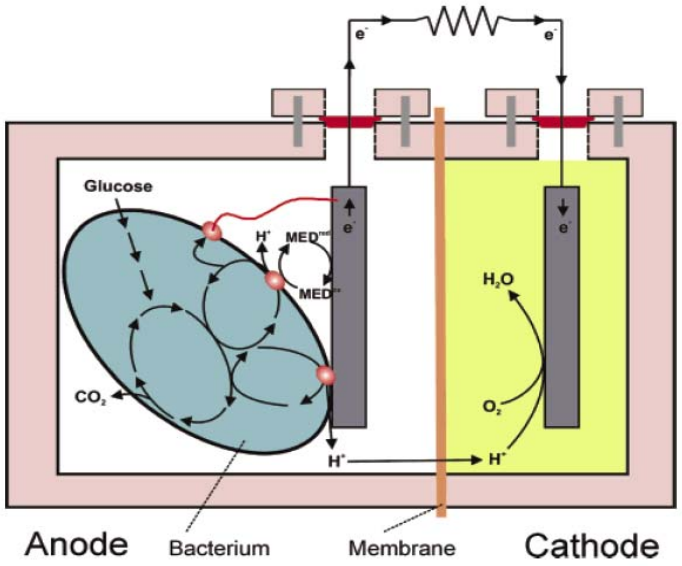

Figure 4-1. Classic two-chamber MFC design with air cathode (Logan et al., 2006).

It is well known that only small amounts of microorganisms called electrogenic microbes can obtain electrons from external sources or transfer electrons to the external electron acceptors like the electrodes. However, most of the microbes are not electrochemically active. As mentioned in Chapter 2, there are mainly two extracellular electron transport methods related to electron transport between the biofilm and electrodes, namely direct electron transport (DET) and mediated electron transport (MET). For DET, direct contact of the bacteria through cytochrome protein or formation of pili (nanowires) is required; while for MET, mediators that can transfer electrons through cytoplasm to the electrode surface are needed (Du et al., 2007; Schröder, 2007).

One of the most pivotal steps in MFC research that can improve the power output of MFC devices, the EET process, was intensively investigated by many researchers, leading to further understanding of MET and DET. All these achievements in EET have actually assisted Ohio University MIC Group to better understand MIC.

Biocathodes are sometimes used in MFC research due to its high catalytic ability and low cost. Biocathodes are different from the conventional cathodes such as Pt cathode for oxygen reduction, where the reduction reaction of the electron acceptors happens within the cytoplasm of the cells in the biofilm. As shown in Figure 4-2A, both DET and MET are adopted by the bacteria to obtain electrons from the electrodes (Castelle et al., 2008; He and Angenent, 2006). As a comparison, the proposed electron transfer pathway in BCSR is depicted in Figure 4-2B. The direction and methods that bacteria use to transfer electrons are identical; the only difference in the two processes being the electron donor. The electrons of biocathodes in the MFC are supplied by the

oxidation of organic matters in the anode, and then transferred through the external wiring to the biocathode. For BCSR, the electron supply is from the electrons released from iron corrosion directly underneath the biofilm. Thus, it is rational to speculate that the methods that can improve the efficiency of EET process of the MFCs could be used to accelerate Type I MIC by SRB or NRB.

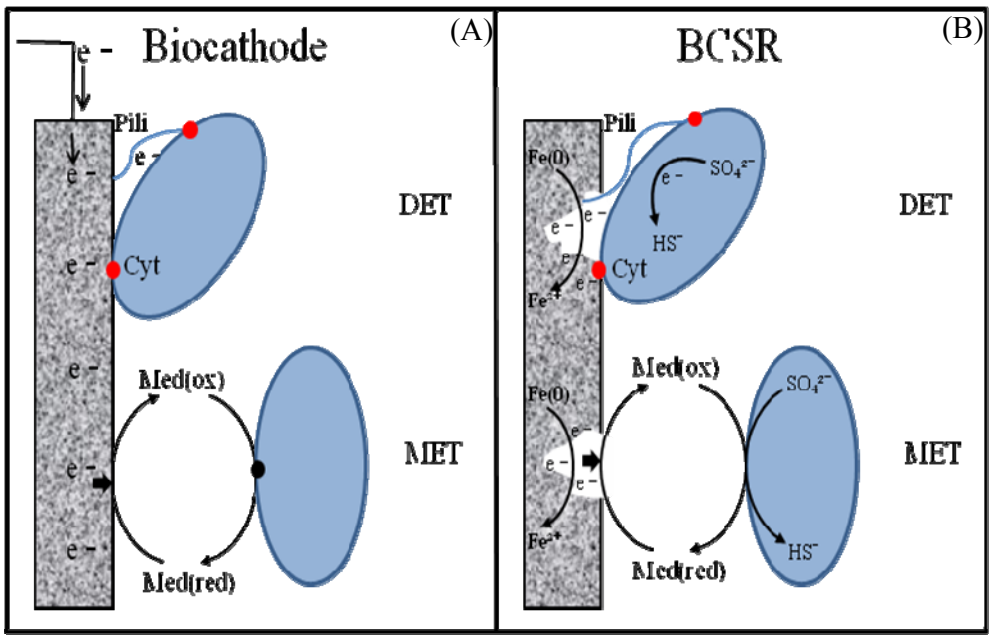

Figure 4-2. The similarity of EET process in MFCs and proposed EET process in BCSR (drawn by Peiyu Zhang and Dake Xu).

Electron mediators facilitate electron transfer between biofilm and electrodes, and are often added to the MFC devices to improve the power output. As discussed above, it is reasonable to speculate that they are able to promote Type I MIC. Flavins like riboflavin and FAD are commonly mediators used by various bacteria. Riboflavin is the water-soluble vitamin B_2, and is also a precursor in the production of FAD and flavin

mononucleotide (FMN) (Fischer and Bacher, 2008). The structure of the isoalloxazine ring enables riboflavin to absorb electrons. The schematic illustration of how electron shuttles promote Type I MIC is shown in Figure 4-3. The electron mediators can shuttle the electrons released by iron oxidation to the sessile cells, and then the mediators are able to be recycled in this procedure. In this work, riboflavin and FAD were used to prove the hypothesis that with the addition of electron mediators, Type I MIC could be accelerated.

4.2 Experimental conditions

The experimental conditions are shown in Table 4-1. The carbon steel coupons were identical to those in Chapter 3, with 1.12 cm^2 exposed top surface without Teflon coating. All the other surfaces were coated with inert Teflon. The manipulations involving microbes were all performed in the anaerobic chamber filled with N_2 gas. The ATCC 1249 medium was used to culture *Desulfovibrio vulgaris*. The medium components are listed in Table 4-2. The culture medium was sparged with N_2 gas for more than one hour. The bacterium and three carbon steel coupons were placed into each anaerobic vial. The initial cell concentration immediately following inoculation in each vial was approximately 10^6 cells/ml. To avoid accidental oxygen leakage, cysteine at a concentration of 100 ppm (w/w) was added as the oxygen scavenger. FAD and riboflavin were dissolved by adjusting the pH of the distilled water. These two electron mediators were tested separately at a concentration of 10 ppm (w/w). There were three duplicate vials for each test condition. The test was repeated three times.

The planktonic SRB cells were enumerated on a hemocytometer at 400X magnification every 24 hours for 7 days. The sessile cells were observed under SEM. The preparation of coupons for SEM observation was described in Chapter 3. The sessile cell counts were quantified by an SRB test kit (Sani-Check Product #100, Warren, Michigan, USA) after a 7-day test. The kit contained a brush dipstick in a vial filled with a solid SRB medium that turns black when SRB are present. The procedure followed Xu et al. (2012). The MPN (Most Probable Number) enumeration method using the ATCC liquid SRB medium was only occasionally used to confirm the results obtained by the test kit because it was time-consuming and labor-intensive. The IFM was used to depict the pit profile caused by SRB under different conditions. The IFM at low resolution (50X) was first used to locate the deepest pits on the entire coupon surface. High resolution (200X) was then used to scan every region to yield the detail of the pit profiles. The procedure to measure the weight loss of the coupons was introduced in Chapter 3.

4.3 Results and discussion

The growth curve after 7 days of SRB with different treatments is present in Figure 4-4. For each data point, the value was averaged from the readings of the three coupons obtained from the same vial. The results demonstrate that both FAD and riboflavin did not increase the cell concentrations, which suggests that the growth of planktonic cells was not promoted by the addition of electron mediators. This is not surprising because the amount of the mediator was far less than the amount of lactate in the medium. The sessile cell counts listed in Table 4-3 indicate that the sessile cell growth was not influenced by the addition of electron mediators. The SRB test kit was

used to quantify sessile cells because it is difficult to count the sessile cells using a hemocytometer. The detection threshold of the hemocytometer requires at least 5 x 10^4 cells/ml. The interference of FeS particles was another concern because they resembled SRB cells. Fortunately, viable *D. vulgaris* cells were motile on the hemocytometer. The normalized weight loss data after 7 days in Figure 4-5 suggest that when an electron mediator was added, the weight loss increased significantly. The average weight loss of the abiotic control was 0.00017 g/cm^2. With the addition of mediators, the weight loss did not increase suggesting that the mediators themselves were not corrosive. This result, consistent with Figure 4-6, suggests that there were no obvious surface changes on the coupon surface when mediators were added. With the addition of SRB without a mediator, the average weight loss was 0.0021±0.00063 g/cm^2. When 10 ppm FAD and riboflavin was added separately, the average weight loss reached 0.0034±0.00070 g/cm^2 and 0.0031±0.00063 g/cm^2, respectively. The considerable increase in weight loss appeared when the mediators were added. The statistical significance for weight loss between the SRB culture without a mediator and the addition of a mediator was confirmed based on the P values obtained (t-test), which were 0.0011 (riboflavin) and 0.0053 (FAD), respectively, and both were less than the threshold of 0.05. The sessile cell count data in Table 4-3 confirm that the electron mediator did not promote sessile cell growth. The general corrosion rate in Figure 4-7 indicates that when adding mediators, corrosion became more severe.

In Figure 4-8A, the largest pit caused by the SRB culture without a mediator was approximately 10 μm (horizontal surface diameter). With the addition of an electron

mediator, the largest pit diameter substantially increased, confirming that the electron transfer promoted by the mediators resulted in more severe corrosion. When adding 10 ppm riboflavin, the largest pit shown in Figure 4-8B was approximately 100 μm (horizontal surface diameter), which was 10 times larger than the pits caused by the SRB without a mediator. With the addition of 10 ppm FAD, the largest pit size reached 40 μm (horizontal surface diameter) as shown in Figure 4-8C. The pit size data were consistent with the weight loss data obtained above.

The pit depth profile in Figure 4-9 shows that the largest pit depth caused by SRB was 10 μm. As shown in Figures 4-10 and 4-11, with the addition of either 10 ppm riboflavin or 10 ppm FAD, the largest pit depths in both treatments were approximately 20 μm. The effect of the electron mediator achieved doubling of the pit depth in comparison pitting by SRB without a mediator. The acceleration of corrosion was not dependent on the cell growth because neither sessile nor planktonic cells were affected by the addition of a mediator. Thus, it is reasonable to conclude that FAD and riboflavin, functioning as electron mediators, substantially enhanced the electron transport in Type I MIC by *D. vulgaris*. According to the largest pit depth data, a worst-case scenario pitting corrosion rate can be obtained, which were 0.52 mm/year (SRB alone), 1.14 mm/year (SRB + 10 ppm riboflavin), and 1.04 mm/year (SRB + 10 ppm FAD), respectively.

In MFC research, a mixed culture biofilm tends to produce a higher power output than a pure culture. The reason for this phenomenon is sometimes because non-electrogenic strains are able to produce electron mediators to promote electron transport. In return, these microbes share the energy released by the redox reaction. Similarly, the

non-corrosive sessile cells may also secrete electron mediators, enhancing the transport of the extracellular electrons released by the iron corrosion into the cytoplasm of the corrosive sessile cells. In return, all the sessile cells can benefit from the energy released from the corrosion reaction, which is an exergonic reaction. This may explain the presence of *S. putrefaciens* coexisting with SRB in oil pipelines and water tanks (Martín-Gil et al., 2004; McLeod et al., 2004). *S. putrefaciens* is able to produce extracellular electron mediators such as FAD and riboflavin, which was confirmed in MFC research (Canstein et al., 2008; Wang et al., 2011). In a biofilm community, *S. putrefaciens* may secrete electron mediators to assist the electron transfer of MIC caused by SRB and share the energy released by MIC in return.

It should be mentioned that the compatibility of the electron mediators and the bacteria is relevant since not all microbes are able to utilize the various electron mediators. It must be noted that the toxicity of the electron mediators is a concern.

4.4 Summary

(1) In this work, the mediator test verified that FAD and riboflavin enhanced the electron transport as a proposed mechanism shown in Figure 4-3.

(2) Type I MIC became more severe when an electron mediator was added.

(3) Electron mediators play an important role in the biofilm community

(4) The electron mediator can be used in lab investigations to achieve a worst-case MIC scenario.

(5) Electron mediators should be detected in severe MIC cases as part of the MIC forensics procedures.

Table 4-1. Experimental Conditions

Parameters	Conditions
SRB strain	*Desulfovibrio vulgaris* (ATCC 7757)
Temperature	37ºC
Culture medium	ATCC 1249 medium
Initial pH	7.0±0.2
Test duration	7 days
Material	C1018 carbon steel
Mediator	10 ppm FAD or 10 ppm riboflavin

Table 4-2. Composition of ATCC 1249 medium for SRB

Component I	$MgSO_4$	2.0 g
	Sodium Citrate	5.0 g
	$CaSO_4$	1.0 g
	NH_4Cl	1.0 g
	Distilled water	400 ml
Component II	K_2HPO_4	0.5 g
	Distilled water	200 ml
Component III	Sodium Lactate	3.5 g
	Yeast Extract	1.0 g
	Distilled water	400 ml
Component IV	$Fe(NH_4)_2(SO_4)_2$	Filter-sterilize 5% (w/w) ferrous ammonium sulfate. Add 0.1 ml of this solution to 5.0 ml of medium prior to inoculation.

Table 4-3. Sessile Cell Count after 7 days by SRB test kit (Gu and Xu, 2013).

Treatment	Sessile cell count (cells/cm^2)
No electron mediator (SRB only)	$\geq 10^7$
SRB + 10 ppm riboflavin	$\geq 10^7$
SRB + 10 ppm FAD	$\geq 10^7$

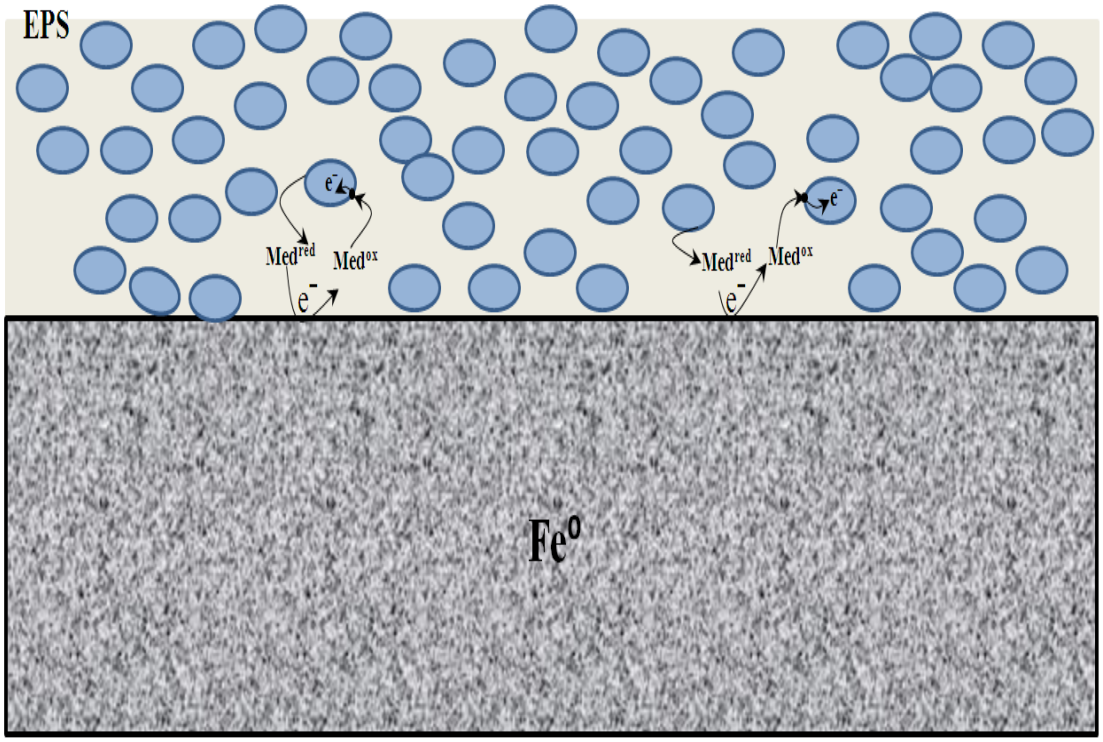

Figure 4-3. Schematic illustration to explain how electron mediators promote MIC (drawn by Peiyu Zhang and Dake Xu).

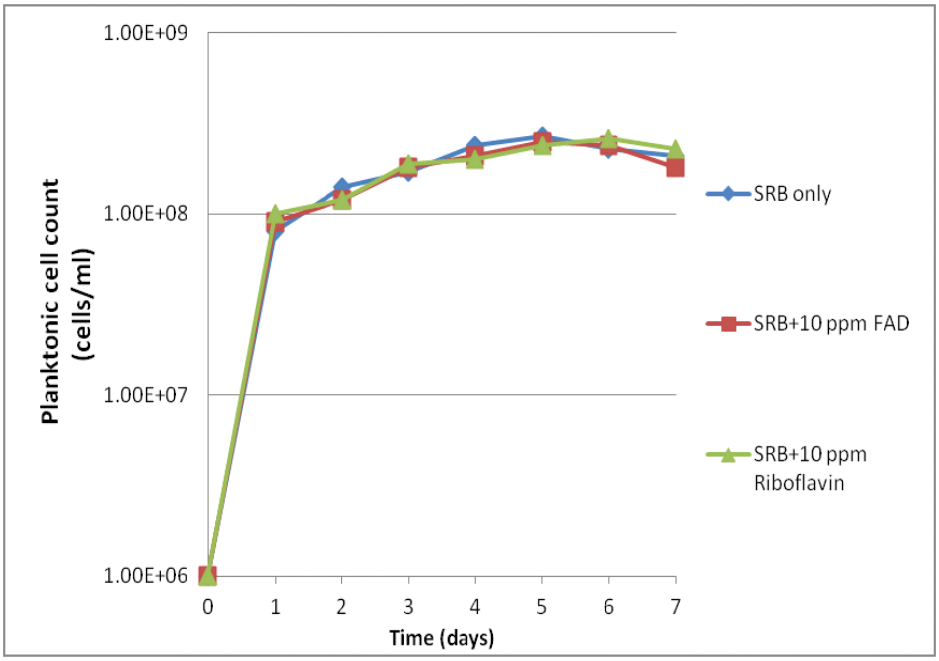

Figure 4-4. Planktonic cell counts with and without addition of electron mediators after 7 days (Gu and Xu, 2013).

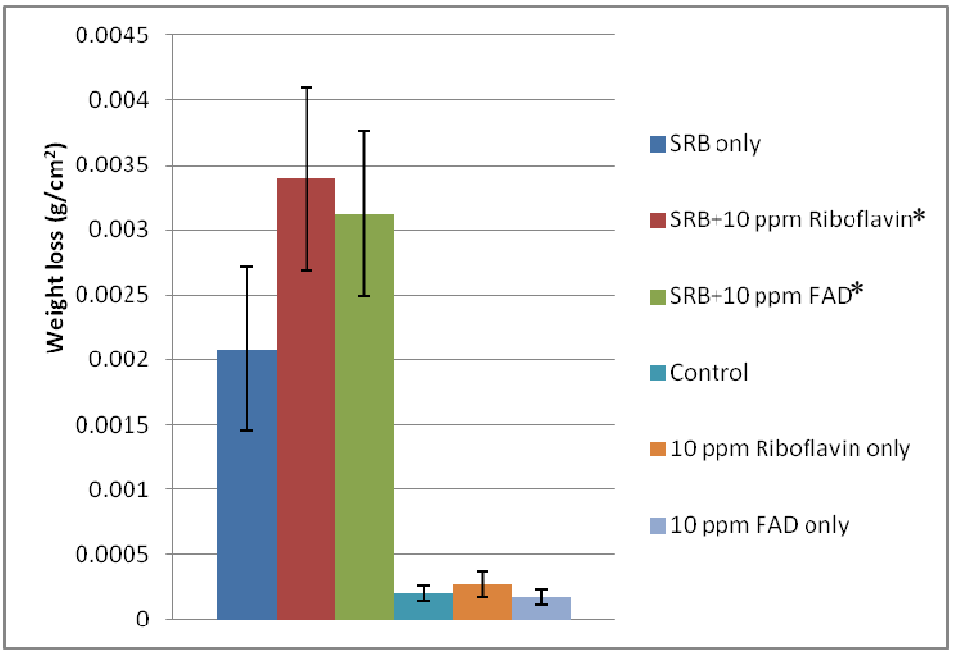

Figure 4-5. Average weight loss data under different conditions after 7 days, and error bars representing standard deviations (Gu and Xu, 2013). *stands for significant difference compared with "SRB only" case.

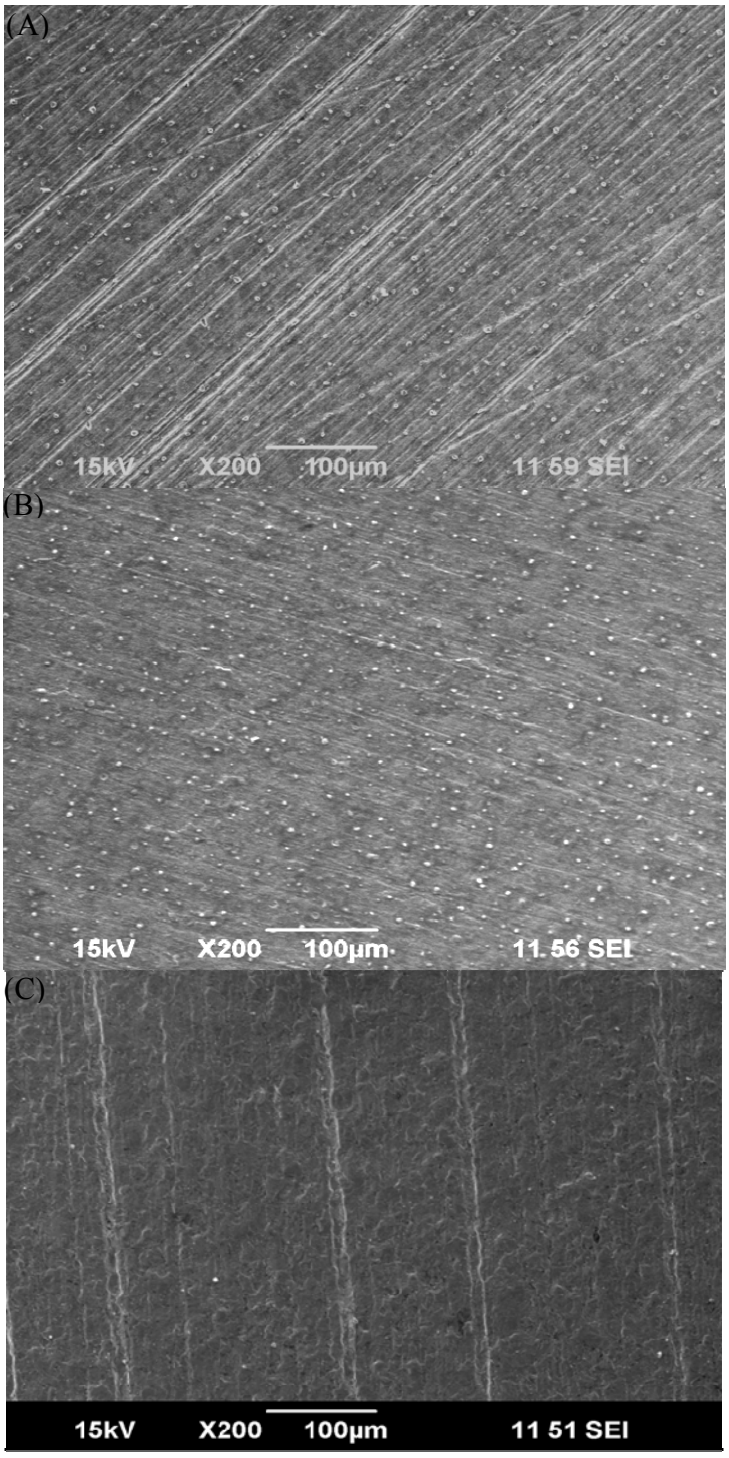

Figure 4-6. Surface morphology after 7 days: (A) SRB culture without mediator, (B) SRB culture with 10 ppm FAD, and (C) SRB culture with 10 ppm riboflavin.

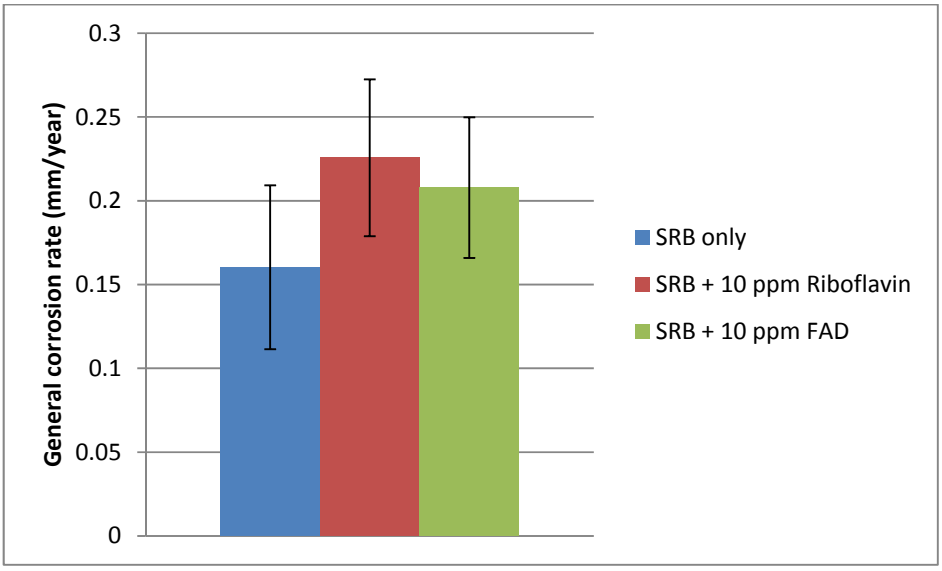

Figure 4-7. General corrosion rate calculated from weight loss (Gu and Xu, 2013). Error bars represent standard deviation.

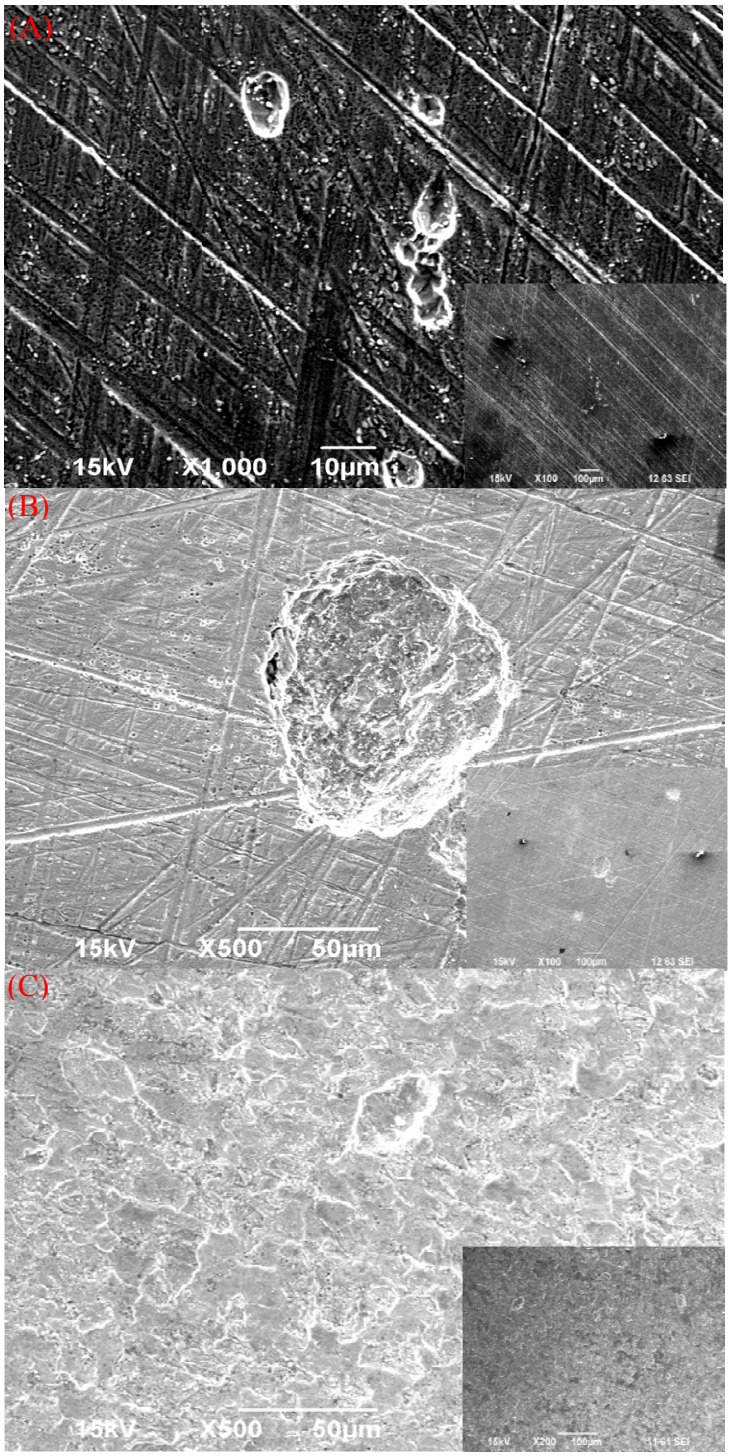

Figure 4-8. Largest pits in horizontal surface diameter after 7 days found in: (A) SRB culture without a mediator, (B) SRB culture with 10 ppm riboflavin, and (C) SRB culture with 10 ppm FAD (Gu and Xu, 2013).

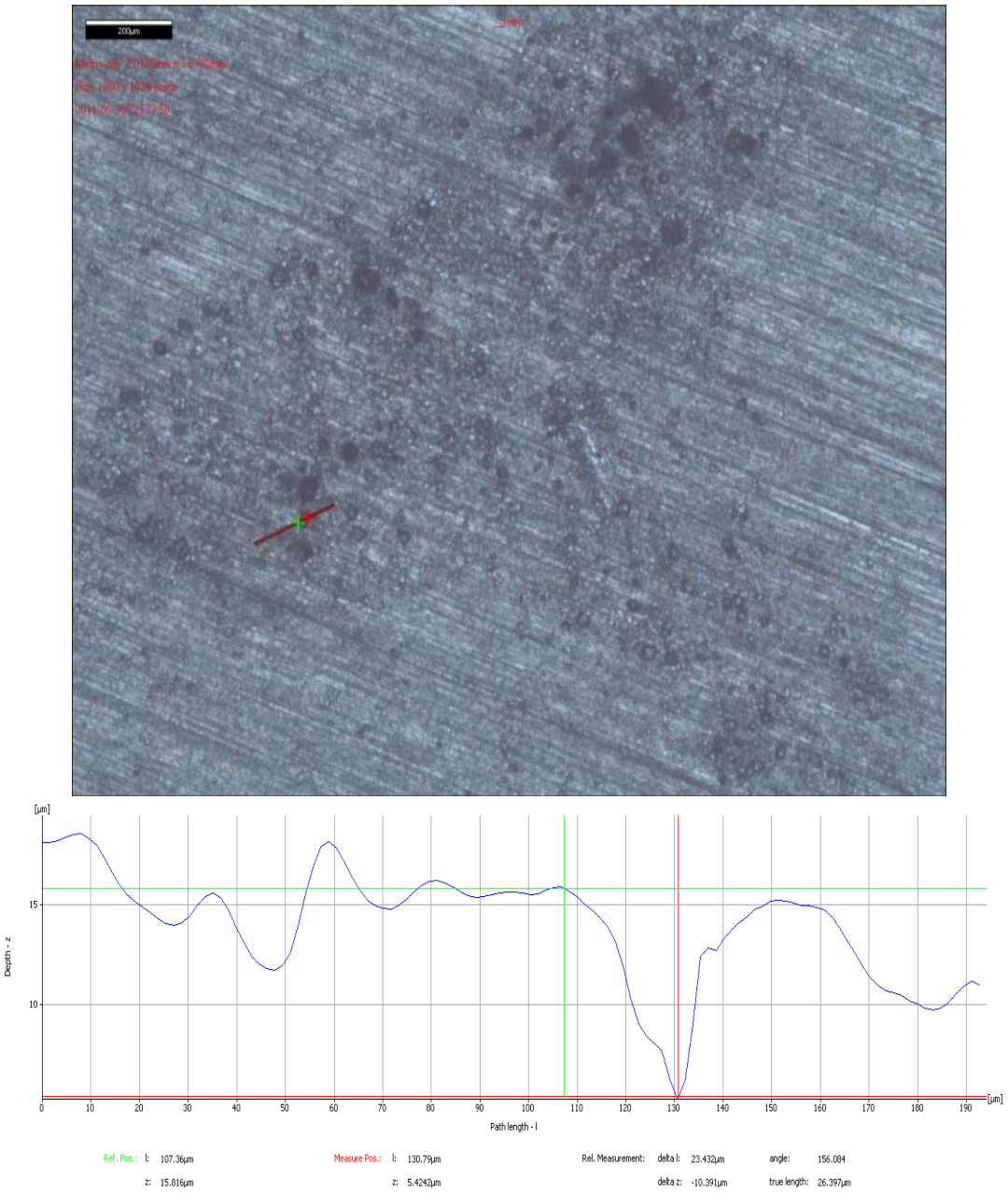

Figure 4-9. Largest pit depth on a coupon without a mediator after 7 days was approximately 10 µm (Gu and Xu, 2013).

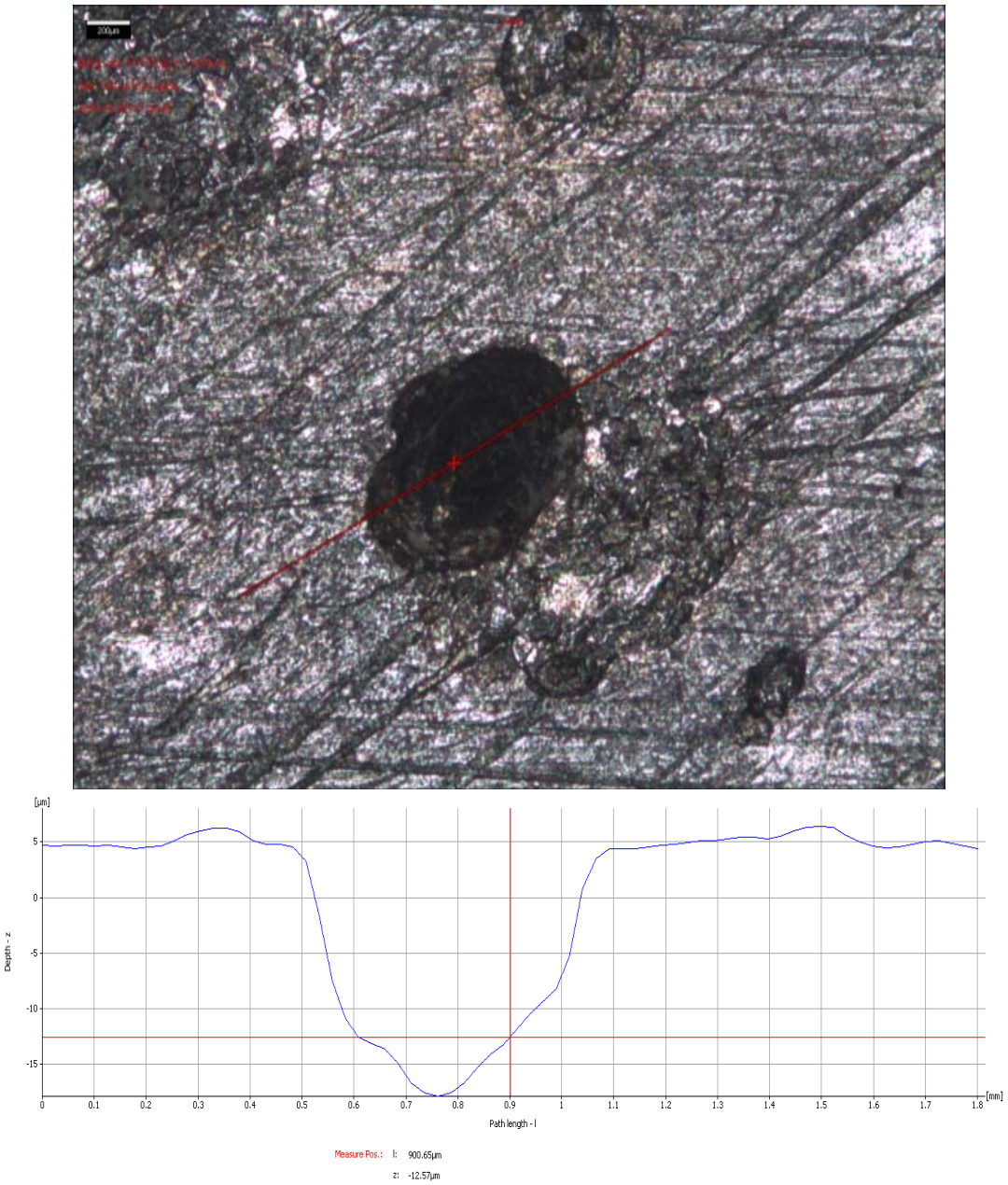

Figure 4-10. Largest pit depth on a coupon with 10 ppm riboflavin after 7 days was approximately 22 µm (Gu and Xu, 2013).

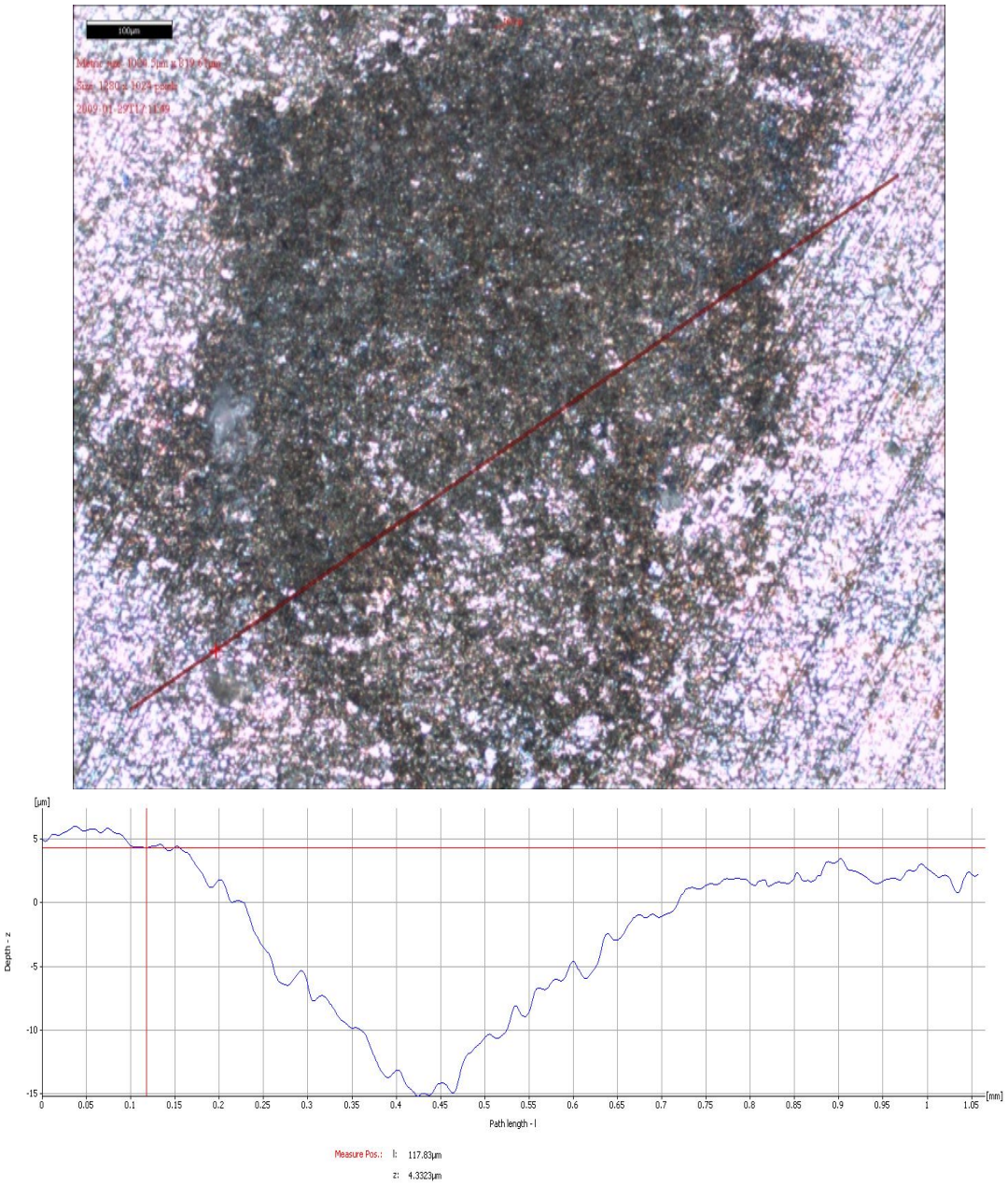

Figure 4-11. Largest pit depth on a coupon with 10 ppm FAD after 7 days was approximately 20 µm (Gu and Xu, 2013).

CHAPTER 5 STARVATION TEST TO SUPPORT BCSR

BCSR has been introduced and explained in both Chapters 2 and 4. The detailed depiction of the EET process given in Chapter 4 clarified how Type I MIC happens. In this chapter, a starvation test of SRB biofilm was designed to verify the motive behind why SRB want to attack carbon steel.

5.1 Introduction

The APS (Adenosine-5'-phosphosulfate) pathway describes how sulfate transfers, activates, and then, gets reduced in the cytoplasm. Those processes, including the transportation, activation and reduction of sulfate in the cytoplasm for dissimilatory sulfate reduction, are actually energy consuming reactions. The process is described in Figure 5-1 (Pereira et al., 2007).

$$SO_4^{2-} + ATP + 2H^+ \rightarrow APS + PPi \qquad 5\text{-}(1)$$

$$APS + H^+ + 2e^- \rightarrow HSO_3^- + AMP \qquad 5\text{-}(2)$$

Sulfate activation in Reaction 5-(1) and APS reduction in Reaction 5-(2) consumed two ATPs to prepare sulfate for reduction, which means that at least two ATP molecules must be synthesized by electron-transport phosphorylation to compensate for the energy loss for each sulfate (Thauer et al., 2007; Muyzer and Stams, 2008). Under typical cellular conditions, the hydrolyses of 1 mole ATP molecule releases approximately 50 kJ energy (Berg et al., 2002) suggesting that when 1 mol of sulfate is activated, 2 mol of ATP, equivalent to 100 kJ, is needed. In BCSR, the iron oxidation coupled with sulfate reduction yields a negative Gibbs free energy change of −180 kJ/mol

sulfate based on the conditions define for $E^{o'}$. The derivations of the parameters such as temperature, concentration and pH may change the value to some extent, but the Gibbs free energy released should still be large enough to compensate for the loss of two ATP molecules and the maintenance energy needed for SRB. It should be noted that the energy released by BCSR could already be the net energy gain, which has already compensated for all the energy losses including APS consumption.

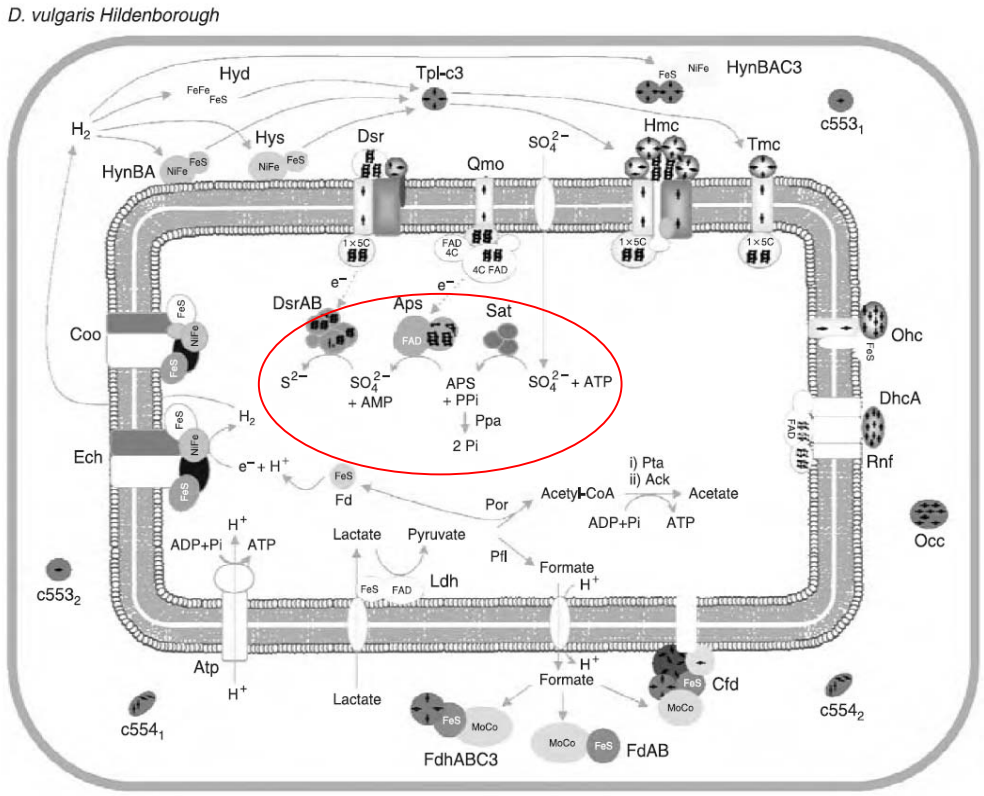

Figure 5-1. Bioenergetics explains how *D. vulgaris Hildenborough* derives energy for growth by coupling the oxidation of lactate to acetate and CO_2 with the reduction of sulfate to sulfide. The red circle depicts the detail of how sulfate was transported, activated and reduced (Pereira et al., 2007).

The BCSR theory demonstrated that due to the diffusion barrier and consumption of the top layer biofilm, the bottom layer biofilm is in a starvation mode because of a lack of digestible organic carbon. Bioenergetically speaking, $E^{o\prime} = -447$ mV for Fe^{2+}/Fe is even slightly more than the $E^{o\prime} = -430$ mV for acetate+CO_2/ lactate. This means elemental iron is a slightly more energetic source than lactate under the conditions defined for $E^{o\prime}$. To obtain maintenance energy, microbes such as SRB can switch from lactate oxidation coupled with sulfate reduction to iron oxidization coupled with sulfate reduction.

Coincidentally, Sherar et al. (2011) recently found that due to lack of organic carbon, SRB cells in their field isolated consortia secreted pili as shown in Figure 2-3. It is rational to speculate that the pili were formed on demand to transfer electrons, which provides direct evidence to support the bioenergetics in BCSR. The electrons released from iron oxidation transported through pili, enter the cytoplasm of SRB where sulfate reduction occurs. The energy released by this redox reaction is needed for SRB to obtain maintenance energy for survival.

The bioenergetics theory for MIC, introduced above, is contrary to the conventional thoughts on MIC, which consider a well-fed biofilm to be more aggressive in a MIC attack. In this chapter, a lab investigation was designed to verify whether a starving biofilm was more aggressive than a well-fed one.

5.2 Material and methods

Table 5-1 shows the test matrix used in this work. All the samples and chemicals were the same as those in Chapter 4. All the medium and coupon preparation procedures and experimental manipulation were also identical to that in Chapter 4.

After 7 days, the coupons covered with established SRB biofilms growth in the same full strength ATCC 1249 medium were transferred to new 125 ml vials containing fresh full medium or a medium with reduced carbon source to test starvation effects. All SRB biofilms were grown under the identical conditions used before the carbon starvation test. After 7 days, the coupons covered with established SRB biofilms were moved to new anaerobic vials containing 100 ml fresh full ATCC 1249 medium or modified ATCC 1249 medium with reduced carbon sources. In the starvation tests, full medium (control), full medium minus 90% lactate and citrate (moderate carbon starvation), full medium minus 99% lactate and citrate (severe carbon starvation), and full medium minus all the lactate and citrate (extreme carbon starvation) were prepared to simulate different degrees of carbon source starvation. In ATCC 1249 medium, lactate is used as the carbon source while citrate functions as a chelating agent to prevent precipitation of FeS particles (Lloyd et al., 1999). Normally, citrate cannot be digested by SRB as a carbon source (Thauer et al. 2007; Muyzer and Stams, 2008). To eliminate the possibility, citrate amount was controlled together with the lactate amount. After incubation in fresh media with different degrees of carbon starvation for 7 days, coupons were removed from the vials for analysis. The sessile cell counts, coupon weight loss,

SEM observation, and IFM for pit depth profile followed the procedure introduced in Chapters 3 and 4.

5.3 Results and discussion

For the starvation test, the sessile cell counts listed in Table 5-2 indicate that severe and extreme organic carbon starvation conditions such as reduction of 99% carbon source and 100% carbon source triggered a huge amount of sessile cell loss. In comparison with the sessile cell count in full medium, severe organic carbon starvation showed two orders of magnitude lower, while moderate starvation with 90% reduction of organic carbon was 10 times lower. The biofilm SEM images shown in Figures 5-2A, 5-3A, 5-4A and 5-5A were consistent with the sessile cell count data shown in Table 5-2.

Figure 5-2B shows the SEM image of pits for the full medium (control) case. When the degrees of starvation were 90% less carbon (Figure 5-3B) and 99% less carbon (Figure 5-4B), the increase in the surface diameter of the pit sizes was obvious. However, due to the irregular shape of the pits, it was difficult to measure the widths accurately, but they were substantially larger in comparison with those produced in the full medium without a carbon source reduction. The pit largest in diameter was under 90% less carbon source condition (moderate carbon starvation). The pits formed under 99% less carbon source (severe carbon starvation) appeared to be relatively shallower than the ones under moderate carbon starvation. The explanation of this phenomenon was that the biofilm was unable to grow more deeply into newly created pit bottoms due to severe carbon starvation. For EET to occur, a biofilm must advance into the newly created pit. As introduced in Chapter 4, the DET method to transfer electrons was either by direct

contact through c-type cytochrome or production of pili. In bioelectrochemistry, either of these two ways required a close proximity between the sessile cells and electrodes in order to make the extracellular electron transport available (iron coupon surface in this case). Even for MET, a very close distance (no more than a few layers of sessile cells) to the iron coupon surface was also needed (Gu, 2012). In this work, when 100% of the carbon source was removed from the medium (extreme carbon starvation), the coupon surface, as shown in Figure 5-5B while relatively rough, had no well-developed MIC pits. This condition could be used as the negative control for measuring MIC before starvation started. The pit depth profiles obtained by IFM in Figure 5-6 describe a trend that is consistent with SEM pit images. The largest pit depth was 10 μm obtained under 90% less carbon source condition (moderate carbon starvation), while 99% less carbon source (severe carbon starvation) and full medium yielded 5.1 μm and 7.3 μm, respectively. The pit depth of 100% carbon source removal (extreme carbon starvation) was not measurable due to its shallow shape. All these data were obtained from three separate repeated experiments.

Figure 5-7A shows the average normalized weight loss data. The weight loss values for full medium, moderate carbon starvation, severe carbon starvation and extreme carbon starvation were 0.0015±0.00007 g/cm^2, 0.0017±0.00009 g/cm^2, 0.0019±0.00011 g/cm^2 and 0.0012±0.00014 g/cm^2, respectively. From the figure, it can be concluded that less organic carbon yielded larger weight loss. However, this trend was reversed for the case of extreme carbon starvation. Under extreme carbon starvation conditions, sessile cells became too few and too weak (lacking enzymes). The statistical significance was

confirmed by calculating the P value for weight loss (t-test). The value of the comparison between the full medium and the full medium minus 90% carbon source was 0.0078, while the value in the comparison between full medium and the full medium minus 99% carbon source was 0.0018. Both were smaller than the commonly accepted 0.05 threshold, indicating a statistical significance. Figure 5-7B shows that all the pH values of the bulk medium at different conditions ranged narrowly between 6.3 and 6.6. Due to the slight difference and low acidity of the medium under all conditions, it is reasonable to exclude the contribution of acidity to the weight loss and pitting. Thus, Type II MIC, due to corrosive metabolites produced by the biofilm was not of concern in this work.

As discussed in Chapter 4, Fe^0 can serve as an energy source for bacteria, and abundant literature has confirmed that Fe^0 can be used for growth of SRB, NRB and even methanogens in non-MIC studies (Biswas and Bose, 2005; Chastain and Kral, 2010; Ginner et al., 2004; Gu and Xu, 2013). In this study, due to a lack of organic carbon, the starved sessile cells utilized Fe^0 as their energy source, and the electrons released by iron corrosion were captured by the sessile cells and, then, transferred into the cytoplasm of the cells where biocatalytic sulfate reduction occurred. The energy released by this process supplied maintenance energy for the sessile cells. This can explain why under moderate and severe starvation conditions, more weight loss and severe MIC attack occurred.

Yeast extract served as growth factors and supplement of vitamins in the medium used in this work. The yeast extract was not diluted in the ATCC 1249 medium when treated for different degrees of starvation tests. It should be noted that sessile cells in a

biofilm can scavenge dead cells and EPS as their organic supply (Costerton, 2007). Thus, even total removal of lactate and citrate did not guarantee complete deprivation of organic carbon for sessile cells survival.

5.4 Summary

(1) Moderate and severe carbon starvation conditions triggered more severe MIC attack compared with the control (full medium).

(2) The energy source of sessile cells switching from organic carbon to Fe^0 was verified and supported by the starvation test.

(3) The BCSR theory was supported by the SRB starvation test.

Table 5-1. Test matrix.

Parameters	Conditions
SRB strain	*D. vulgaris* (ATCC 7757)
Temperature	37ºC
Culture medium	ATCC 1249 medium
Carbon source reduction	0%, 90%, 99%, 100%
Initial pH	7.0±0.2
Starvation duration	7 days
Coupon material	C1018 carbon steel

Table 5-2. Sessile cell count in different culture media by SRB test kit (Xu and Gu, 2011).

Medium	Sessile Cell Count (cells/cm^2)
Full medium (ATCC 1249 Medium)	$\geq 10^6$
Full medium minus 90% carbon source	$\geq 10^5$
Full medium minus 99% carbon source	$\geq 10^4$
Full medium minus 100% carbon source	$\geq 10^4$

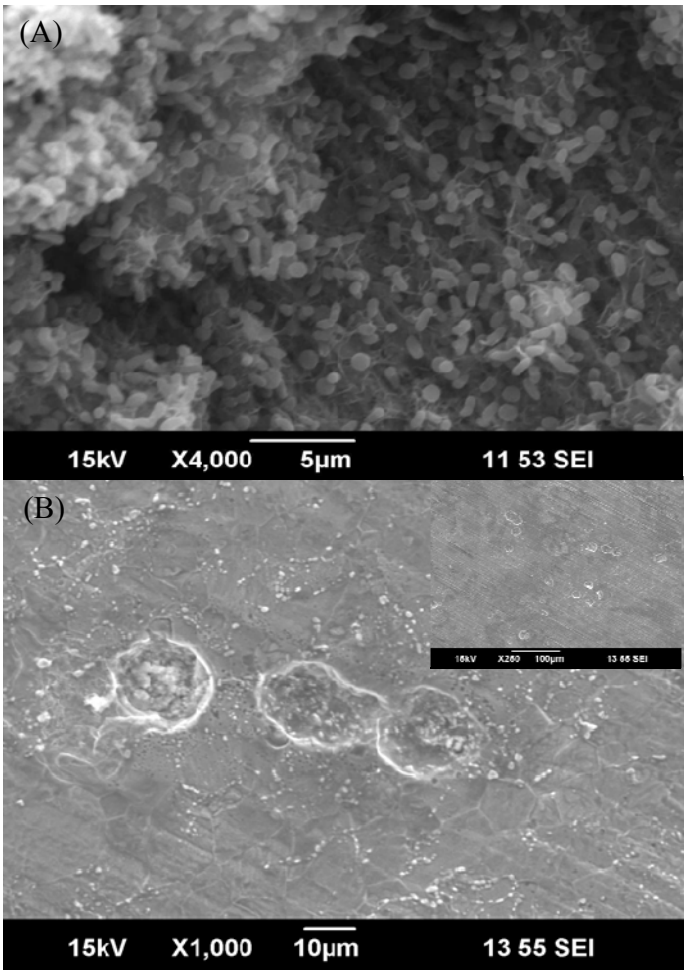

Figure 5-2. SEM images for (A) sessile SRB, and (B) MIC pits obtained using full medium (control) in the starvation test (Xu and Gu, 2011).

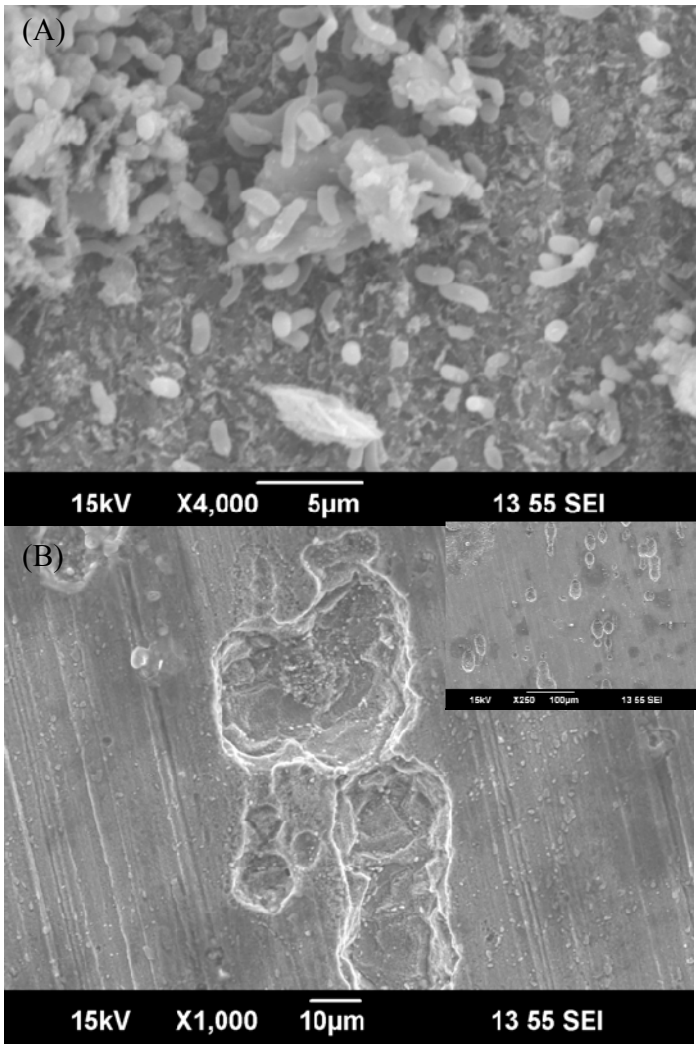

Figure 5-3. SEM images for (A) sessile SRB, and (B) MIC pits obtained using full medium minus 90% carbon source (moderate carbon starvation) in the starvation test (Xu and Gu, 2011).

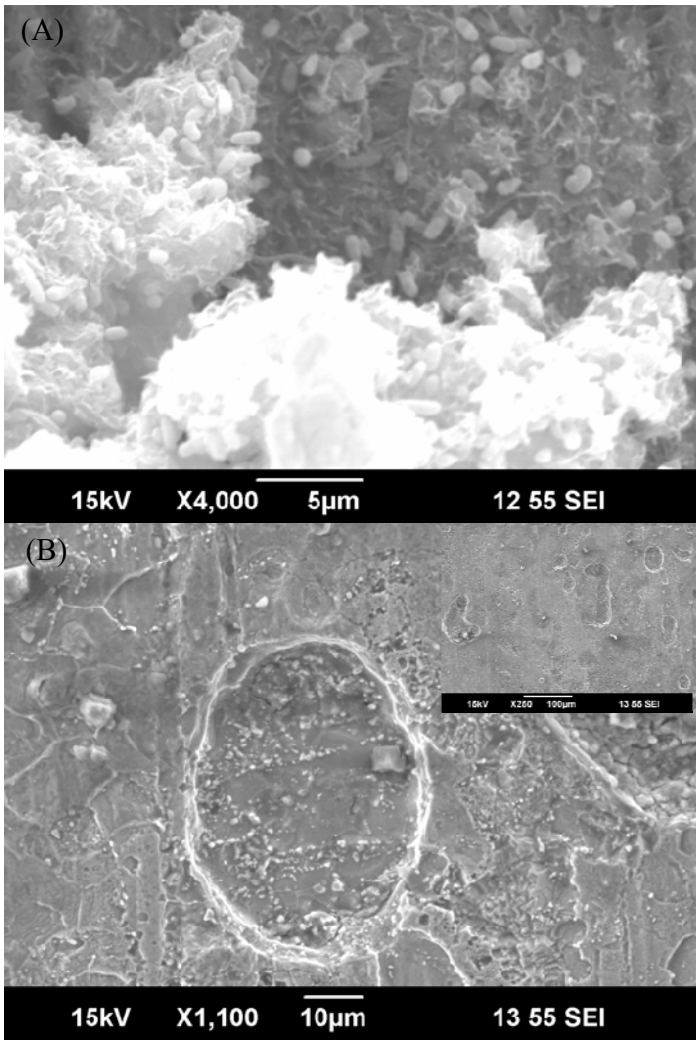

Figure 5-4. SEM images for (A) sessile SRB, and (B) MIC pits obtained using full medium minus 99% carbon source (severe carbon starvation) in the starvation test (Xu and Gu, 2011).

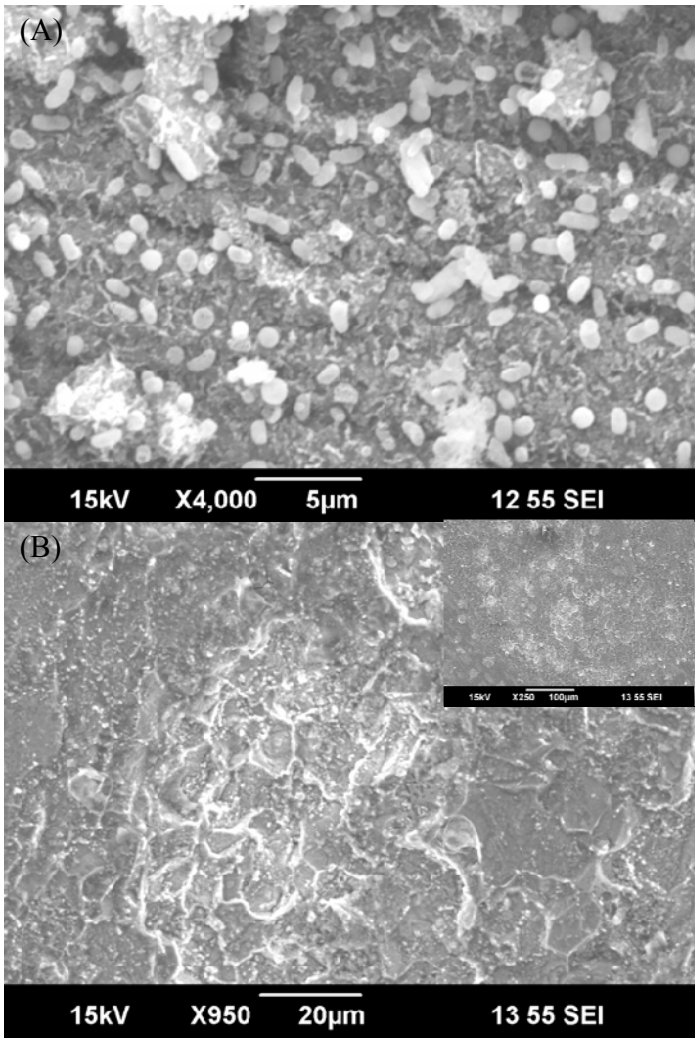

Figure 5-5. SEM images for (A) sessile SRB, and (B) MIC pits obtained using full medium minus 100% carbon source (extreme carbon starvation) in the starvation test (Xu and Gu, 2011).

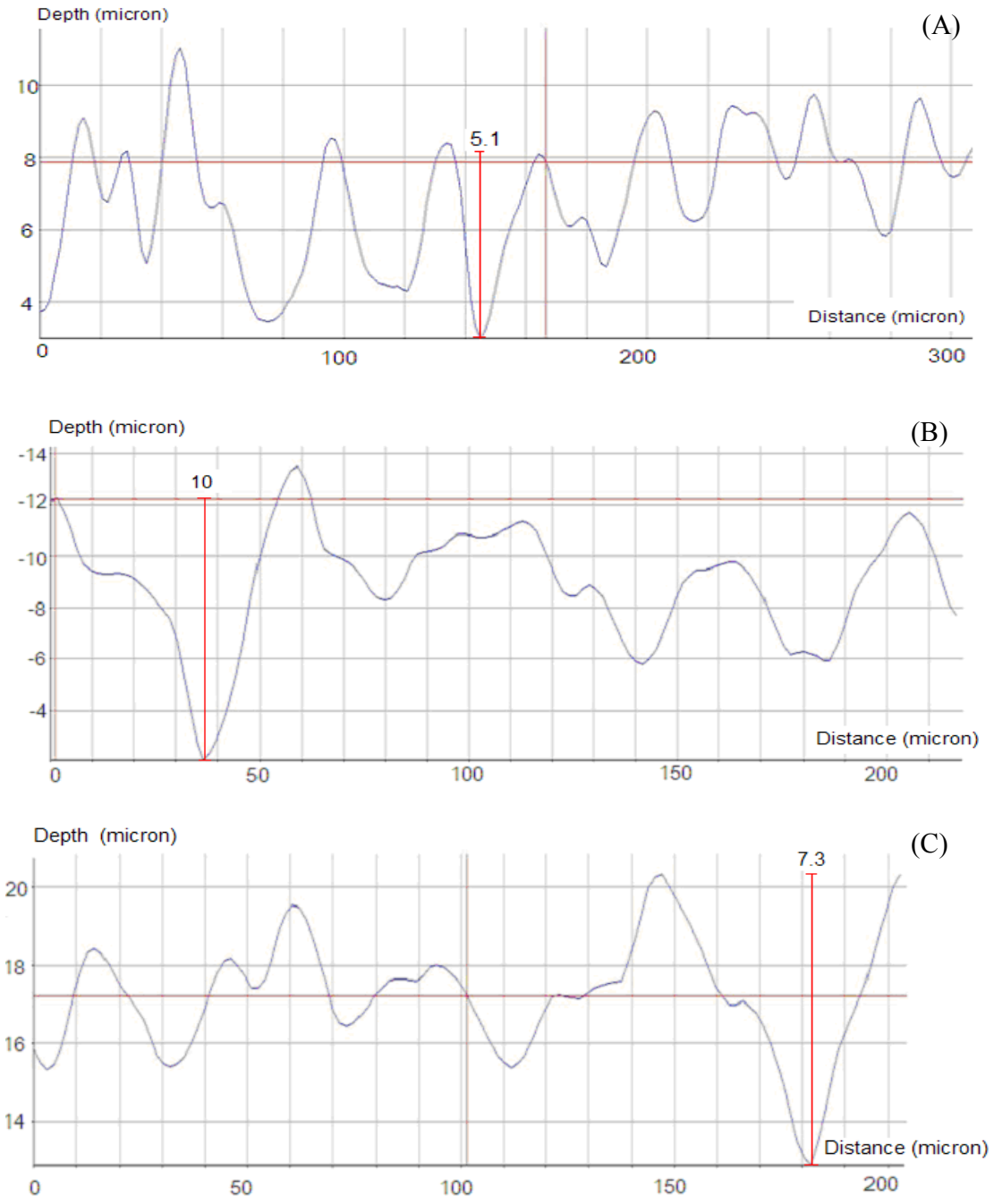

Figure 5-6. IFM pit profile for a coupon (A) full medium (control) , (B) full medium minus 90% carbon source (moderate carbon starvation), and (C) full medium minus 99% carbon source (severe carbon starvation) (Xu and Gu, 2011).

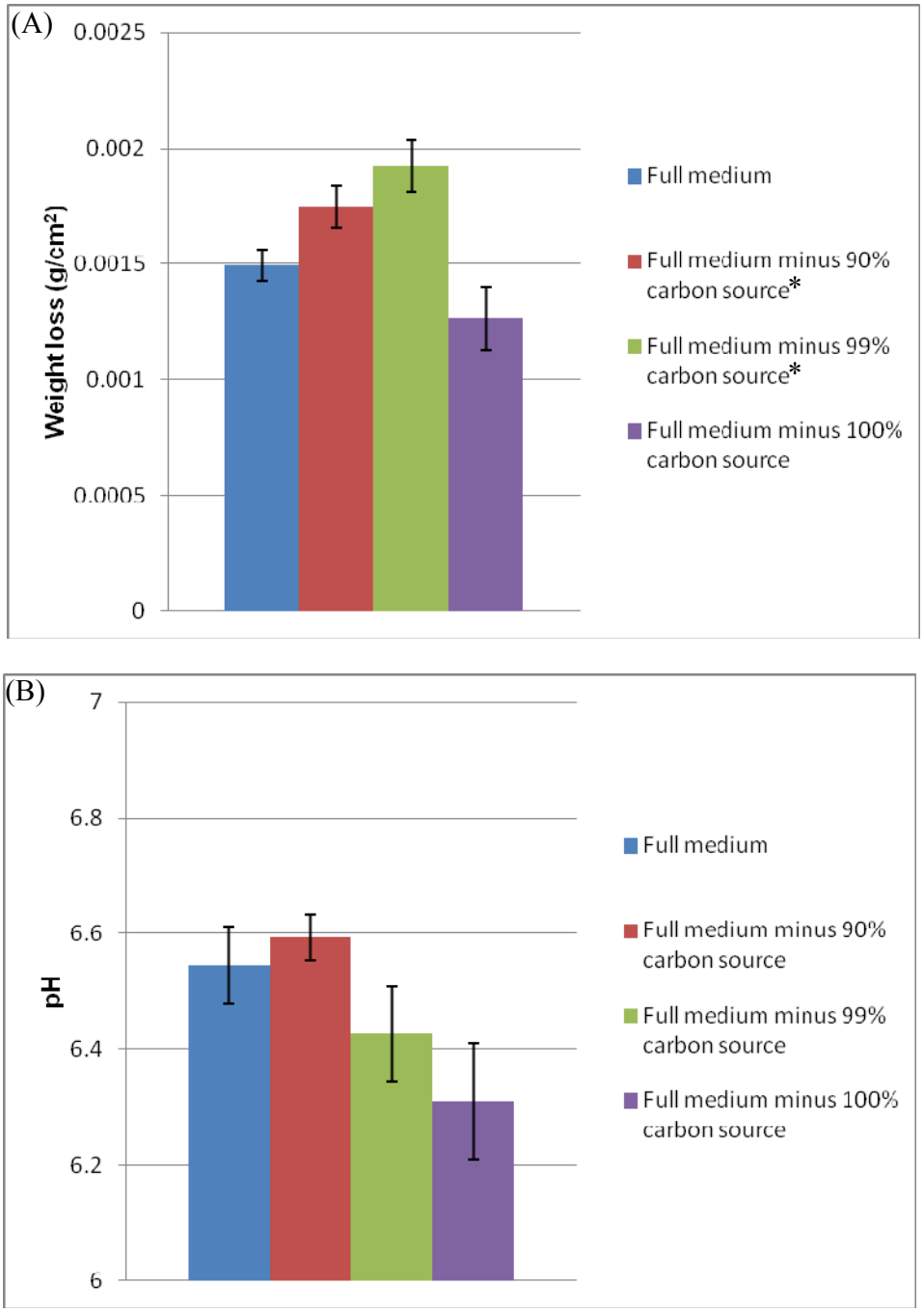

Figure 5-7. (A) Weight loss and (B) pH data after 7-day starvation test. Error bars represent standard deviations (Xu and Gu, 2011). *stands for significant difference compared with "full medium" case.

CHAPTER 6 D-AMINO ACIDS AS BIOCIDE ENHANCERS

As introduced in Chapter 2, chelators (EDTA and EDDS) and alcohols (ethanol or methanol) can be used as biocide enhancers. Their efficacy requires high concentrations, suggesting that their large-scale application is costly. Another concern is the potential reaction between biocides and biocide enhancers during transport and storage.

D-amino acids were reported to be effective in dispersing biofilms. It is well known that planktonic cells are much more vulnerable than sessile cells. In biofilm mitigation, it is advantageous to convert sessile cells to planktonic cells. Some D-amino acids are able to replace the D-ala in the peptidoglycan of bacterial cell walls, resulting in the disassembly of the biofilm. D-amino acids are regarded as signal molecules to control the biofilm.

6.1 D-amino acid mixture to enhance current treatment method containing biocide and chelator

To effectively enhance the biocidal effect of THPS against SRB biofilm, at least 1000 ppm (w/w) or even 2000 ppm EDDS is required. Such high concentrations are unacceptable in large scale applications due to their cost. A more effective combination of biocides and enhancers is needed.

The test matrix in this work is described in Table 6-1. D-amino acids (D-tyr, D-met, D-trp and D-leu) were mixed at equimolar concentrations. Based on the molecular weight of each D-amino acid, 1 mM equimolar concentration was equivalent to 660 ppm (w/w) D-amino acid mixture concentration. Experimental procedure in this chapter

followed Xu et al. (2012).

6.1.1 Prevention of SRB biofilm establishment

Figure 6-1 shows the *D. vulgaris* biofilm morphology following different treatments. When treated with the D-amino acid mixture alone at the concentration of 6.6 ppm and 660 ppm, there were still numerous sessile cells, indicating that the D-amino acid mixture alone was not effective in preventing the biofilm formation. With the addition of 30 ppm THPS + 6.6 ppm D-amino acid mixture, 30 ppm THPS + 660 ppm D-amino acid mixture, 100 ppm THPS, and 30 ppm THPS + 500 ppm EDDS, respectively, no obvious inhibition effect was achieved. Figure 6-2A demonstrates that by adding 6.6 ppb D-amino acid mixture (equivalent to 10 nM for each D-amino acid in the mixture) to the biocide cocktail consisting of 30 ppm THPS + 500 ppm EDDS, the sessile cell number was substantially reduced compared with either 30 ppm THPS + 6.6 ppm D-amino acid mixture or 30 ppm THPS + 500 ppm EDDS, shown in Figures 6-1D and 6-1F. By increasing the D-amino acid mixture concentration to 6.6 ppm in the triple combination biocide cocktail, the sessile cells were barely detectable as shown in Figure 6-2B. Based on the data above, the triple combination of 30 ppm THPS + 500 ppm EDDS + 6.6 ppm D-amino acid mixture was confirmed to successfully prevent SRB biofilm establishment on the carbon steel coupon surface after a 7-day treatment.

Table 6-2 shows the sessile cell count data obtained from the Biosan SRB test kit. Without any treatment, the sessile cells on the coupon surface reached 10^8 cells/cm^2. When treated with 30 ppm THPS, 2 log kill was achieved and the cell numbers decreased to 10^6 cells/cm^2. When the combination of 30 ppm THPS with 6.6 ppm D-amino acid

mixture was used, there was no improvement. With the addition of 30 ppm THPS + 500 ppm EDDS, the sessile cell count decreased to 10^5 cells/cm^2. When treated with 30 ppm THPS + 500 ppm EDDS + 6.6 ppm D-amino acid mixture, the sessile cell count decreased significantly to 10^3 cells/cm^2, resulting in the most effective inhibition with a 5 log reduction when compared with the sessile cell numbers with no treatment.

6.1.2 Removal of the established SRB biofilm

Similar results were obtained in removing established SRB biofilm tests. Figure 6-3 demonstrates that with the D-amino acid mixture alone at 6.6 ppm or 660 ppm, there was no removal effect. When treated with THPS alone even at a high concentration of 250 ppm, sessile cells could still be detected. When treated with the combination of 30 ppm THPS with either 500ppm EDDS, 6.6 ppm, or 660 ppm D-amino acid mixture, sessile cells appeared less abundant but could still be easily detected. With the addition of 6.6 ppb D-amino acid mixture + 30 ppm THPS + 500 ppm EDDS triple combination biocide cocktail, only a few cells could be seen on the coupon surface. Complete removal of sessile cells was achieved when the D-amino acid concentration increased to 6.6 ppm. The sessile cell counts as shown in Table 6-3 are consistent with Figures 6-3 and 6-4. The best efficacy of a 4 log reduction of sessile cells was achieved when the triple combination of 30 ppm THPS + 500 ppm EDDS + 6.6 ppm D-amino acid mixture was treated. Treatment of 30 ppm THPS alone and 30 ppm THPS + 6.6 ppm D-amino acid mixture showed only 1 log reduction, while a combination of 30 ppm THPS + 500 ppm EDDS obtained a 2 log reduction.

6.1.3 Discussion

The D-amino acid mixture containing D-tyr, D-met, D-trp and D-leu may be signal molecules that can disperse biofilm (Kolodkin-Gal et al., 2010), and the combination of these four D-amino acids together showed a synergistic effect and better inhibition ability than individual D-amino acids. A variety of equimolar mixtures of these four D-amino acids were tested at 2.5, 5, and 15 nM for each individual D-amino acid. The minimum inhibitory concentration was 2.5 nM. The D-amino acid mixture successfully dispersed the biofilms of *Staphylococcus aureus*, *Bacillus subtilis* and *Pseudomonas aeruginosa*. These biofilms were fluffy and more easily eradicated than *D. vulgaris* biofilms on carbon steel coupons.

In this study, due to the tenacity of SRB biofilm, D-amino acids alone showed no dispersion effect on the SRB biofilm. The explanation for this phenomenon was that the morphology of the SRB biofilm was thin and dense, which made it attach tenaciously to the coupon surface. The D-amino acids mixture cannot function effectively as dispersion signal molecules. The SRB cells need additional stress to disperse. With the help of the stress from a biocide (e.g., THPS), D-amino acids are capable of convincing the biofilm to disassemble. In this work, D-amino acids enhanced the efficacy of a double combination of THPS and EDDS. It successfully prevented biofilm establishment and removed the established biofilm with the addition of only a ppm level of a D-amino acid mixture, lowering effective EDDS concentrations from 1000 ppm to 500 ppm.

Table 6-1. Test matrix.

Parameters	Conditions
SRB strain	*D. vulgaris* (ATCC 7757)
Temperature	37ºC
Culture medium	ATCC 1249 medium
Biocide	30 ppm THPS
Chelator	500 ppm EDDS
D-amino acids mixture	6.6 ppb, 6.6 ppm and 660 ppm
Initial pH	7.0±0.2
Coupon material	C1018 carbon steel

Table 6-2. Sessile cell counts 7 days after using different treatment methods for the prevention of SRB biofilm establishment in ATCC 1249 medium (Xu et al., 2012).

Treatment	Sessile cell count (cells/cm^2)
No treatment	$\geq 10^8$
30 ppm THPS	$\geq 10^6$
30 ppm THPS + 6.6 ppm D-amino acid mixture	$\geq 10^6$
30 ppm THPS+ 500 ppm EDDS	$\geq 10^5$
30 ppm THPS + 500 ppm EDDS + 6.6 ppm D-amino acid mixture	$\geq 10^3$

Table 6-3. Sessile cell counts 7 days after using different treatment methods to treat established SRB biofilms in ATCC 1249 medium (Xu et al., 2012).

Treatment	Sessile cell count (cells/cm^2)
No treatment	$\geq 10^7$
30 ppm THPS	$\geq 10^6$
30 ppm THPS + 6.6 ppm D-amino acid mixture	$\geq 10^6$
30 ppm THPS + 500 ppm EDDS	$\geq 10^5$
30 ppm THPS + 500 ppm EDDS + 6.6 ppm D-amino acid mixture	$\geq 10^3$

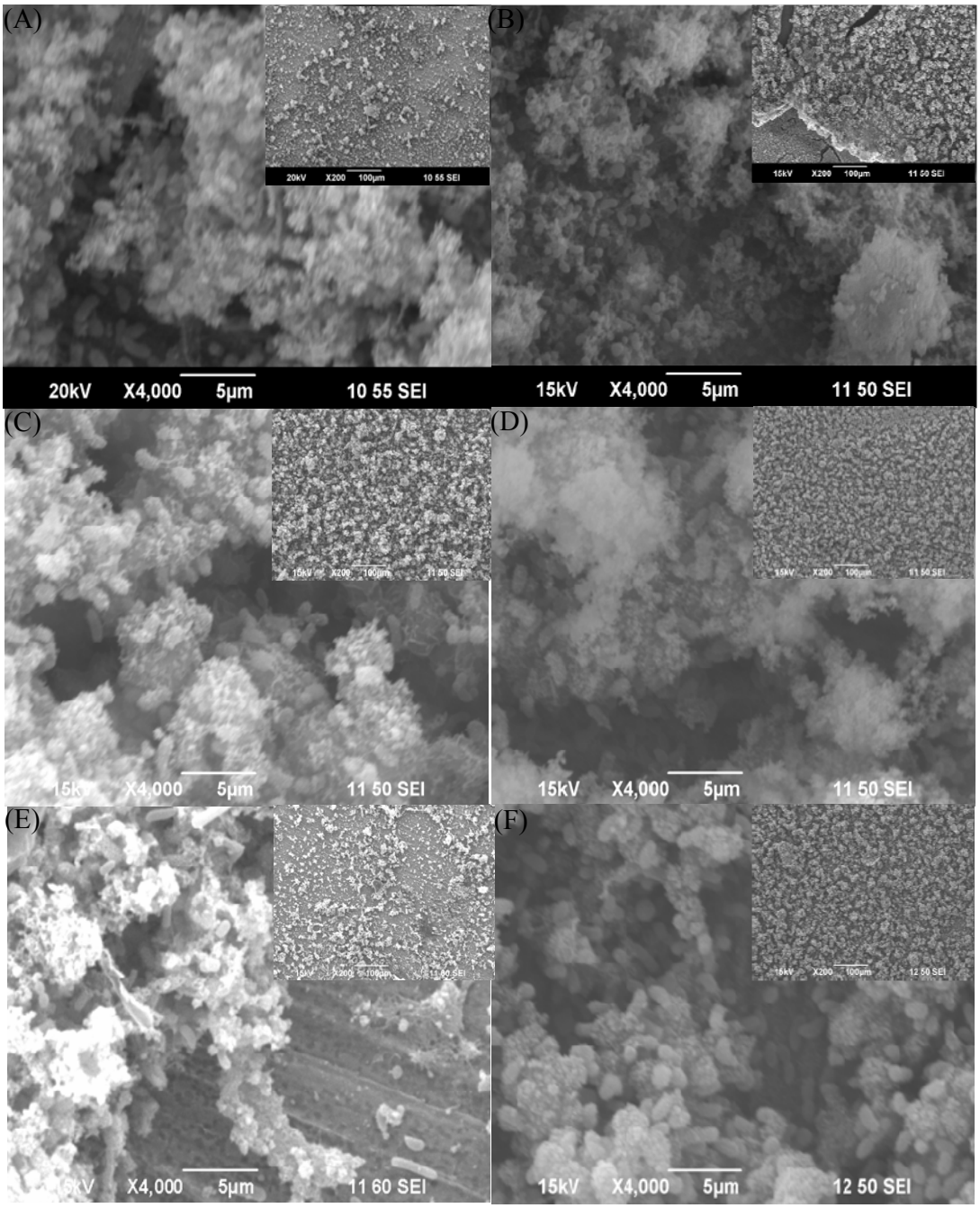

Figure 6-1. SEM images for 7-day coupons in ATCC 1249 medium with (A) 6.6 ppm D-amino acid mixture, (B) 30 ppm THPS + 6.6 ppm D-amino acid mixture, (C) 660 ppm D-amino acid mixture, (D) 30 ppm THPS + 660 ppm D-amino acid mixture, (E) 100 ppm THPS treatment, (F) 30 ppm THPS + 500 ppm EDDS. Scale bars for the small inserted images are 100 µm (Xu et al. 2012).

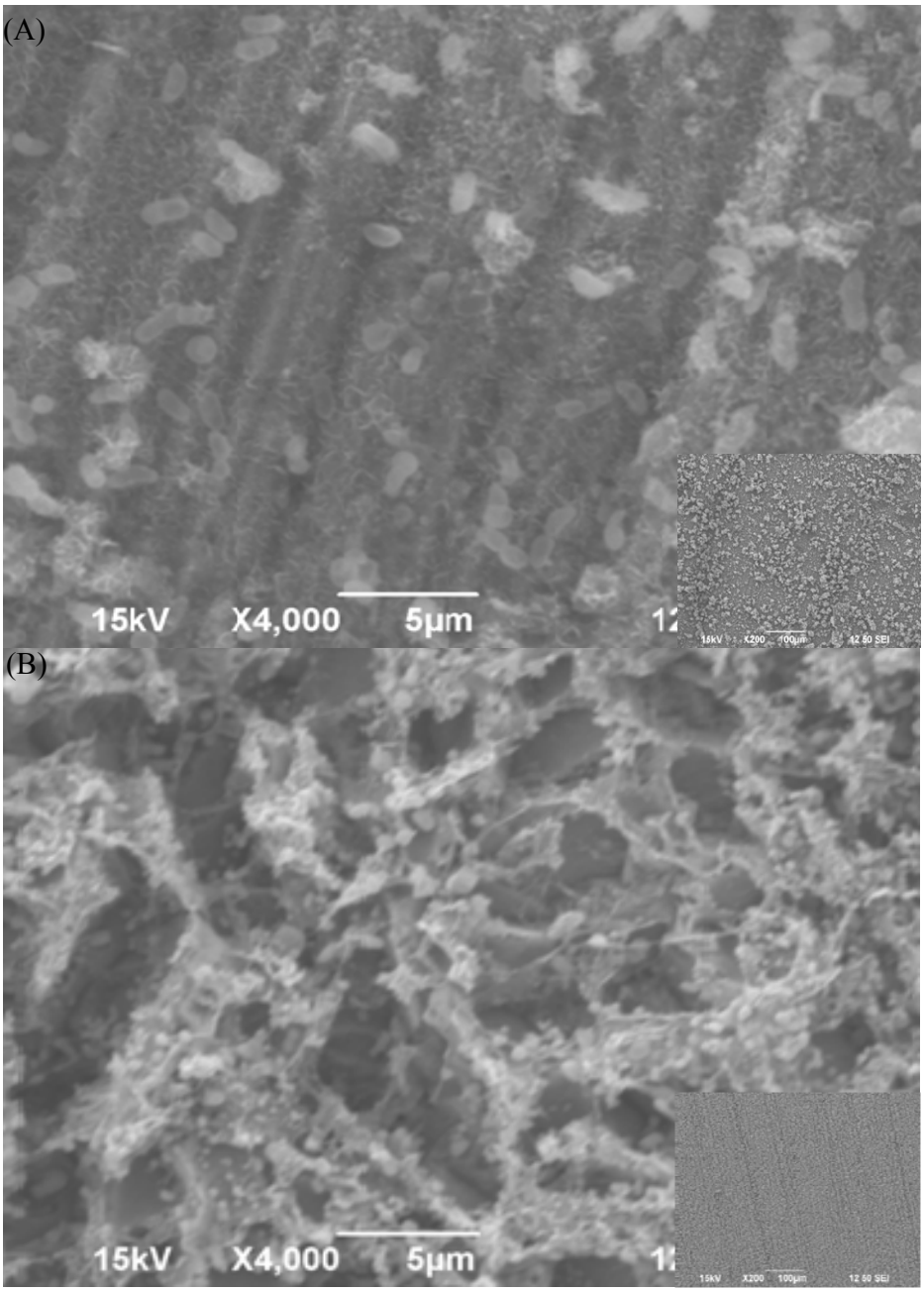

Figure 6-2. SEM images for 7-day coupons in ATCC 1249 medium with (A) 30 ppm THPS + 500 ppm EDDS + 6.6 ppb D-amino acid mixture, (B) 30 ppm THPS + 500 ppm EDDS + 6.6 ppm D-amino acid mixture. Scale bars for the small inserted images are 100 μm. 6.6 ppb D-amino acid mixture is equal to 10 nM D-amino acid mixture (Xu et al. 2012).

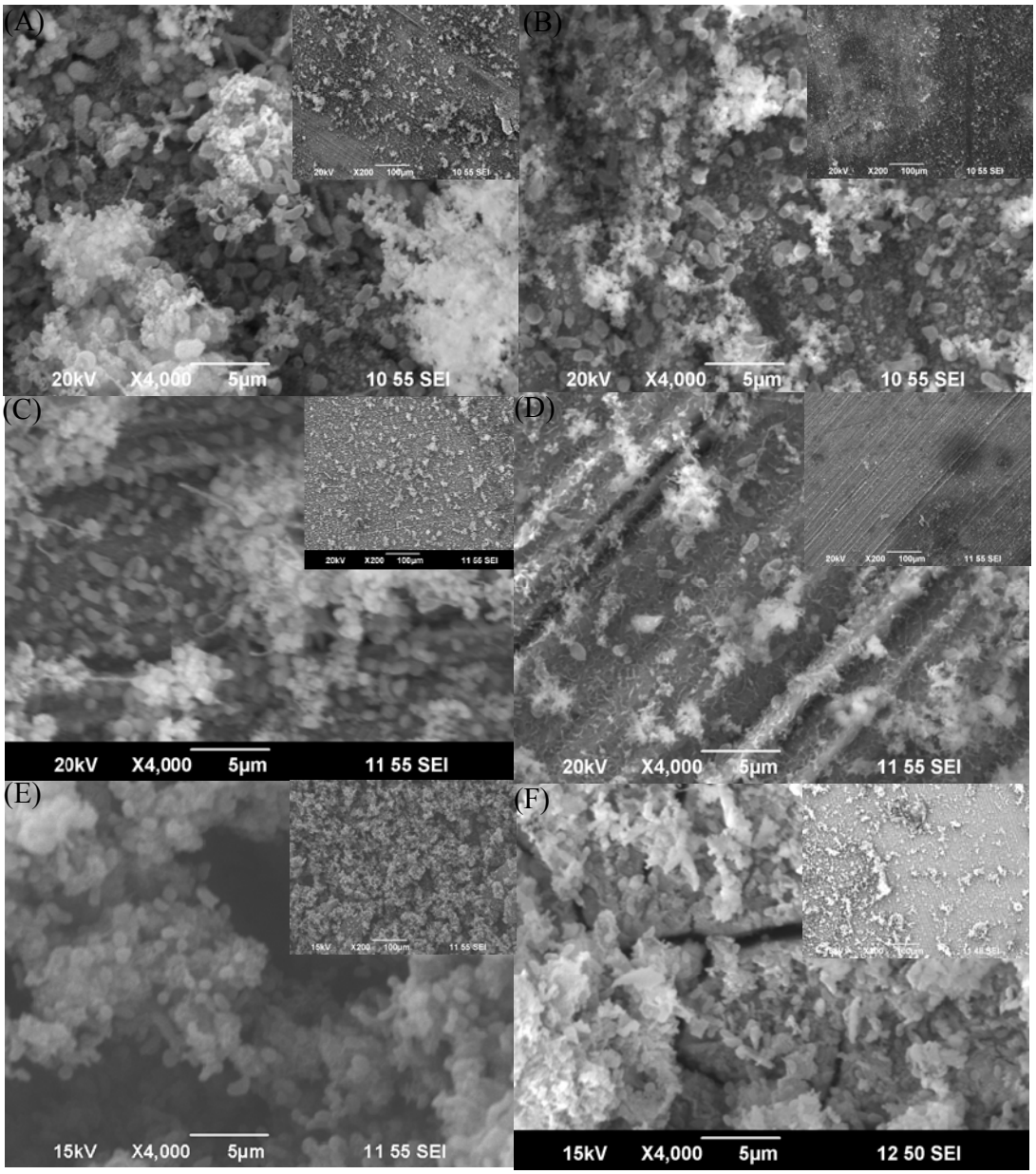

Figure 6-3. SEM images for coupons in ATCC 1249 medium covered with mature biofilms for 7 days then they were treated with (A) 6.6 ppm D-amino acid mixture, (B) 30 ppm THPS + 6.6 ppm D-amino acid mixture, (C) 660 ppm D-amino acid mixture, (D) 30 ppm THPS + 660 ppm D-amino acid mixture, (E) 250 ppm THPS treatment, (F) 30 ppm THPS + 500 ppm EDDS. Scale bars for the small inserted images are 100 μm (Xu et al. 2012).

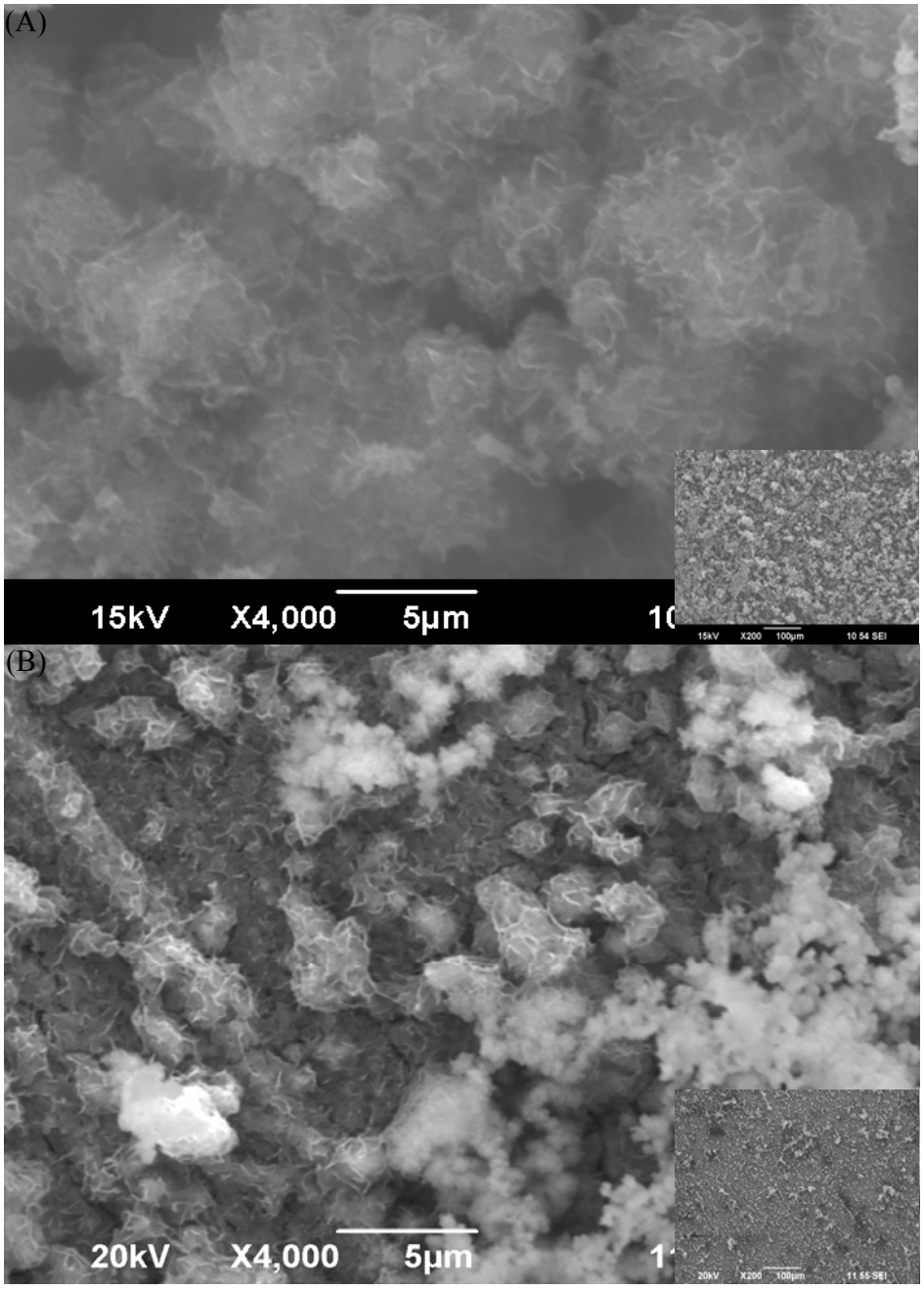

Figure 6-4. SEM images for coupons in ATCC 1249 medium covered with mature biofilms for 7 days then they were treated with (A) 30 ppm THPS + 500 ppm EDDS + 6.6 ppb D-amino acid mixture, (B) 30 ppm THPS + 500 ppm EDDS + 6.6 ppm D-amino acid mixture. Scale bars for the small inserted images are 100 µm (Xu et al. 2012).

6.2 D-tyr as a biocide enhancer

The potential of the D-amino acid mixture as a biocide enhancer was demonstrated in Section 6.1. The advantages of D-amino acids were their green nature–a lack of toxicity and low cost.

A triple combination biocide cocktail is not recommended if a dual combination can achieve a similar efficacy. D-tyr was chosen as the potential biocide enhancer in this work given its high dispersal ability of biofilm, reported in the literature (Kolodkin-Gal et al., 2010). All the preparations and manipulations followed Xu el al. (2012). In this part of the research, the efficacy of low concentrations of D-tyr to enhance THPS was investigated. The objective was to demonstrate that under the stress of THPS, D-tyr shows strong biofilm dispersal ability, and can achieve the synergistic effect together with THPS in both biofilm prevention and removal tests.

6.2.1 Prevention of SRB biofilm establishment

As shown in Table 6-4, the sessile *D. vulgaris* cell count on the control coupon without biocidal treatment was more than 10^7 cells/cm^2 after a 7-day test. When treated with 100 ppm THPS, a 5 log reduction was achieved, which means that 99.999% of the SRB sessile cells were killed. D-tyr alone at a concentration of 100 ppm did not effectively disperse the sessile cells on the coupon surface, only decreasing to 10^6 cells/cm^2 SRB sessile cells. There were still 10^4 cells/cm^2 SRB sessile cells on the coupon surface when treated with 50 ppm THPS. However, with the addition of a binary combination of 50 ppm THPS + 1 ppm D-tyr, SRB sessile cells were undetectable. Again,

experimental data demonstrated that a biocide stress is needed for D-amino acid treatment of a tenacious biofilm.

The SEM observation shown in Figure 6-5 fully supported the data listed in Table 6-4. Figure 6-5A shows a large number of sessile cells on the coupon surface after a 7-day test without any treatment (control). When adding 100 ppm THPS, the sessile cells obviously decreased (6-5B). With the addition of only 100 ppm D-tyr, the sessile SRB cells were abundant (6-5C), and were similar to the untreated control (6-5A). However, the binary combination of 50 ppm THPS + 1 ppm D-tyr achieved almost complete biofilm prevention because no sessile cells could be seen in Figure 6-5D. However, confirmation by sessile cell count through MPN was needed and is shown below. D-tyr at only 1 ppm concentration effectively halved the dosage of THPS from 100 ppm to 50 ppm, which achieved an even better biofilm prevention as shown in Figures 6-5B and 6-5D.

6.2.2 Shock treatment to remove established biofilm

Shock treatment in this test was used to simulate the slug treatment with a certain contact time in the pipelines. To avoid the osmotic shock caused by the changing environment from the ATCC 1249 medium to a solution lacking ionic strength such as distilled water, a solution containing $MgSO_4$ and $(NH_4)_2Fe(SO_4)_2$, two salts, in the ATCC 1249 medium, was used.

Table 6-5 demonstrates that 100 ppm D-tyr alone slightly decreased the sessile cell count from 10^6 to 10^5 cells/cm^2, while 50 ppm THPS alone showed better efficacy with a 2 log reduction. However, the sessile cell count was undetectable when treated

with the combination of 50 ppm THPS + 1 ppm D-tyr, indicating a successful eradication of sessile cells. The same performance was obtained with 100 ppm THPS, suggesting that 1 ppm D-tyr could halve the THPS dosage. The data obtained from the 1-hour and 3-hour shock treatments were similar, indicating that 1 ppm D-tyr sufficiently improved the performance of 50 ppm THPS and that the test duration of 1 hour was adequate for the current test conditions.

The SEM observation shown in Figure 6-6 confirms the sessile cell count data in Table 6-5 for a 1-hour shock treatment. An abundant number of sessile cells were present after being in the solution containing $MgSO_4$ and $(NH_4)_2Fe(SO_4)_2$ at the same concentration as in the ATCC 1249 medium for 1 hour. There were still numerous sessile cells found on the coupon surface when treated with 50 ppm THPS alone for the 1-hour test. D-tyr at a concentration of 100 ppm was ineffective in dispersing the sessile cells as shown by the numerous cells remaining on the coupon surface. When adding 30 ppm THPS + 1 ppm D-tyr, the combination partially removed the sessile cells, and only a few sessile cells were visible on the coupon surface. Increasing the amount of THPS by using 50 ppm THPS + 1 ppm D-tyr, the sessile cells were barely detectable.

6.2.3 Discussion

Xu and Liu found that D-tyr could inhibit the secretion of EPS, achieving mitigation of membrane fouling, and disperse the attached biofilm without influencing the growth of the sessile cell (Xu and Liu, 2011). A low concentration of 3 mM of D-tyr was capable of effectively preventing the attachment of *P. aeruginosa* to the nanofiltration membrane surface. The growth of the planktonic *P. aeruginosa* was not

inhibited by D-tyr (Yu et al., 2012). In this study, our experimental results also confirmed that D-tyr had no effect on planktonic cell growth. The initial planktonic cell count was 10^6 cells/ml. After 7-day incubation, both the sessile cells treated with 100 ppm D-tyr and without treatment of D-tyr, increased to 10^8 cells/ml, indicating that the addition of D-tyr had no inhibiting effect on *D. vulgaris* growth.

D-ala is naturally found in the peptidoglycan of most bacteria, including both Gram-negative and Gram-positive bacteria (Lam et al., 2009). D-ala presented in significant quantities, appeared in the terminus of both DAP and Lys types of peptidoglycan. The possible explanation for the mechanism of how D-amino acids dispersed biofilm was that other D-amino acids substituted for the D-ala terminus of the peptidoglycan, resulted in the breakdown of the peptidoglycan of the cell wall. This tremendous change in the constitution of the cell wall finally triggered the biofilm dispersal (Kolodkin-Gal et al., 2010). In our experiment as shown in Figure 6-7, with the addition of a high concentration of D-ala into the binary combination of 50 ppm THPS + 1 ppm D-tyr biocide cocktail, the binary cocktail no longer was able to remove the sessile cells in comparison with those shown in Figure 6-6E. This interesting phenomenon suggests that in the presence of large amount of D-ala, D-tyr cannot replace the D-ala terminus in the SRB cell wall. The substitution of D-ala by D-tyr was interfered with the existence of high concentrations of D-ala.

Another interesting find in this work was that D-tyr alone had limitations in dispersing the SRB sessile cells, even at high concentrations of 100 ppm. This can be explained by the fact that SRB biofilms are far more tenacious than the reported fluffy

biofilm dispersed by D-amino acids alone. Only in the presence of a biocide stress, does a very small amount of D-tyr prove to be effective at biofilm dispersal. In this work, the binary combination of 50 ppm THPS + 1 ppm D-tyr succeed in preventing biofilm establishment and in removing established biofilm.

Table 6-4. Sessile cell counts on coupons taken from 7-day SRB cultures in ATCC 1249 medium mixed with different treatment chemicals to prevent SRB biofilm establishment (Xu et al., 2012).

Treatment	Sessile cell count (cells cm^{-2})
No treatment (control)	$\geq 10^7$
100 ppm D-tyr	$\geq 10^6$
50 ppm THPS	$\geq 10^4$
50 ppm THPS + 1 ppm D-tyr	<10
100 ppm THPS	$\geq 10^2$

Table 6-5. Sessile cell counts on coupons (initially covered with mature SRB biofilms) after undergoing 1-hour treatment and 3-hour treatment, respectively (Xu et al., 2012).

Treatment	Sessile cell count for 1-hour treatment (cells cm^{-2})	Sessile cell count for 3-hour treatment (cells cm^{-2})
No treatment (control)	$\geq 10^6$	$\geq 10^6$
100 ppm D-tyr	$\geq 10^5$	$\geq 10^5$
50 ppm THPS	$\geq 10^4$	$\geq 10^3$
50 ppm THPS + 1 ppm D- tyr	<10	<10
100 ppm THPS	<10	<10

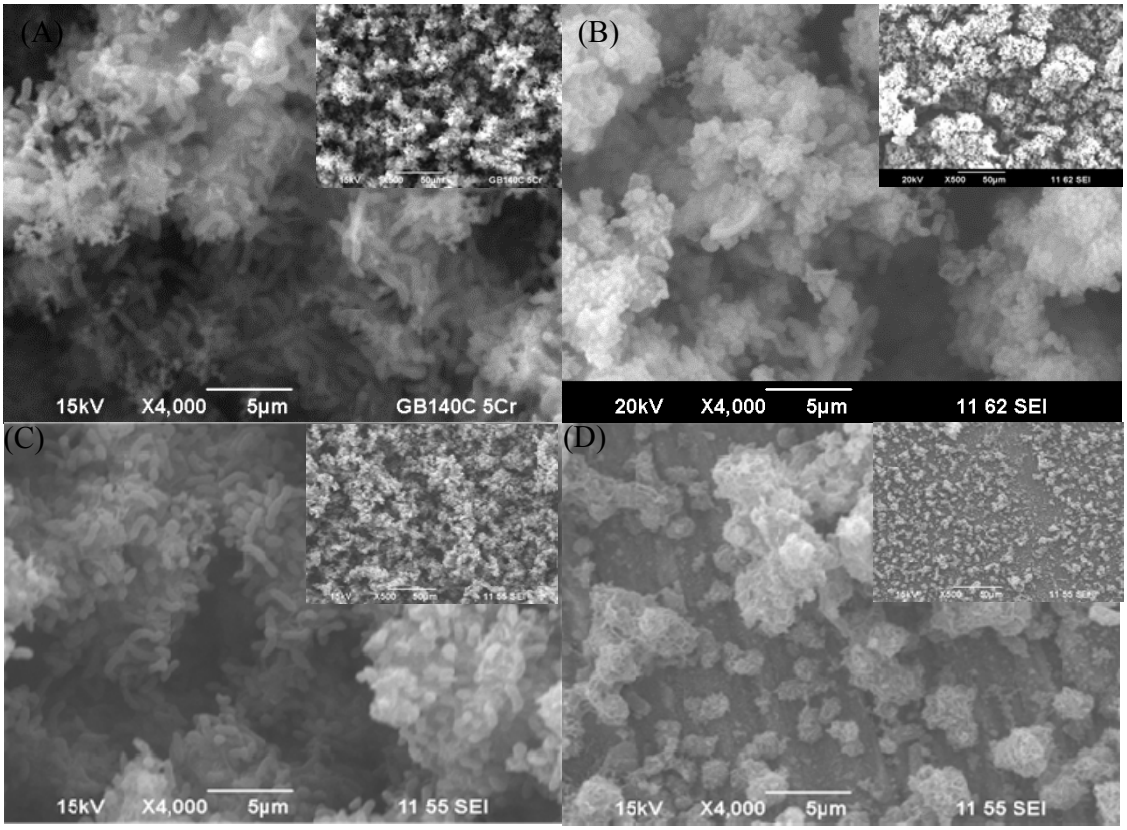

Figure 6-5. SEM images for 7-day coupons from SRB cultures in ATCC 1249 medium. (A) control with no treatment chemicals added to the culture medium, (B) 100 ppm THPS added, (C) 100 ppm D-tyr added, and (D) 50 ppm THPS + 1 ppm D-tyr added, respectively. Scale bars for the small inserted images are 50 µm (Xu et al. 2012).

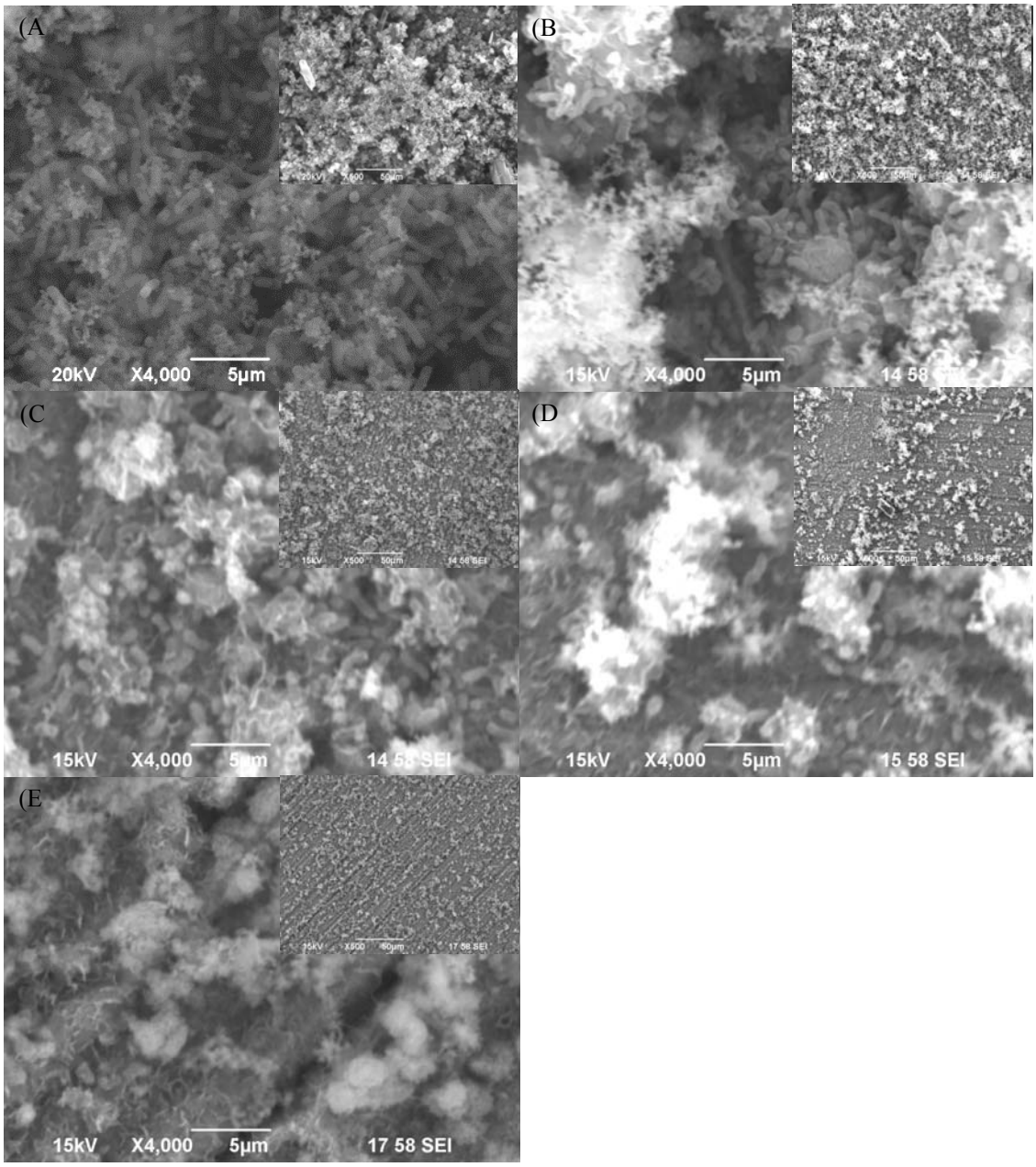

Figure 6-6. SEM images for coupons (initially covered with mature SRB biofilms) after undergoing 1-hour shock treatment. (A) Coupon treated with a solution containing $MgSO_4$ and $(NH_4)_2Fe(SO_4)_2$ at the same concentration as in the full strength culture medium (control), (B) treated with 50 ppm THPS, (C) treated with 100 ppm D-tyr, (D) treated with 30 ppm THPS + 1 ppm D-tyr, (E) treated with 50 ppm THPS + 1 ppm D-tyr, respectively. Scale bars for the small inserted images are 50 µm (Xu et al. 2012).

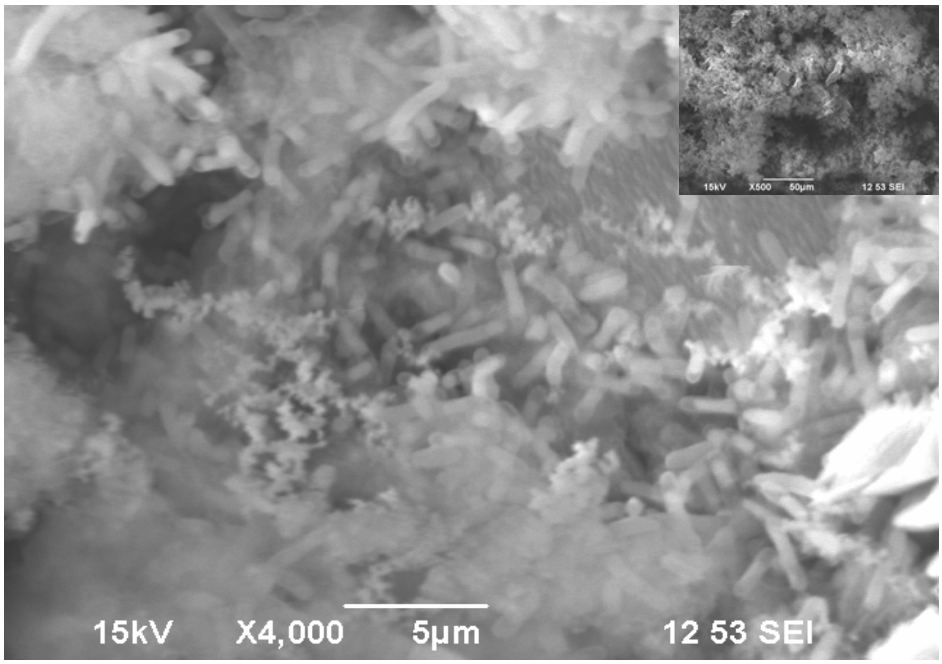

Figure 6-7. SEM images for coupons (initially covered with mature SRB biofilms) after undergoing 3-hour shock treatment with 50 ppm THPS + 1 ppm D-tyr + 1000 ppm D-ala. Scale bars for the small inserted images are 50 µm (Xu et al. 2012).

6.3 D-met as a biocide enhancer

D-methionine (D-met) is a green chemical that is readily biodegradable, and does not show any known OSHA hazards (Cooper, 1966; Leuchtenberger et al., 2005; Sigma, 2009). The test of feeding 1.16 g/day D-met in food showed no adverse effects for humans (Kies et al., 1975; Vuyyuri et al., 2008). D-met is also safe in nature compared with the unknown safety profile of D-tyr.

In this study, the SRB biofilm and MIC pitting corrosion mitigation effect of the binary combination of THPS + D-met was investigated. All the preparations and manipulations followed Xu et al. (2013b).

6.3.1 Prevention of SRB biofilm establishment

Table 6-6 shows the sessile *D. vulgaris* cell count data obtained in different treatments. THPS at 30 ppm had no preventive effect after a 7-day test, while 100 ppm D-met showed a slight dispersal effect because the sessile cell count decreased from 10^6 cells/cm^2 to 10^5 cells/cm^2. The treatment of 30 ppm THPS + 100 ppm D-met, 50 ppm THPS, and 50 ppm THPS + 10 ppm D-met, respectively, all yielded the same sessile cell counts of 10^4 cells/cm^2. A low concentration of 10 ppm D-met showed no enhanced inhibition with 50 ppm THPS; however, when D-met was increased to 50 ppm, the sessile cell counts decreased to 10^3 cells/cm^2. The best prevention effect of a 5 log reduction was obtained by further increasing D-met to 100 ppm combined with 50 ppm THPS. Under this treatment, sessile cells were barely detectable. This combination was even more effective than treatment with 100 ppm THPS alone given that the latter only achieved a 4 log reduction.

The SEM images shown in Figure 6-8 confirmed the data shown in Table 6-6. When treated with 100 ppm THPS alone and 500 ppm D-met alone, numerous sessile cells were present. When a combination of 50 ppm THPS and 100 ppm D-met was used, sessile cells could not be detected, suggesting that the successful prevention of SRB biofilm after a 7-day test have been achieved.

6.3.2 Removal of established biofilm

Figure 6-9 indicates that treatment of THPS alone at 500 ppm cannot effectively eradicate the sessile cells because some sessile cells remained on the coupon surface after 7 days. The sessile cells were abundant on the coupon surface when treated with 1000 ppm D-met alone. However, when treated with the binary combination of 50 ppm THPS and 100 ppm D-met, no sessile cells could be found on the coupon surface after a 7-day test, suggesting successful removal of established biofilm.

To simulate a less nutritious environment close to reality for treating established SRB biofilms, magnesium sulfate, sodium lactate, ferrous ammonium sulfate hexahydrate and yeast extract at concentrations 1/4 of those in the full ATCC 1249 medium were also used. In comparison with full ATCC 1249 medium, similar results were obtained in 1/4 strength medium as shown in Figure 6-10. Despite the biofilm being weaker than the biofilm in the full ATCC 1249 medium, 50 ppm THPS was still insufficient for eradicating the pre-established SRB biofilm. However, when treated with the binary combination of 50 ppm THPS + 100 ppm D-met, the pre-established biofilm was thoroughly removed.

The 3-hour shock treatment shown in Figure 6-11 confirmed the same trend. Only

the binary cocktail containing 50 ppm THPS + 100 ppm D-met effectively removed the pre-established SRB biofilm, and the efficacy was far better than 50 ppm THPS alone and 100 ppm D-met alone.

6.3.3 Mitigation of MIC pitting corrosion

Figure 6-12 shows the different surface morphologies of bare coupons after removing the corrosion products and biofilm under different treatments. When treated with 50 ppm THPS alone and with 500 ppm D-met alone, MIC pitting was not prevented as evidenced by the corroded carbon steel coupon surfaces. It is well known that biofilm is the major contributor to MIC pitting corrosion. Based on this, Figures 6-12A and 6-12B showed the consistency on sessile cell count data and biofilm SEM observation described above. The binary combination of 50 ppm THPS + 100 ppm D-met achieved MIC pitting corrosion mitigation, and no pits were found on the coupon surfaces. The normalized weight loss confirmed the mitigation of MIC pitting corrosion because the binary combination of 50 ppm THPS + 100 ppm D-met resulted in the lowest weight loss of 0.00045±0.00008 g/cm^2 as shown in Figure 6-13. The treatment of 50 THPS alone yielded an average weight loss of 0.00065±0.00005 g/cm^2. The P value (t-test) from these two treatments was 0.012, which was smaller than the 0.05 threshold for statistical significance.

6.3.4 Discussion

Table 6-7 indicates that 100 ppm D-met alone failed to suppress planktonic SRB growth. This phenomenon was consistent with the literature mentioned in Chapter 2, indicating that D-amino acids alone had no impact on planktonic cell growth. Further

addition of D-met did not enhance the efficacy of THPS against planktonic SRB growth, suggesting that D-met was not biocidal but rather the signal molecule, and was only effective for sessile cell dispersion.

Currently, chemical synthesis of a 50:50 mixture of D/L-met is used to supply D/L-met. The production of D-met is presently through the enzymatic catalyzed conversion of D- to L-met. If L-met does not interfere with D-met efficacy, D/L-met could replace pure D-met due to its cheaper cost. Thus, it is desirable to prove that L-met poses no adverse effect in biofilm mitigation. Figure 6-14 verifies that L-met was not able to enhance the THPS efficacy against SRB sessile cells because it is not a signal molecule to disperse SRB biofilm. When the SRB biofilm was treated with a 50:50 mixture of D/L-met, the synergy of THPS and D-met was still observed, indicating that L-met did not interfere with the dispersal ability of D-met.

As expected, with the addition of a high concentration of D-ala (1000 ppm), the synergistic effect of 50 ppm THPS + 100 ppm D-met was inhibited. This is because the high concentration of D-ala interfered with the displacement of D-ala in the peptidoglycan in the SRB cell walls by D-met. This result is consistent with Kolodkin-Gal et al. (2010). They proposed that the working mechanism for D-met was that D-met substituted the D-ala terminus in the peptidoglycan of the bacterial cell wall. They also reported that with the existence of high concentrations of D-ala, the signal effect and substitution of D-met to D-ala were interfered, resulting in loss of dispersal ability of the D-met for SRB biofilm.

Table 6-6. Sessile cell counts in ATCC 1249 medium 7 days after using different treatment methods to prevent SRB biofilm establishment (Xu et al., 2013b).

Treatment	Sessile cell count (cells/cm^2)
No treatment	$\geq 10^6$
30 ppm THPS	$\geq 10^6$
100 ppm D-met	$\geq 10^5$
30 ppm THPS + 100 ppm D-met	$\geq 10^4$
50 ppm THPS	$\geq 10^4$
50 ppm THPS + 10 ppm D-met	$\geq 10^4$
50 ppm THPS + 50 ppm D-met	$\geq 10^3$
100 ppm THPS	$\geq 10^2$
50 ppm THPS + 100 ppm D-met	≤ 10

Table 6-7. Planktonic cell counts in ATCC 1249 medium 7 days after using different treatment methods to prevent SRB biofilm establishment (Xu et al., 2013b).

Treatment	Planktonic cell count (cells/ml)
No treatment	$\geq 10^8$
100 ppm D-met	$\geq 10^8$
50 ppm THPS	$\geq 10^2$
50 ppm THPS + 100 ppm D-met	$\geq 10^2$

*Initial cell concentration was 10^6 cells/ml and the experiment was repeated three times.

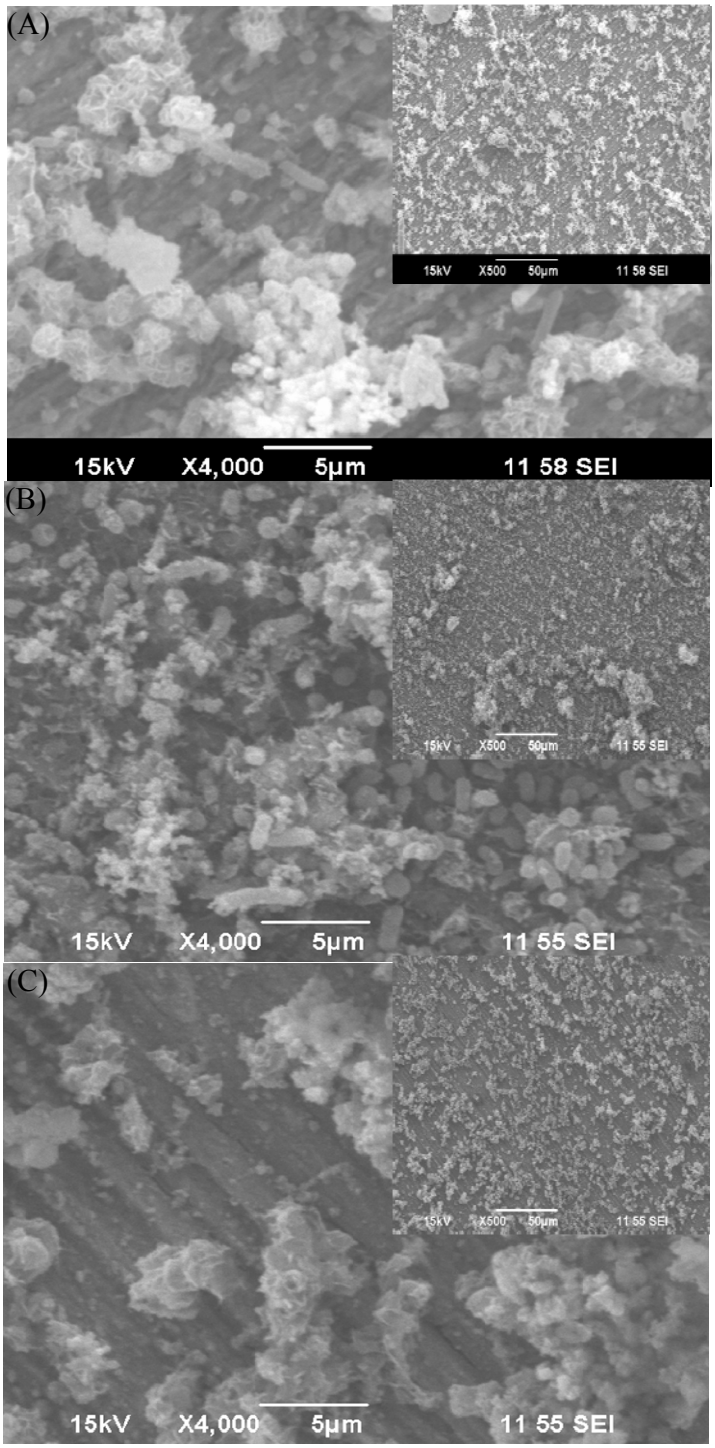

Figure 6-8. SEM images for 7-day coupons in SRB cultures with ATCC 1249 medium treated with (A) 100 ppm THPS, (B) 500 ppm D-met, and (C) 50 ppm THPS + 100 ppm D-met, respectively (Xu et al., 2013b). Scale bars for the small inserted images are 50 µm.

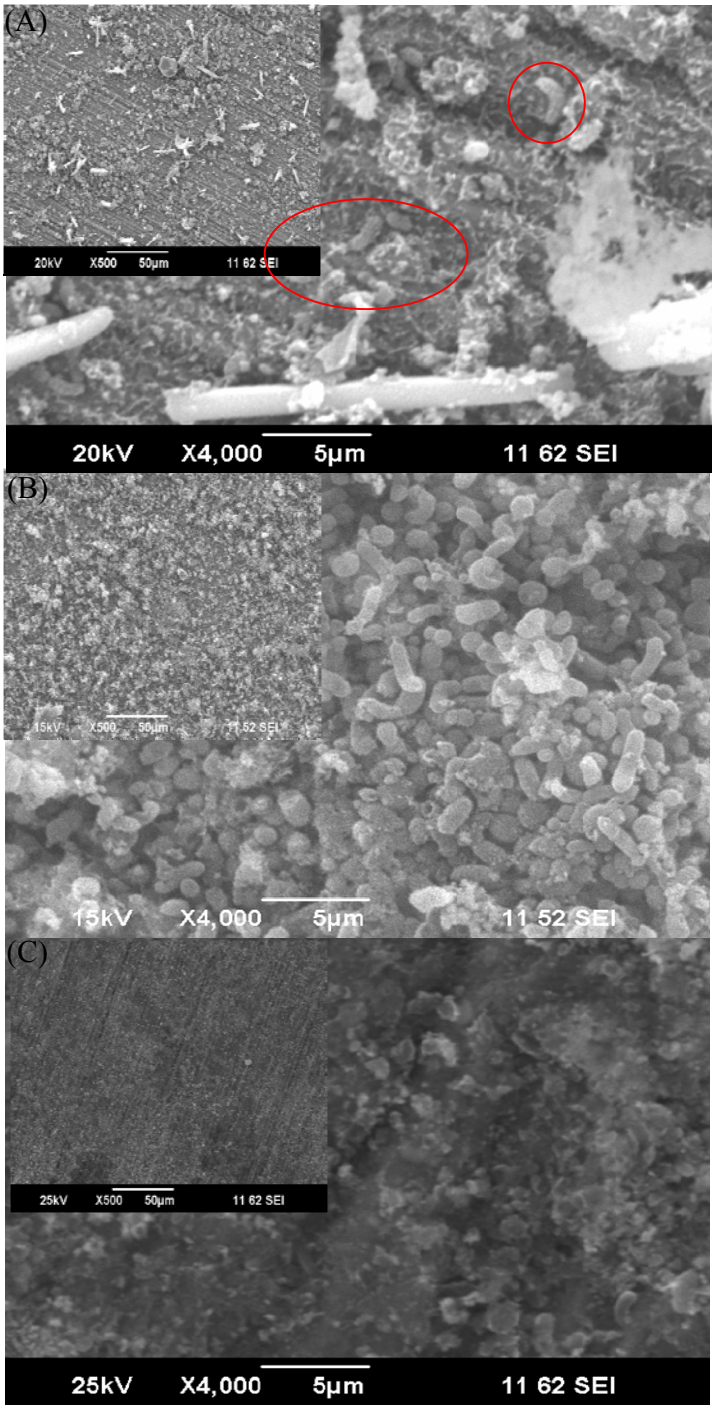

Figure 6-9. SEM images for coupons (initially covered with established biofilms) in ATCC 1249 medium after they were treated for 7 days with (A) 500 ppm THPS, (B) 1000 ppm D-met, and (C) 50 ppm THPS + 100 ppm D-met, respectively (Xu et al., 2013b). Scale bars for the small inserted images are 50 µm. Circle indicates SRB sessile cell location.

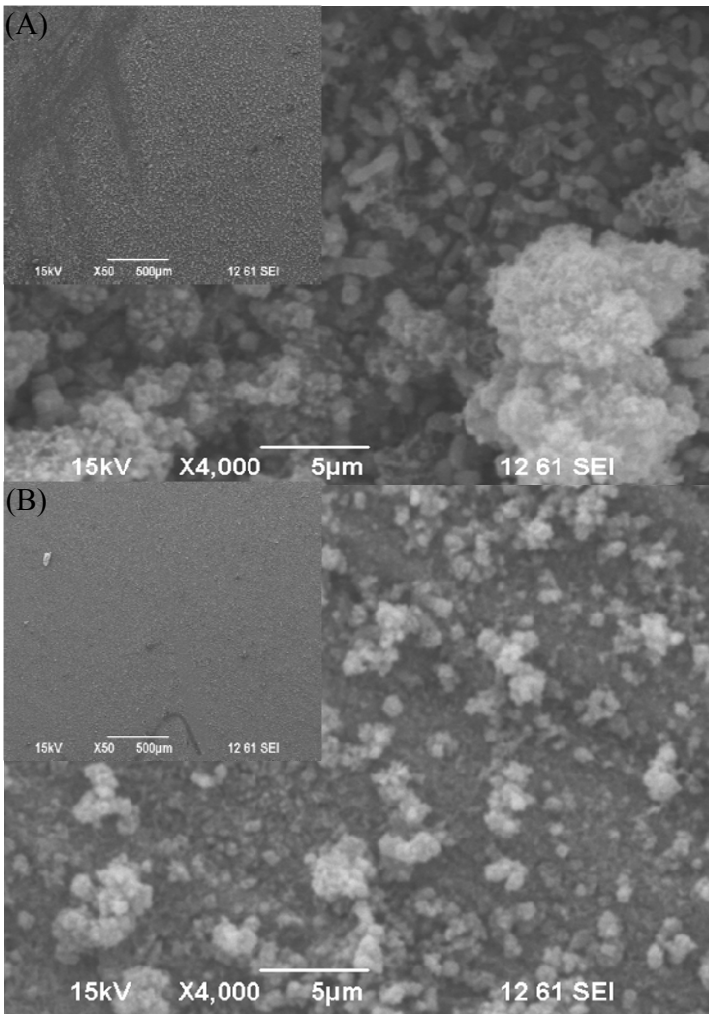

Figure 6-10. SEM images for coupons (initially covered with established biofilms) in 1/4 strength medium after they were treated for 7 days with (A) 50 ppm THPS, (B) 50 ppm THPS + 100 ppm D-met, respectively (Xu et al. 2013b). Scale bars for the small inserted images are 500 µm.

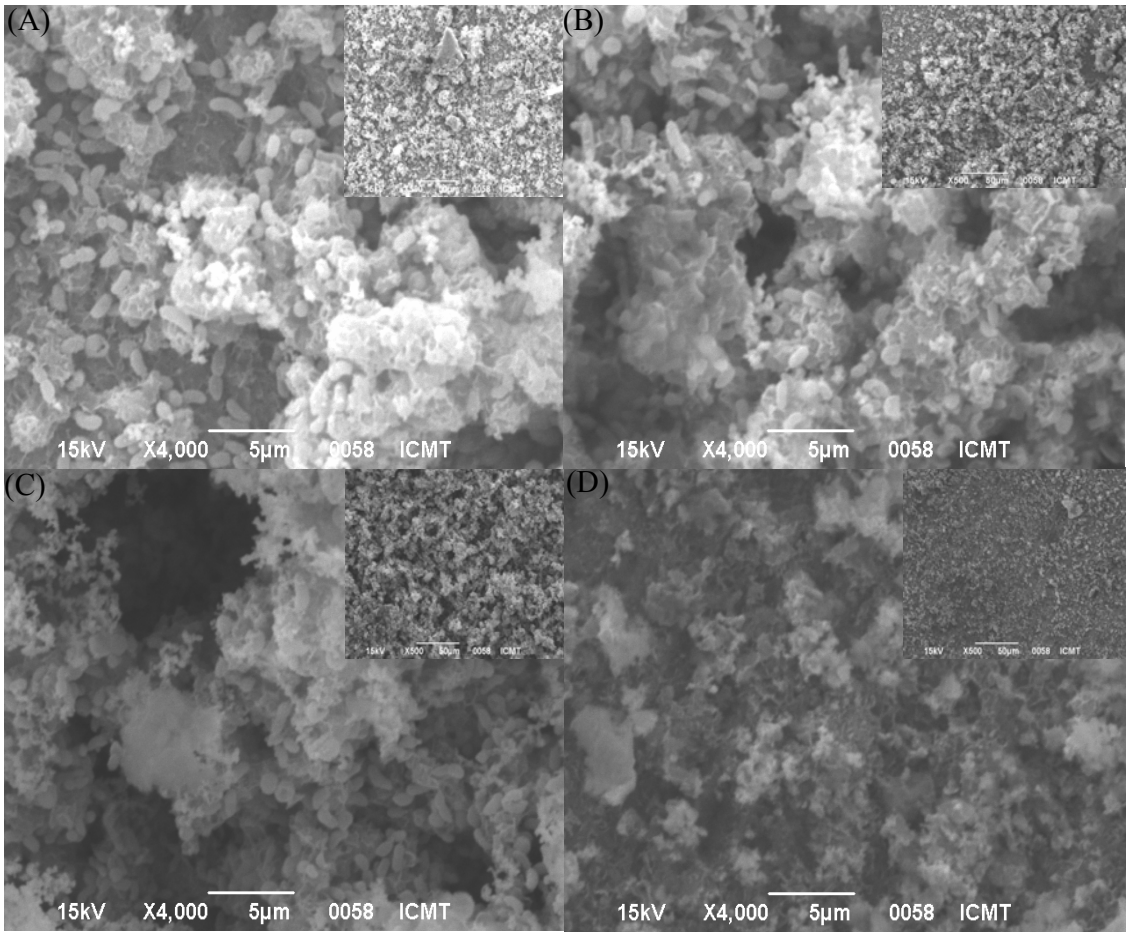

Figure 6-11. SEM images for coupons (initially covered with established biofilms) after being soaked for 3 hours in (A) deoxygenated water, (B) 50 ppm THPS, (C) 500 ppm D-met treatment, (D) 50 ppm THPS + 100 ppm D-met, resepctively (Xu et al. 2013b). Scale bars for the small inserted images are 50 μm.

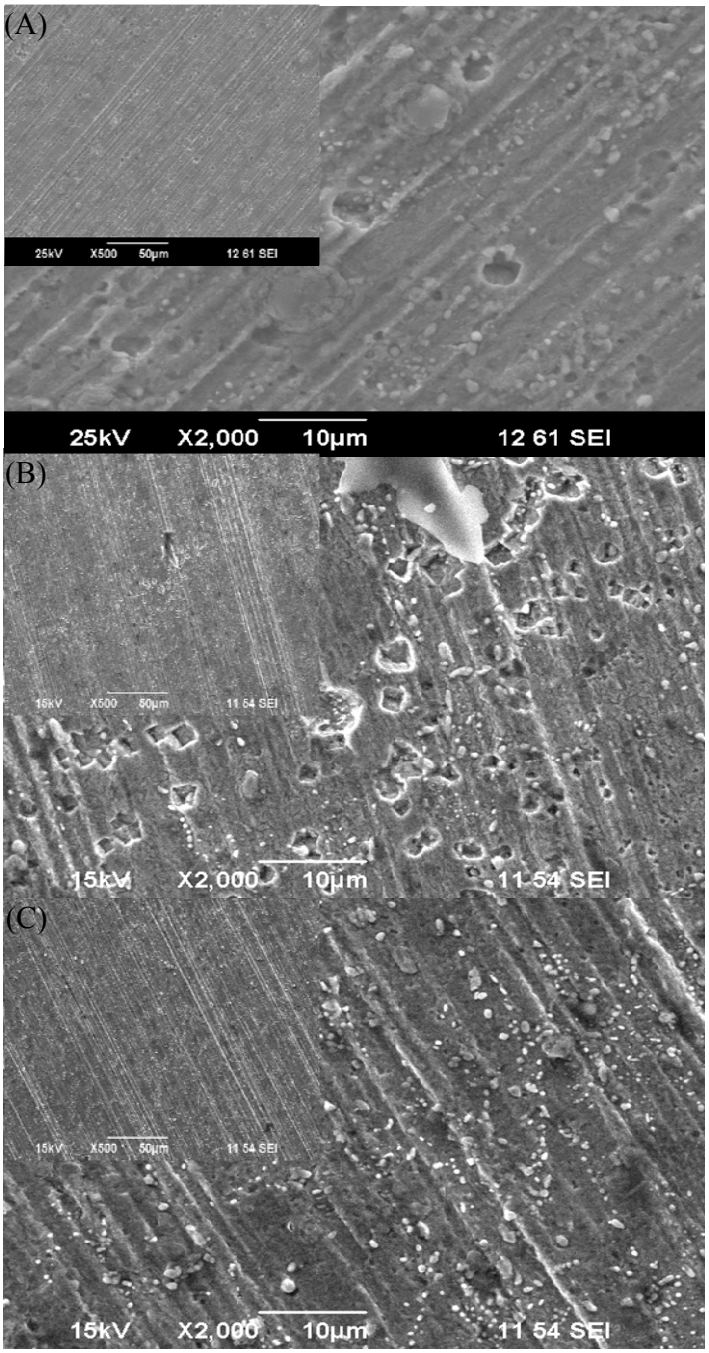

Figure 6-12. SEM images of coupon surfaces after biofilm removal for coupons obtained from ATCC 1249 medium 7 days after treatment with (A) 50 ppm THPS treatment, (B) 500 ppm D-met treatment, and (C) with 50 ppm THPS + 100 ppm D-met, respectively (Xu et al., 2013b). Scale bars for the small inserted images are 50 µm.

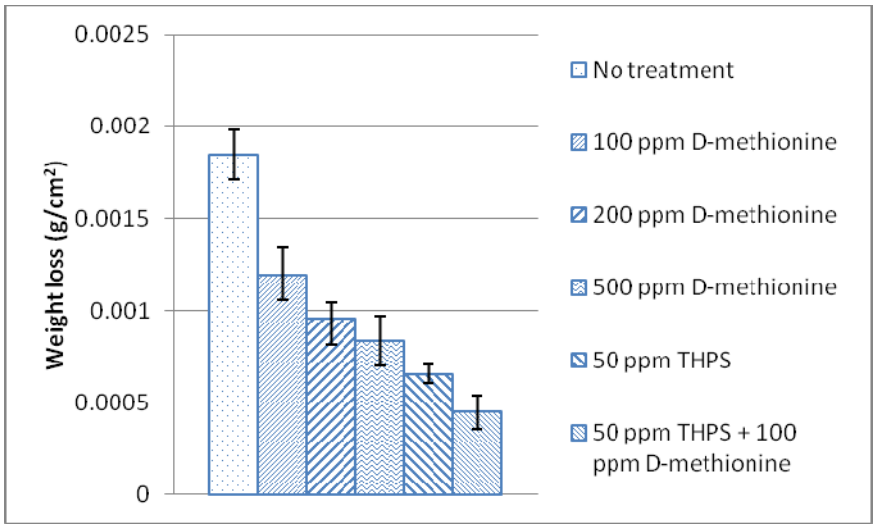

Figure 6-13. Normalized weight loss data based on exposed coupon surface areas for different treatment methods in the mitigation of MIC pitting at 37°C in ATCC 1249 medium for 7 days. Each data point was the average of the data from at least five coupons. Error bars represent standard deviations (Xu et al., 2013b).

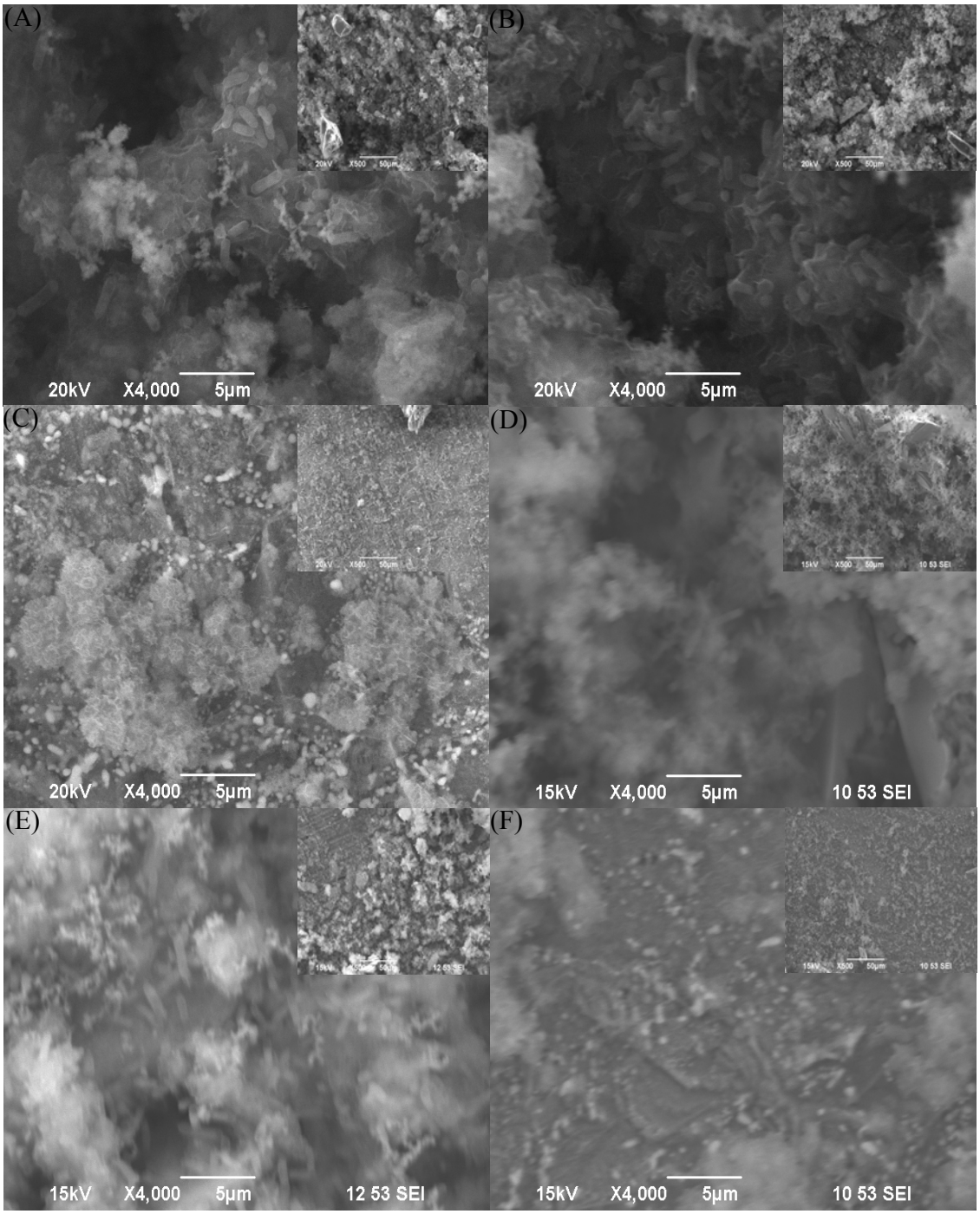

Figure 6-14. SEM images for coupons (initially covered with established biofilms) after being soaked for 3 hours in (A) 50 ppm THPS, (B) 500 ppm D-met, (C) 50 ppm THPS + 100 ppm D-met, (D) 50 ppm THPS + 100 ppm L-met, (E) 50 ppm THPS + 100 ppm D-met + 1000 ppm D-ala, and (F) 50 ppm THPS + 100 ppm D-met + 100 ppm L-met, respectively (Xu et al. 2013b). Scale bars for the small inserted images are 50 µm.

CHAPTER 7 CONCLUSION

Lab investigation of MIC caused by *B. licheniformis* confirmed that NRB could cause severe MIC pitting on C1018 carbon steel in anaerobic conditions. The BCNR mechanism successfully explains the "why and how" of MIC caused by *B. licheniformis* from the aspect of bioenergetics and EET. The BCSR theory was fully supported by the electron mediator test using riboflavin and FAD and biofilm starvation test using *D. vulgaris*, which were designed to verify the electron transfer pathway and bioenergetics proposed in BCSR. The *B. licheniformis* test and *D. vulgaris* proved the validity of the foundation of Type I MIC mechanism proposed by Ohio University MIC Group. Details of how electron transfer occurs from an iron surface to the cytoplasm are needed to fully understand Type I MIC. The pathway of how electron mediators shuttle the electrons to pass into/out of the cell membrane is also worth further research.

D-amino acid mixture consisting of D-tyr, D-met, D-trp and D-leu was capable of significantly enhancing the efficacy of binary combinations of biocide and the chelator, EDDS. Individual D-tyr at the concentration of 1 ppm demonstrated considerable enhancement of THPS when treating on SRB biofilms. D-met also showed its potent biofilm dispersal ability at the concentration of 100 ppm combined with 50 ppm THPS. It should be pointed out that glutaraldehyde is not a suitable choice for D-amino acids because it is a cross-linking agent that renders D-amino acids ineffective. Additional combinations of different D-amino acids, including those unreported ones should also be tested for both biofilm prevention and removal tests. A combination with better efficacy and lower effective dosage is desired. Such further research will promote greener and

much efficient treatment for treatment of biofilm mitigation. It is expected that different D-amino acid combinations may be needed for different field biofilm consortia and a mixture likely works better than a single D-amino acid used as a biocide enhancer.

REFERENCES

Abedi, S.S., Abdolmaleki, A., Adibi, N., 2007. Failure analysis of SCC and SRB induced cracking of a transmission oil products pipeline. Eng. Fail. Anal. 14, 250–261.

Axelsen, S.B., Rogne, T., 1998. Do micro-organisms "eat" metal?" Microbiologically influenced corrosion of industrial materials (Contract No. BRRT-CT98-5084).

Bade, K., Manz, W., Szewzyk, U., 2000. Behavior of sulfate reducing bacteria under oligotrophic conditions and oxygen stress in particle-free systems related to drinking water. Fems Microbiol. Ecol. 32, 215–223.

Baena, S., Fardeau, M.L., Labat, M., Ollivier, B., Garcia, J.L., Patel, B.K., 1998. *Desulfovibrio aminophilus* sp. nov., a novel amino acid degrading and sulfate reducing bacterium from an anaerobic dairy wastewater lagoon. Syst. Appl. Microbiol. 21, 498–504.

Bagarinao, T., Vetter, R.D., 1989. Sulfide tolerance and detoxification in shallow-water marine fishes. Mar. Biol. 103, 291–302.

Beech, I.B., Gaylarde, C.C., 1999. Recent advances in the study of biocorrosion: an overview. Rev. Microbiol. 30, 117–190.

Berg, J.M., Tymoczko, J.L., Stryer, L., 2002. Section 14.1, Metabolism is composed of many coupled, interconnecting reactions. in: Biochemistry. 5th edition. New York: W H Freeman. Available from: http://www.ncbi.nlm.nih.gov/books/NBK22439/

Bhat, S., Sharma, V.K., Thomas, S., Anto, P.F., Singh, S.K., 2011. 8-in pipeline from group gathering station to central tank farm. Mater. Perform. 50, 50–53.

Biswas, S., Bose, P., 2005. Zero-valent iron-assisted autotrophic denitrification. J. Environ. Eng. 131, 1212–1220.

Canstein, H. von., Ogawa, J., Shimizu, S., Lloyd, J.R., 2008. Secretion of flavins by Shewanella species and their role in extracellular electron transfer. Appl. Environ. Microbiol. 74, 615–623.

Carew, J., Al-Hashem, A., El-Mohemeed, E., Al-Enezi, H., 2009. North Kuwait oil field sea water flood experience in pipeline integrity management program, in: Corrosion/2009 Paper No. 09117. NACE International, Houston, TX.

Carlson, C.A., Ingraham, J.L., 1983. Comparison of denitrification by *Pseudomonas stutzeri*, *Pseudomonas aeruginosa*, *and Paracoccus denitrificans*. Appl. Environ. Microbiol. 45, 1247–1253.

Castelle, C., Guiral, M., Malarte, G., Ledgham, F., Leroy, G., Brugna, M., Giudici-Orticoni, M.-T., 2008. A new iron-oxidizing/O_2-reducing supercomplex spanning both inner and outer membranes, isolated from the extreme acidophile *Acidithiobacillus ferrooxidans*. J. Biol. Chem. 283, 25803–25811.

Cava, F., Lam, H., de Pedro, M., Waldor, M., 2011. Emerging knowledge of regulatory roles of D-amino acids in bacteria. Cell. Mol. Life Sci. 68, 817–831.

Chan, K.-Y., Xu, L.-C., Fang, H.H.P., 2002. Anaerobic Electrochemical corrosion of mild steel in the presence of extracellular polymeric substances produced by a culture enriched in sulfate-reducing bacteria. Environ. Sci. Technol. 36, 1720–1727.

Chen, F., Johns, M., 1996. Relationship between substrate inhibition and maintenance energy of *Chlamydomonas reinhardtii* in heterotrophic culture. J. Appl. Phycol. 8, 15–19.

Chen, G.-W., Choi, S.-J., Lee, T.-H., Lee, G.-Y., Cha, J.-H., Kim, C.-W., 2008. Application of biocathode in microbial fuel cells: cell performance and microbial community. Appl. Microbiol. Biotechnol. 79, 379–388.

Cooper, S., 1966. Utilization of D-Methionine by *Escherichia Coli*. J. Bacteriol. 92, 328–332.

Costerton, J.W., 2007. The Biofilm Primer, 1st ed. Springer, Berlin-New York, pp. 3–85.

Cournet, A., Délia, M.-L., Bergel, A., Roques, C., Bergé, M., 2010. Electrochemical reduction of oxygen catalyzed by a wide range of bacteria including Gram-positive. Electrochem. Commun. 12, 505–508.

Davis, F., Higson, S.P.J., 2007. Biofuel cells--recent advances and applications. Biosens. Bioelectron. 22, 1224–1235.

Donlan, R.M., 2002. Biofilms: Microbial Life on Surfaces. Emerg. Infect. Dis. 8, 881–890.

Du, Z., Li, H., Gu, T., 2007. A state of the art review on microbial fuel cells: A promising technology for wastewater treatment and bioenergy. Biotechnol. Adv. 25, 464–482.

Dunsmore, B., Whitfield, T., Lawson, P.A., Collins, M.D., 2004. Corrosion by Sulfate Reducing Bacteria that Utilize Nitrate, in: Corrosion/2004 Paper No. 04763. NACE International, Houston, TX.

Feio, M.J., Reis, M.A., Lino, A.R., Rainha, V., Fonseca, I.T.E., 2000. The Influence of the *Desulfovibrio desulfuricans* 14 ATCC 27774 on the corrosion of mild steel. Mater. Corros. 51, 691–697.

Fischer, M., Bacher, A., 2008. Biosynthesis of vitamin B2: Structure and mechanism of riboflavin synthase. Arch. Biochem. Biophys. 474, 252–265.

Flemming, H.-C., 1996. Biofouling and microbiologically influenced corrosion (MIC)-an economic and technical overview, in: Heitz, E., Sand W., and Flemming. H.-C. (eds.), Microbial Deterioration of Materials. Springer-Verlag, Berlin-New York, pp. 5–14.

Folmsbee, M., Duncan, K., Han, S.O., Nagle, D., Jennings, E., McInerney, M., 2006. Re-identification of the halotolerant, biosurfactant-producing *Bacillus licheniformis* strain JF-2 as Bacillus mojavensis strain JF-2. Syst. Appl. Microbiol. 29, 645–649.

Friedman, M., 2010. Origin, microbiology, nutrition, and pharmacology of D-Amino Acids. Chem. Biodivers. 7, 1491–1530.

Fukui, M., Takii, S., 1990. Survival of sulfate-reducing bacteria in oxic surface sediment of a seawater lake. Fems Microbiol. Lett. 73, 317–322.

Gardner, L.R., Stewart, P.S., 2002. Action of glutaraldehyde and nitrite against sulfate-reducing bacterial biofilms. J. Ind. Microbiol. Biotechnol. 29, 354–360.

Geets, J., Borremans, B., Diels, L., Springael, D., Vangronsveld, J., van der Lelie, D., Vanbroekhoven, K., 2006. DsrB gene-based DGGE for community and diversity surveys of sulfate-reducing bacteria. J. Microbiol. Methods 66, 194–205.

Ghafari, S., Hasan, M., Aroua, M.K., 2008. Bio-electrochemical removal of nitrate from water and wastewater—A review. Bioresour. Technol. 99, 3965–3974.

Gieg, L., Jack, T., Foght, J., 2011. Biological souring and mitigation in oil reservoirs. Appl. Microbiol. Biotechnol. 92, 263–282.

Ginner, J.L., Alvarez, P.J.J., Smith, S.L., Scherer, M.M., 2004. Nitrate and nitrite reduction by Fe^0: influence of mass transport, temperature, and denitrifying microbes. Environ. Eng. Sci. 21, 219–229.

Gu, T., 2012. New understandings of biocorrosion mechanisms and their classifications. J. Microb. Biochem. Technol. 04, 3–6.

Gu, T., Xu, D., 2010. Demystifying MIC mechanisms, in: Corrosion/2010 Paper No. 10213. NACE International, Houston, TX.

Gu, T., Zhao, K., Nesic, S., 2009. A practical mechanistic model for MIC based on a biocatalytic cathodic sulfate reduction (BCSR) theory, in: Corrosion/2009 Paper No. 09390. NACE International, Houston, TX.

Gu, T., Xu, D., 2013. Why are some microbes corrosive and some not? in: Corrosion/2013 Paper No. C2013-0002336. NACE International, Houston, TX.

Halim, A., Gubner, R., Watkin, E., 2011. Preliminary study on nitrate injection to control souring problem in oil reservoir:benefits and side effects on steel material, in: Corrosion/2011 Paper No. 11229. NACE International, Houston, TX.

Hall-Stoodley, L., Costerton, J.W., Stoodley, P., 2004. Bacterial biofilms: from the Natural environment to infectious diseases. Nat. Rev. Microbiol. 2, 95–108.

Hamilton, W.A., 1998a. Sulfate-reducing bacteria: Physiology determines their environmental impact. Geomicrobiol. J. 15, 19–28.

Hamilton, W.A., 1998b. Bioenergetics of sulphate-reducing bacteria in relation to their environmental impact. Biodegradation 9, 201–212.

He, Z., Angenent, L.T., 2006. Application of bacterial biocathodes in microbial fuel cells. Electroanalysis 18, 2009–2015.

Heidelberg, J.F., Seshadri, R., Haveman, S.A., Hemme, C.L., Paulsen, I.T., Kolonay, J.F., Eisen, J.A., Ward, N., Methe, B., Brinkac, L.M., Daugherty, S.C., Deboy, R.T., Dodson, R.J., Durkin, A.S., Madupu, R., Nelson, W.C., Sullivan, S.A., Fouts, D., Haft, D.H., Selengut, J., Peterson, J.D., Davidsen, T.M., Zafar, N., Zhou, L., Radune, D., Dimitrov, G., Hance, M., Tran, K., Khouri, H., Gill, J., Utterback, T.R., Feldblyum, T.V., Wall, J.D., Voordouw, G., Fraser, C.M., 2004. The genome sequence of the anaerobic, sulfate-reducing bacterium *Desulfovibrio vulgaris* Hildenborough. Nat. Biotechnol. 22, 554–559.

Henstra, A.M., Dijkema, C., Stams, A.J.M., 2007. Archaeoglobus fulgidus couples CO oxidation to sulfate reduction and acetogenesis with transient formate accumulation. Environ. Microbiol. 9, 1836–1841.

Hernandez, M.E., Newman, D.K., 2001. Extracellular electron transfer. Cell. Mol. Life Sci. 58, 1562–1571.

Pereira, Inês, A.C., Haveman, S.A., Voordouw, G., 2007. Biochemical, genetic and genomic characterization of anaerobic electron transport pathways in sulfate-reducing Delta proteobacteria, in: Sulphate-Reducing Bacteria: Environmental

and Engineered Systems, Barton, L.L., Hamilton, W.A., (eds.), Cambriged: Cambridge University Press, pp 215-240.

Inoue, K., Qian, X., Morgado, L., Kim, B.-C., Mester, T., Izallalen, M., Salgueiro, C.A., Lovley, D.R., 2010. Purification and characterization of OmcZ, an outer-surface, octaheme c-type cytochrome essential for optimal current production by *Geobacter sulfurreducens*. Appl. Environ. Microbiol. 76, 3999–4007.

Jacobson, G.A., 2007. Corrosion at prudhoe bay: a lesson on the line. Mater. Perform. 46, 26–34.

Jahn, A., Nielsen, P.H., 1998. Cell biomass and exopolymer composition in sewer biofilms. Water Sci. Technol. 37, 17–24.

Jeanthon, C., L'Haridon, S., Cueff, V., Banta, A., Reysenbach, A.-L., Prieur, D., 2002. *Thermodesulfobacterium hydrogeniphilum* sp. nov., a thermophilic, chemolithoautotrophic, sulfate-reducing bacterium isolated from a deep-sea hydrothermal vent at Guaymas Basin, and emendation of the genus Thermodesulfobacterium. Int. J. Syst. Evol. Microbiol. 52, 765–772.

Kane, R.D., 1985. Roles of H_2S in behaviour of engineering alloys. Int. Met. Rev. 30, 291–301.

Karim, S., Mustafa, C.M., Assaduzzaman Md., Mayeedui Islam, 2010. Effect of nitrate ion on corrosion inhibition of mild steel in simulated cooling water, Chem. Eng. Res. Bull. 14, 87–91.

Keasler, V., Bennett, B., Bromage, B., Franco, R.J., Lefevre, D., Shafer, J., Moninuola, B., 2010. Bacterial characterization and biocide qualification for full well stream crude oil pipelines, in: Corrosion/2010 Paper No. 10250. NACE International, San Antonio, TX.

Kies, C., Fox, H., Aprahamian, S., 1975. Comparative value of L-, and D-methionine supplementation of an oat-based diet for humans. J. Nutr. 105, 809–814.

G.H. Koch, M.P.H. Brongers, N.G. Thompson, Y.P. Virmani, J.H. Payer, 2001. Corrosion costs and preventive strategies in the United States. FHWA-RD-01–156, Federal Highway Administration, Washington, D.C..

Kolodkin-Gal, I., Romero, D., Cao, S., Clardy, J., Kolter, R., Losick, R., 2010. D-amino acids trigger biofilm disassembly. Science 328, 627–629.

Konno, R., Bruckner, H., D'Aniello, A., Fisher, G.H., Fujii, N. (eds.), 2009. D-amino acids practical methods and protocols: Analytical Methods for D-Amino Acids. Nova Science Pub Inc.

Korenblum, E., Valoni, E., Penna, M., Seldin, L., 2010. Bacterial diversity in water injection systems of Brazilian offshore oil platforms. Appl. Microbiol. Biotechnol. 85, 791–800.

Lam, H., Oh, D.-C., Cava, F., Takacs, C.N., Clardy, J., de Pedro, M.A., Waldor, M.K., 2009. D-Amino acids govern stationary phase cell wall remodeling in bacteria. Science 325, 1552–1555.

Larsen, J., Rasmussen, K., Pedersen, H., Sorensen, K., Lundgaard, T., Skovhus, L.T., 2010. Consortia of MIC bacteria and archaea cauing pitting corrosion in top side oil production facilities, in: Corrosion/2010 Paper No. 10252. NACE International, Houston, TX.

Lee, D.-J., Pan, X., Wang, A., Ho, K.-L., 2013. Facultative autotrophic denitrifiers in denitrifying sulfide removal granules. Bioresour. Technol. 132, 356–360.

Lee, W., Lewandowski, Z., Nielsen, P.H., Hamilton, W.A., 1995. Role of sulfate-reducing bacteria in corrosion of mild steel: A review. Biofouling 8, 165–194.

Leuchtenberger, W., Huthmacher, K., Drauz, K., 2005. Biotechnological production of amino acids and derivatives: current status and prospects. Appl. Microbiol. Biotechnol. 69, 1–8.

Little B J, Ray, R.I., Pope, R.K., 2000. The relationship between corrosion and the biological sulfur cycle, in: Corrosion/2000 Paper No. 00394. NACE International, Houston, TX.

Little, B., Wagner, P., 1997. Myths related to microbiologically influenced corrosion. Mater. Perform. 36, 40–44.

Little, B.J., Ray, R.I., Pope, R.K., 2000. Relationship between corrosion and the biological sulfur cycle: a review. Corrosion 56, 433–443.

Lloyd, J.R., Ridley, J., Khizniak, T., Lyalikova, N.N., Macaskie, L.E., 1999. Reduction of technetium by *Desulfovibrio desulfuricans*: biocatalyst characterization and use in a flow through bioreactor. Appl. Environ. Microbiol. 65, 2691–2696.

Logan, B.E., Hamelers, B., Rozendal, R., Schröder, U., Keller, J., Freguia, S., Aelterman, P., Verstraete, W., Rabaey, K., 2006. Microbial fuel cells: methodology and technology. Environ. Sci. Technol. 40, 5181–5192.

López, M.A., Javier Zavala Díaz de la Serna, F., Jan-Roblero, J., Romero, J.M., Hernández-Rodríguez, C., 2006. Phylogenetic analysis of a biofilm bacterial population in a water pipeline in the Gulf of Mexico. Fems Microbiol. Ecol. 58, 145–154.

Lovley, D.R., 2006. Microbial fuel cells: novel microbial physiologies and engineering approaches. Curr. Opin. Biotechnol. 17, 327–332.

Lovley, D.R., Phillips, E.J.P., 1994. Novel processes for anaerobic sulfate production from elemental sulfur by sulfate-reducing bacteria. Appl. Environ. Microbiol. 60, 2394–2399.

Mah, T.-F.C., O'Toole, G.A., 2001. Mechanisms of biofilm resistance to antimicrobial agents. Trends Microbiol. 9, 34–39.

Maloy, J.T., 1985. Nitrogen, phosphorus, arsenic, antimony, and bismuth, in: Standard potentials in aqueous solution, Monographs in electroanalytical chemistry and electrochemistry, Bard, A.J., Parsons, R., Jordan, J., (eds.), New York: M. Dekker, pp 127–188.

Martín-Gil, J., Ramos-Sánchez, M.C., Martín-Gil, F.J., 2004. *Shewanella putrefaciens* in a fuel-in-water emulsion from the Prestige oil spill. Antonie Van Leeuwenhoek 86, 283–285.

McLeod, E.S., MacDonald, R., Brozel, V.S., 2004. Distribution of *Shewanella putrefaciens* and *Desulfovibrio vulgaris* in sulphidogenic biofilms of industrial cooling water systems determined by fluorescent in situ hybridisation. Water SA 28, 123–128.

McNeil, M.B., Jones, J.M., Little, B.J., 1991. Production of sulfide minerals by sulfate-reducing bacteria during microbiologically influenced corrosion of copper. DTIC Document.

Minz, D., Flax, J.L., Green, S.J., Muyzer, G., Cohen, Y., Wagner, M., Rittmann, B.E., Stahl, D.A., 1999. Diversity of sulfate-reducing bacteria in oxic and anoxic regions of a microbial mat characterized by comparative analysis of dissimilatory sulfite reductase genes. Appl. Environ. Microbiol. 65, 4666–4671.

Mishra, M., Jain, S., Thakur, A.R., RayChaudhuri, S., 2013. Microbial community in packed bed bioreactor involved in nitrate remediation from low level radioactive waste. J. Basic Microbiol. (In Press).

Monteny, J., Vincke, E., Beeldens, A., De Belie, N., Taerwe, L., Van Gemert, D., Verstraete, W., 2000. Chemical, microbiological, and in situ test methods for biogenic sulfuric acid corrosion of concrete. Cem. Concr. Res. 30, 623–634.

Muyzer, G., Stams, A.J.M., 2008. The ecology and biotechnology of sulphate-reducing bacteria. Nat. Rev. Microbiol. 6, 441–454.

Nanninga, H.J., Gottschal, J.C., 1987. Properties of *Desulfovibrio carbinolicus* sp. nov. and other sulfate-reducing bacteria isolated from an anaerobic-purification plant. Appl. Environ. Microbiol. 53, 802–809.

Nevin, K.P., Kim, B.-C., Glaven, R.H., Johnson, J.P., Woodard, T.L., Methé, B.A., DiDonato, R.J., Covalla, S.F., Franks, A.E., Liu, A., Lovley, D.R., 2009. Anode biofilm transcriptomics reveals outer surface components essential for high density current production in *Geobacter sulfurreducens* fuel cells. PLOS ONE 4, e5628.

Nijburg, J.W., Gerards, S., Laanbroek, H.J., 1998. Competition for nitrate and glucose between *Pseudomonas fluorescens* and *Bacillus licheniformis* under continuous or fluctuating anoxic conditions. Fems Microbiol. Ecol. 26, 345–356.

O'Toole, G., Kaplan, H.B., Kolter, R., 2000. Biofilm Formation as microbial development. Annu. Rev. Microbiol. 54, 49–79.

Oliet, S.H.R., Mothet, J.-P., 2006. Molecular determinants of D-serine-mediated gliotransmission: from release to function. Glia 54, 726–737.

Örnek, D., Jayaraman, A., Syrett, B., Hsu, C.H., Mansfeld, F., Wood, T., 2002. Pitting corrosion inhibition of aluminum 2024 by Bacillus biofilms secreting polyaspartate or γ-polyglutamate. Appl. Microbiol. Biotechnol. 58, 651–657.

Pollegioni, L., Sacchi, S., 2010. Metabolism of the neuromodulator D-serine. Cell. Mol. Life Sci. Cmls 67, 2387–2404.

Valensi, G., van Muylder, J., Pourbaix, M., Sulphur, Section 19.2 in: M. Pourbaix, (ed.), Atlas of Electrochemical Equilibria in Aqueous Solutions, translated from the French by J. A. Franklin, Pergamon Press Oxford, New York, 1966: pp. 545-553.

Raad, I., Chatzinikolaou, I., Chaiban, G., Hanna, H., Hachem, R., Dvorak, T., Cook, G., Costerton, W., 2003. In vitro and ex vivo activities of minocycline and EDTA against microorganisms embedded in biofilm on catheter surfaces. Antimicrob. Agents Chemother. 47, 3580–3585.

Raad, I., Hanna, H., Dvorak, T., Chaiban, G., Hachem, R., 2007. Optimal antimicrobial catheter lock solution, using different combinations of minocycline, EDTA, and

25-Percent ethanol, rapidly eradicates organisms embedded in biofilm. Antimicrob. Agents Chemother. 51, 78–83.
Ravenschlag, K., Sahm, K., Knoblauch, C., Jørgensen, B.B., Amann, R., 2000. Community Structure, Cellular rRNA Content, and Activity of Sulfate-Reducing Bacteria in Marine Arctic Sediments. Appl. Environ. Microbiol. 66, 3592–3602.
Risatti, J.B., Capman, W.C., Stahl, D.A., 1994. Community structure of a microbial mat: the phylogenetic dimension. Proc. Natl. Acad. Sci. U. S. A. 91, 10173–10177.
Rodriguez, M.M., Bill, E., Brennessel, W.W., Holland, P.L., 2011. N_2 reduction and hydrogenation to ammonia by a molecular iron-potassium complex. Science 334, 780–783.
Rosenbaum, M., Aulenta, F., Villano, M., Angenent, L.T., 2011. Cathodes as electron donors for microbial metabolism: which extracellular electron transfer mechanisms are involved? Bioresour. Technol. 102, 324–333.
Rosnes, J.T., Torsvik, T., Lien, T., 1991. Spore-forming thermophilic sulfate-reducing bacteria isolated from North Sea oil field waters. Appl. Environ. Microbiol. 57, 2302–2307.
Royet, J., Dziarski, R., 2007. Peptidoglycan recognition proteins: pleiotropic sensors and effectors of antimicrobial defences. Nat. Rev. Microbiol. 5, 264–277.
Kakooei, S., Ismail, M.C., Ariwahjoedi, B., 2012. Mechanisms of microbiologically influenced corrosion: a review. World Appl. Sci. J. 17, 524–531.
Sakai, K., Yamanami, T., 2006. Thermotolerant *Bacillus licheniformis* TY7 produces optically active l-lactic acid from kitchen refuse under open condition. J. Biosci. Bioeng. 102, 132–134.
Sakashita, M., Sato, N., 1977. The effect of molybdate anion on the ion-selectivity of hydrous ferric oxide films in chloride solutions. Corros. Sci. 17, 473–486.
Sanchez, Z., Tani, A., Kimbara, K., 2012. Extensive reduction in cell viability and enhanced matrix production in *Pseudomonas aeruginosa* PAO1 flow biofilms treated with D-amino acid mixture. Appl. Environ. Microbiol.
Sass, A., Rütters, H., Cypionka, H., Sass, H., 2002. *Desulfobulbus mediterraneus* sp. nov., a sulfate-reducing bacterium growing on mono- and disaccharides. Arch. Microbiol. 177, 468–474.
Schröder, U., 2007. Anodic electron transfer mechanisms in microbial fuel cells and their energy efficiency. Phys. Chem. Chem. Phys. 9, 2619–2629.
Semkiw, E., 2010. The role of the tetraheme cytochrome c3 in *Desulfovibrio vulgaris* Hildenborough metabolism.
Sen, A., 2001. Acidophilic sulphate reducing bacteria: candidates for bioremediation of acid mine drainage pollution. (Ph.D.). University of Wales, Bangor.
Sherar, B.W.A., Power, I.M., Keech, P.G., Mitlin, S., Southam, G., Shoesmith, D.W., 2011. Characterizing the effect of carbon steel exposure in sulfide containing solutions to microbially induced corrosion. Corros. Sci. 53, 955–960.
Sigma, 2009. MSDS of D-methionine from Sigma-Aldrich Corporation.
Stadnitskaia, A., Muyzer, G., Abbas, B., Coolen, M.J.L., Hopmans, E.C., Baas, M., van Weering, T.C.E., Ivanov, M.K., Poludetkina, E., Sinninghe Damsté, J.S., 2005. Biomarker and 16S rDNA evidence for anaerobic oxidation of methane and

related carbonate precipitation in deep-sea mud volcanoes of the Sorokin Trough, Black Sea. Mar. Geol. 217, 67–96.
Stahl, D.A., Loy, L., Wagner, M., 2007. Sulphate-reducing bacteria from oil field environments and deep-sea hydrothermal vents, in: Sulphate-Reducing Bacteria: Environmental and Engineered Systems, Barton, L.L., Hamilton, W.A., (eds.), Cambriged: Cambridge University Press, pp 305-328.
Stoodley, P., Sauer, K., Davies, D.G., Costerton, J.W., 2002. Biofilms as Complex Differentiated Communities. Annu. Rev. Microbiol. 56, 187–209.
Stott, J.F.D., Skerry, B.S., King, R.A., 1988. Laboratory evaluation of materials for resistance to anaerobic corrosion caused by sulphate reducing bacteria: philosophy and practical design, the use of synthetic environments for corrosion testing. ASTM STP 970, Francis P.E., Lee T.S., (eds.), ASTM.
Su, W., Zhang, L., Li, D., Zhan, G., Qian, J., Tao, Y., 2012. Dissimilatory nitrate reduction by *Pseudomonas alcaliphila* with an electrode as the sole electron donor. Biotechnol. Bioeng. DOI: 10.1002/bit.24554.
The Dow Chemical Company, 2009. AQUCAR^{TM} THPS 75 water treatment microbiocide antimicrobial for industrial water treatment applications (No. Form No. 253-01944-09/01/09 PS).
Thauer, R.K., Stackebrandt, E., Hamilton, W.A., 2007. Energy metabolism phylogenetic diversity of sulphate-reducing bacteria, in: Sulphate-Reducing Bacteria: Environmental and Engineered Systems, Barton, L.L., Hamilton, W.A., (eds.), Cambriged: Cambridge University Press, pp 1-38.
Thierry, D., Sand, W., 2002. Microbially Influenced Corrosion, in: Marcus, P., (ed.), Corrosion Mechanisms in Theory and Practice. CRC Press, pp. 583–603.
Thomas, C.J., Edyvean, R.G.J., Brook, R., 1988. Biologically enhanced corrosion fatigue. Biofouling 1, 65–77.
Till, B.A., Weathers, L.J., Alvarez, P.J.J., 1998. Fe(0) supported autotrophic denitrification. Env. Sci Technol 32, 634–639.
Uchiyama, T., Ito, K., Mori, K., Tsurumaru, H., Harayama, S., 2010. Iron corroding methanogen isolated from a crude-oil storage tank. Appl. Environ. Microbiol. 76, 1783–1788.
Vance, I., Thrasher, D.R., 2005. Reservoir souring: mechanism and prevention, in: Ollivier, B., Magot, M., (eds.) Petroleum Microbiology. American Society for Microbiology. ASM press: Washington, D.C., pp. 123–142.
Venzlaff, H., Enning, D., Srinivasan, J., Mayrhofer, K.J.J., Hassel, A.W., Widdel, F., Stratmann, M., 2013. Accelerated cathodic reaction in microbial corrosion of iron due to direct electron uptake by sulfate-reducing bacteria. Corros. Sci. 66, 88–96.
Videla, H.A., 1996. Manual of Biocorrosion, 1st ed. CRC-Press, pp 13–45.
Videla, H.A., 2002. Prevention and control of biocorrosion. Int. Biodeterior. Biodegrad. 49, 259–270.
Videla, H.A., Herrera, L.K., 2005. Microbiologically influenced corrosion: looking to the future. Int. Microbiol. Off. J. Span. Soc. Microbiol. 8, 169–180.
Von Wolzogen Kuehr, C.A.H., Van der Vlugt, L., 1934. The graphitization, of cast iron as an electrochemical process in anaerobic soils. Water 18, 147–165.

Vuyyuri, S.B., Hamstra, D.A., Khanna, D., Hamilton, C.A., Markwart, S.M., Campbell, K.C.M., Sunkara, P., Ross, B.D., Rehemtulla, A., 2008. Evaluation of D-methionine as a novel oral radiation protector for prevention of mucositis. Clin. Cancer Res. Off. J. Am. Assoc. Cancer Res. 14, 2161–2170.

Wade, D., Boman, A., Wåhlin, B., Drain, C.M., Andreu, D., Boman, H.G., Merrifield, R.B., 1990. All D-amino acid containing channel forming antibiotic peptides. Proc. Natl. Acad. Sci. 87, 4761–4765.

Walsh, D., Pope, D., Danford, M., Huff, T., 1993. The effect of microstructure on microbiologically influenced corrosion. Jom J. Miner. Met. Mater. Soc. 45, 22–30.

Wang, Q., Zhao, X., Chamu, J., Shanmugam, K.T., 2011. Isolation, characterization and evolution of a new thermophilic *Bacillus licheniformis* for lactic acid production in mineral salts medium. Bioresour. Technol. 102, 8152–8158.

Wen, J., Zhao, K., Gu, T., Raad, I.I., 2009. A green biocide enhancer for the treatment of sulfate-reducing bacteria (SRB) biofilms on carbon steel surfaces using glutaraldehyde. Int. Biodeterior. Biodegrad. 63, 1102–1106.

Wen, J., Zhao, K., Gu, T., Raad, I.I., 2010. Chelators enhanced biocide inhibition of planktonic sulfate-reducing bacterial growth. World J. Microbiol. Biotechnol. 26, 1053–1057.

Woolley, K.J., 1987. The c-type cytochromes of the gram-positive bacterium *Bacillus licheniformis*. Arch. Biochem. Biophys. 254, 376–379.

Xu, D., Gu, T., 2011. Bioenergetics explains when and why more severe MIC pitting by SRB can occur, in: Corrosion/2011 Paper No 11426. NACE International, Houston, TX.

Xu, D., Huang, W., Ruschau, G., Hornemann, J., Wen, J., Gu, T., 2013a. Laboratory investigation of MIC threat due to hydrotest using untreated seawater and subsequent exposure to pipeline fluids with and without SRB spiking. Eng. Fail. Anal. 28, 149–159.

Xu, D., Li, Y., Gu, T., 2012. A synergistic D-tyrosine and tetrakis hydroxymethyl phosphonium sulfate biocide combination for the mitigation of an SRB biofilm. World J. Microbiol. Biotechnol. 28, 3067–3074.

Xu, D., Li, Y., Gu, T., 2013b. D-Methionine as a biofilm dispersal signaling molecule enhanced tetrakis hydroxymethyl phosphonium sulfate mitigation of *Desulfovibrio vulgaris* biofilm and biocorrosion pitting. Mater. Corros. In press.

Xu, D., Wen, J., Fu, W., Gu, T., Raad, I.I., 2012. D-amino acids for the enhancement of a binary biocide cocktail consisting of THPS and EDDS against an SRB biofilm. World J. Microbiol. Biotechnol. 28, 1641–1646.

Xu, D., Wen, J., Gu, T., Raad, I., 2012. Biocide cocktail consisting of glutaraldehyde, ethylene diamine disuccinate (EDDS), and methanol for the mitigation of souring and biocorrosion. Corrosion 68, 994–1002.

Xu, H., Liu, Y., 2011. d-Amino acid mitigated membrane biofouling and promoted biofilm detachment. J. Membr. Sci. 376, 266–274.

Xu, L.-C., Fang, H.H.P., Chan, K.-Y., 1999. Atomic force microscopy study of microbiologically influenced corrosion of mild steel. J. Electrochem. Soc. 146, 4455–4460.

Yu, C., Wu, J., Contreras, A.E., Li, Q., 2012. Control of nanofiltration membrane biofouling by *Pseudomonas aeruginosa* using d-tyrosine. J. Membr. Sci. 487–494.

Zhou, M., Wang, H., Hassett, D.J., Gu, T., 2013. Recent advances in Microbial Fuel Cells (MFCs) and Microbial Electrolysis Cells (MECs) for wastewater treatment, bioenergy and bioproducts. J. Chem. Technol. Biotechnol. in press., DOI: 10.1002/jctb.4004.

Zumft, W.G., 1997. Cell biology and molecular basis of denitrification. Microbiol. Mol. Biol. Rev. 61, 533–616.

Zuo, R., 2007. Biofilms: strategies for metal corrosion inhibition employing microorganisms. Appl. Microbiol. Biotechnol. 76, 1245–1253.

Thesis and Dissertation Services